

**Metal Ion Sensor with Catalytic DNA in a Nanofluidic  
Intelligent Processor**

**SERDP Project Number CS-1265**

**U.S. Army Corps of Engineers  
Construction Engineering Research Laboratory**

**Lead Principal Investigator: Dr. Donald M. Cropek**

**8 February 2005**

Distribution Statement A: Approved for Public Release, Distribution is Unlimited

## Report Documentation Page

*Form Approved*  
*OMB No. 0704-0188*

Public reporting burden for the collection of information is estimated to average 1 hour per response, including the time for reviewing instructions, searching existing data sources, gathering and maintaining the data needed, and completing and reviewing the collection of information. Send comments regarding this burden estimate or any other aspect of this collection of information, including suggestions for reducing this burden, to Washington Headquarters Services, Directorate for Information Operations and Reports, 1215 Jefferson Davis Highway, Suite 1204, Arlington VA 22202-4302. Respondents should be aware that notwithstanding any other provision of law, no person shall be subject to a penalty for failing to comply with a collection of information if it does not display a currently valid OMB control number.

1. REPORT DATE <b>08 FEB 2005</b>	2. REPORT TYPE	3. DATES COVERED <b>00-00-2005 to 00-00-2005</b>			
4. TITLE AND SUBTITLE <b>Metal Ion Sensor with Catalytic DNA in a Nanofluidic Intelligent Processor</b>		5a. CONTRACT NUMBER			
		5b. GRANT NUMBER			
		5c. PROGRAM ELEMENT NUMBER			
6. AUTHOR(S)		5d. PROJECT NUMBER			
		5e. TASK NUMBER			
		5f. WORK UNIT NUMBER			
7. PERFORMING ORGANIZATION NAME(S) AND ADDRESS(ES) <b>U.S. Army Corps of Engineers, Construction Engineering Research Laboratory, 3909 Halls Ferry Road, Vicksburg, MS, 39180-6199</b>		8. PERFORMING ORGANIZATION REPORT NUMBER			
9. SPONSORING/MONITORING AGENCY NAME(S) AND ADDRESS(ES)		10. SPONSOR/MONITOR'S ACRONYM(S)			
		11. SPONSOR/MONITOR'S REPORT NUMBER(S)			
12. DISTRIBUTION/AVAILABILITY STATEMENT <b>Approved for public release; distribution unlimited</b>					
13. SUPPLEMENTARY NOTES					
14. ABSTRACT					
15. SUBJECT TERMS					
16. SECURITY CLASSIFICATION OF:			17. LIMITATION OF ABSTRACT	18. NUMBER OF PAGES	19a. NAME OF RESPONSIBLE PERSON
a. REPORT <b>unclassified</b>	b. ABSTRACT <b>unclassified</b>	c. THIS PAGE <b>unclassified</b>	<b>Same as Report (SAR)</b>	<b>96</b>	

This report was prepared under contract to the Department of Defense Strategic Environmental Research and Development Program (SERDP). The publication of this report does not indicate endorsement by the Department of Defense, nor should the contents be construed as reflecting the official policy or position of the Department of Defense. Reference herein to any specific commercial product, process, or service by trade name, trademark, manufacturer, or otherwise, does not necessarily constitute or imply its endorsement, recommendation, or favoring by the Department of Defense.

# Table of Contents

List of Figures and Tables.....	ii
Conversion Factors.....	v
Acknowledgements.....	1
Executive Summary .....	2
Objective .....	3
Background .....	4
Materials and Methods.....	8
Results and Discussion.....	8
Conclusions.....	24
References.....	25
Appendix.....	29

## List of Figures and Tables

Figure 1. (a) Structure of the Pb-sensing catalytic DNA. (b) Fluorosensing mechanism and results .....	6
Figure 2. Sensor selectivity.....	6
Figure 3. Schematic diagram of the molecular gate used as an intelligent nanofluidic processor .....	7
Figure 4: Fluorescence spectra for (a) background and (b) solution after addition of lead .....	10
Figure 5: Immobilization and lead reaction schematic.....	11
Figure 6: Fluorescence intensities produced from reactions of immobilized DNA on Au surfaces.....	11
Figure 7: Calibration curve for immobilized DNAzyme on Au surfaces for fluorescence versus lead solution concentration.....	11
Figure 8: Fluorescence intensities from reactions with lead solutions with immobilized DNAzymes, non-regenerated surfaces, and regenerated surfaces....	12
Figure 9: Transmission electron micrograph of the molecular gate membrane after electroless deposition of gold .....	13
Figure 10: Comparison of total fluorescent intensities for DNAzyme sensors assembled on planar gold-coated glass and gold-coated polycarbonate membranes with identical geometric size after complete reaction with $10\ \mu\text{M Pb}^{2+}$ . Access to $\sim 250\text{nm}$ pores through the membrane allows for $9.2 \pm 3.1$ times higher intensity attributed to the higher surface area.....	14
Figure 11: Intensities of fluorescence after reaction with $10\ \text{nM}$ and $10\ \mu\text{M Pb}^{2+}$ for 60 minutes compared to the intensity of the solution without reaction with $\text{Pb}^{2+}$ after the same time interval. Values of $2.33 \pm 0.98$ times and $4.85 \pm 1.15$ times the control were calculated for $10\ \text{nM}$ and $10\ \mu\text{M Pb}^{2+}$ , respectively .....	14
Figure 12: (A) Schematic of two crossed microfluidic channels with a nanocapillary array interconnect. (B) Optical image of the PDMS gated injection and transport device. (C) Electrical bias configuration for electrokinetic injection and electrophoretic transport of $\text{Pb}^{2+}$ .....	15
Figure 13: Three channel microfluidic system .....	16

Figure 14: Three channel microfluidic sensors.....	16
Figure 15. Fluorescence image series for gated injection of Pb <sup>2+</sup> band across the array of 200 nm diameter capillaries.....	17
Figure 16: Experimental set up for detection of fluorescent emission from the detection channel. A three channel chip is shown .....	17
Figure 17: Fluorescent images of lead injections into the collection channel from background to the on (inject) state to the off state (17A). Results from multiple injections show the system reproducibility .....	18
Figure 18: (Left) Migration of a probe across PCTE nano-capillary arrays with 200 nm-diameters connecting to PDMS channels. Fluorescence intensity to monitor the transport of Pb <sup>2+</sup> in Lactate/HEPES BGE, pH7.2. (Right) Calibration curve of the DNAzyme-based Pb <sup>2+</sup> detection System.....	19
Figure 19: Microchip electrophoretic system with conductivity detection. (A) contact gold electrode chip and (B) contactless aluminum film electrode chip.....	20
Figure 20: Resistance (conductivity) measurements for different standard conductivity solutions (left) and standard lead concentrations (right) at an operation frequency of 100 kHz and an excitation voltage of 1V .....	21
Figure 21: (A) Separation of metal ions using lactate. Carrier electrolyte, 15 mM lactate, 8 mM 4-methylbenzylamine (pH 7.2 adjusted with ammonium hydroxide); Applied separation voltage, 30 kV; capillary, fused-silica, 75 μm ID, 60 cm long. (B) Separation of metal ions using lactate/HEPES. Carrier electrolyte, 25 mM lactate, 25 mM HEPES, 50 mM NaCl, 8 mM 4-methylbenzylamine (pH 7.2 adjusted with ammonium hydroxide); (C) Fluorescence enhancement of the cleaved strand in the presence of Pb <sup>2+</sup> using the lactate/HEPES buffer system .....	22

## Tables

Table 1. DNA labels and sequences.....	9
Table 2. Certified metal content in electroplating sludge reference material .....	23

## Acronyms

The following is a list of the common acronyms used in this report. Chemical element abbreviations are expected to be common knowledge.

AAS	Atomic Absorption Spectrometry
BGE	Background Electrolyte
CD	Conductivity Detection
CE	Capillary Electrophoresis
CZE	Capillary Zone Electrophoresis
Dabcyl	4-(((4-dimethylamino)-phenyl)azo)benzoic acid
DNA	Deoxyribonucleic Acid
DoD	Department of Defense
EPA	Environmental Protection Agency
FI	Flow Injection
HEPES	[4-(2-hydroxyethyl)-1-piperazineethanesulfonic acid
ICP-MS	Inductively Coupled Plasma Mass Spectroscopy
ISE	Ion-Selective Electrode
LCR	Impedance / Conductivity / Resistance
LIF	Laser Induced Fluorescence
MCH	Mercaptohexanol
MEMS	Microelectromechanical System
NAI	Nanocapillary Array Interconnects
PCTE	Polycarbonate Nuclear Track Etched
PDMS	Poly(dimethylsiloxane)
PMT	Photon Multiplier Tube
ppb	parts per billion
ppm	parts per million
RCRA	Resource Conservation and Recovery Act
RNA	Ribonucleic Acid
SAM	Self-assembled Monolayers
TAMRA	Carboxytetramethylrhodamine
TAS	Total Analytical System

## Conversion Factors

Non-SI\* units of measurement used in this report can be converted to SI units as follows:

<b>Multiply</b>	<b>By</b>	<b>To Obtain</b>
acres	4,046.873	square meters
cubic feet	0.02831685	cubic meters
cubic inches	0.00001638706	cubic meters
degrees (angle)	0.01745329	radians
degrees Fahrenheit	$(5/9) \times (^\circ\text{F} - 32)$	degrees Celsius
degrees Fahrenheit	$(5/9) \times (^\circ\text{F} - 32) + 273.15$	kelvins
feet	0.3048	meters
gallons (U.S. liquid)	0.003785412	cubic meters
horsepower (550 ft-lb force per second)	745.6999	watts
inches	0.0254	meters
kips per square foot	47.88026	kilopascals
kips per square inch	6.894757	megapascals
miles (U.S. statute)	1.609347	kilometers
pounds (force)	4.448222	newtons
pounds (force) per square inch	0.006894757	megapascals
pounds (mass)	0.4535924	kilograms
square feet	0.09290304	square meters
square miles	2,589,998	square meters
tons (force)	8,896.443	newtons
tons (2,000 pounds, mass)	907.1847	kilograms
yards	0.9144	meters

---

\* *Système International d'Unités* ("International System of Measurement"), commonly known as the "metric system."

## **Acknowledgements**

This study was conducted for the Strategic Environmental Research and Development Program in the Conservation Pillar. The technical monitor was Dr. Robert Holst.

The Principal Investigator on this project was Dr. Donald M. Cropek, Construction Engineering Research Laboratory (CERL), Environmental Processes Branch. The associated Technical Director was Dr. Kumar Topurdurti, CERL, CNE, and the Director of CERL is Dr. Alan W. Moore. CERL is an element of the U.S. Army Engineer Research and Development Center (ERDC), U.S. Army Corps of Engineers. The Commander and Executive Director of ERDC is COL John Morris III, EN and the Director of ERDC is Dr. James R. Houston.

This work was performed as a collaboration between CERL and the University of Illinois, Urbana-Champaign. The Lead Investigator at the University of Illinois was Dr. Paul W. Bohn, Chemistry. Team at the University of Illinois included the following members: Dr. In-Hyoung Chang, Dr. Jonathan Sweedler, Dr. Yi Lu, Dr. Carla Swearingen, and Mr. Daryl Wernette.

## Executive Summary

Heavy metals are a ubiquitous and troublesome class of pollutants, and lead (Pb) occupies a prominent position as a contaminant requiring constant attention. It is a RCRA metal, and its presence often defines a waste as hazardous. It is also an EPA Urban Air Toxic, meaning its emissions are regulated under the Clean Air Act Amendment of 1990. Anthropogenic sources of Pb from military operations require active monitoring and sensing to ensure environmental compliance and protection. The high profile of Pb is linked to its numerous toxicological effects over a wide exposure range (1).

Origins of Pb in the environment result from both historical and current uses of lead compounds. Runoff along the drip line of buildings, some dating from as far back as World War II, still contain Pb derived from the lead based paints commonly used. Outdoor metal structures, such as bridges, are frequently covered in red and white lead primers, from which Pb is released during weathering and refurbishing. Industrial activities, *e.g.* smelting of lead acid batteries, still produce a waste stream high in Pb. New guidance from DoD Directive 4715 requires a high degree of management and monitoring of firing ranges to maintain operational readiness while protecting human health and the environment. The impact areas on these firing ranges are replete with lead due to use of numerous lead containing munitions. Range managers must carefully monitor leaching of lead from the berms to protect downstream habitats. These examples and others would benefit immensely from a field-portable lead sensor designed and equipped with features and characteristics that would allow real time, *in situ* measurement of lead in ground water.

A further example is the SERDP Ecosystem Management Project. This is an ecosystem monitoring program focused on maintaining and improving the sustainability and native biological diversity on military lands while supporting human needs, including the DoD mission. This program establishes long term monitoring sites on DoD lands to monitor the non-steady state of ecosystems, especially the effects of military activities. Current efforts include measuring equipment and remote sensors for acquisition of water quality field data. Despite the recognized adverse effects of chemical pollutants and contaminants on aquatic and terrestrial biota, these critical parameters are not being measured, in large part due to the lack of a field product that meets all requirements for remote metal sensing, *e.g.* rugged, reliable, sensitive, selective, and remotely operable.

Miniaturization of sensing elements is currently a very important aspect in environmental monitoring due to not only its effectiveness in reducing cost and labor but also its portability. In recent years, considerable interest has focused on the development of miniaturized microfluidic systems (also called lab-on a chip) offering many potential benefits including improved analytical performance, fast and efficient chemical reactions within small volumes, and low manufacturing cost. A further benefit of miniaturization is the reduction in reagent and sample consumption and subsequent reduction in the quantity of waste produced. Through these advantages, it is considered that one could mass produce and mass employ these remote sensors, particularly in long term monitoring of ecosystems. This research furthers the state-of-the-art in microfluidic sensing devices that incorporate molecular beacons for the detection of heavy metal cations, specifically lead (Pb<sup>2+</sup>).

Several literature articles have been published describing the separation and simultaneous determination of metal ions based on microfluidic device (2-9). For example, Jacobson *et al.* have demonstrated a successful separation of Zn, Cd, and Al with detection limits of several tens of ppb on a capillary electrophoresis (CE) microchip (4). Deng and Collins (9) have utilized colorimetric detection to demonstrate the separation of six heavy metals including Pb<sup>2+</sup>. These heavy metals were effectively separated and simultaneously determined on a CE microchip with detection limits of sub ppb concentration level after preconcentration by solid-phase extraction (SPE) (9).

The use of biosensors in environmental pollution monitoring has become a growing interest, as these devices provide rapid, simple and reliable determination of pollutants at a trace levels. Novel lead specific biosensors have been developed and significant progress has been made (10-14). Lu *et al.* (13-15) developed a new biosensor for lead by combining the high selectivity of catalytic DNA with the sensitivity of fluorescent detection, and it can be applied to the quantitative detection of Pb<sup>2+</sup> over a wide concentration range from 0.1 to 10 μM.

This paper presents the potential of combining Pb<sup>2+</sup> specific catalytic DNA enzymes with microfluidic devices. We incorporate the catalytic DNAzyme into a detection channel on the microfluidic device. Lead containing solution is placed in a source channel. By appropriate application of voltages across channels, the lead solution can be injected through nanocapillary array interconnects (NAI) that separate the channels. These gatable microfluidic devices build upon research developed by Bohn and Sweedler *et al.* (16-18). Methods for adapting lead specific biosensors to the NAI microfluidic device are presented. Performances of the developed method were evaluated by studying quantifiable concentration range, method accuracy and precision. Successful application to real sample analysis using an electroplating sludge certified reference material is also presented.

It is important to note that the sensor architecture developed here is not analyte dependent. We can incorporate other molecular beacons on this microfluidic device. Because identifying the Pb<sup>2+</sup>-selective catalytic DNA sequence was accomplished via a novel combinatorial search, *success in the development of this prototype lead sensor lends itself to rapid development of other targeted chemical sensors based on catalytic DNA that are uniquely reactive to any other metal or organic compound.* Thus, relevance of this research is magnified beyond Pb<sup>2+</sup> to include field sensors for other chemicals of interest such as PCBs, PAHs, and other metals (*e.g.* Al, Hg, Cd, and depleted uranium).

## Objective

This work addressed the initial statement of need to develop a miniature sensor for monitoring the waterborne heavy metal pollutant lead (Pb<sup>2+</sup>). We created a highly selective and sensitive miniature sensor for Pb<sup>2+</sup> by combining two recent advances: (a) *catalytic DNA* that is reactive only to Pb<sup>2+</sup> and which can be tagged to produce fluorescence only in the presence of the metal, and (b) *nanoscale fluidic molecular gates* that can manipulate fluid flows and perform molecular separations on tiny volumes of material. This work develops the chemistry needed to combine Pb-specific catalytic DNA with the molecular gates and the protocol for separating, sensing, and

quantifying  $\text{Pb}^{2+}$  in a complex matrix.

The biosensor is a multi-level nanofluidic-microfluidic hybrid device, in which a nanocapillary array membrane is used to control motion of picoliter-volume fluid voxels from the analyte-containing sample stream to the biosensor compartment. These devices employ a membrane containing an array of nanocapillaries located between multilayered microfluidic channels, allowing for the convenient and efficient control of fluids in the device (16-18). In this paper, methods for adapting this lead-selective DNAzyme to the nanofluidic device are explored and the analytical figures of merit including dynamic range, limit of detection, accuracy, and precision are determined. Finally, the microfluidic / DNAzyme molecular beacon is successfully applied to analysis of  $\text{Pb}^{2+}$  in an electroplating sludge certified reference material.

## Background

There are a number of different methods currently used for the determination of lead. Among the various methods, atomic absorption spectrometry (AAS) (19-21) and inductively coupled plasma mass spectrometry (ICP-MS) (22-24) are most widely used for the determination of metal ions with high efficiency, selectivity and sensitivity, and are thus suitable for the determination of metal ions in environmental samples. Unfortunately, these techniques require expensive instrumentation and sophisticated sample pre-treatment procedures. Recently, the combination of flow injection (FI) on-line separation and preconcentration methods provide significant advantages when coupled to conventional spectroscopy methods, *e.g.* less risk of contamination, high enrichment efficiencies, reproducibility, method precision, and simple automated operation. FI-AAS (25,26), FI-ICP-MS (27,28), and FI-spectrophotometry-based methods (29,30) have been reported for the determination of lead in biological and environmental samples. On the other hand, potentiometry (*i.e.* ion-selective electrodes (ISEs)) has become a routine analytical method for rapid determination of numerous analytes include trace metal ions in a cost effective manner in the field of clinical diagnostics and environmental monitoring (31,32). Stripping voltametry using chemically modified electrodes has also been considered as a prospective technique with low detection limit, selectivity, and the possibility of multielement detection (33,34). However, current approaches require that numerous samples be collected and sent to an analytical laboratory for the pretreatment and assessment as to the extent and type of heavy metal present. For the simultaneous determination of trace metals at  $\mu\text{g/L}$  levels in complex matrices, ion chromatography (35,36) and capillary zone electrophoresis (CZE) (37) have been applied. The common disadvantages to these techniques is the cost of the equipment and the required operator skill and attendance that tether these to the laboratory bench.

As mentioned above, miniaturized systems have attracted interest and must compete with the laboratory techniques. Recently, miniaturized high-performance analytical systems, capillary electrophoresis microchip systems, are finding applications in environmental sensing include metals (6,9). These miniaturized devices provide the potential for enhancing the speed of an analytical separation, while reducing the system size and weight, and the consumption of samples and reagents. Through this research project, we propose here a new methodology for the miniaturized lead sensor by combining a biosensor (catalytic DNA) with a microfluidic chip. This research demonstrates the ability of the lead-specific biosensor to determine lead in

complex matrices. All these features are highly desirable for the development of truly portable devices capable of sensitively and rapidly monitoring hazardous metal cations in the field.

**Catalytic DNA.** In 1994, DNA was shown through a technique called *in vitro* selection (*vide infra*) to carry out catalytic functions when single stranded (38). The DNAs (called catalytic DNA or DNA enzymes or deoxyribozymes) have proven capable of catalyzing many reactions including RNA/DNA-cleavage, ligation, phosphorylation, cleavage of phosphoramidate bonds, and porphyrin metallation (39). Catalytic DNAs have shown great promise as anti-viral pharmaceutical agents against diseases such as AIDS and leukemia. Recently Lu and coworkers at Illinois demonstrated that catalytic DNAs can expand out of the realm of biological chemistry and into environmental monitoring by selectively reacting with  $\text{Pb}^{2+}$  in the presence of interfering cations (15).

**Metal ion sensors.** Metal ions play important roles in biological systems. Beneficial metal ions such as  $\text{Ca}^{2+}$ ,  $\text{Fe}^{3+}$  and  $\text{Mg}^{2+}$  are minerals required to maintain normal functions, while toxic metal ions such as  $\text{Pb}^{2+}$ ,  $\text{Hg}^{2+}$  and  $\text{Cr}^{6+}$  can have a number of adverse health effects. Current methods for metal ion determinations, such as atomic absorption spectrometry (40), inductively coupled plasma mass spectrometry (22), and anodic stripping voltammetry (41), often require sophisticated equipment or sample treatment and are unsuitable for field monitoring due to size, power requirements, and fragility. *Simple and inexpensive methods that permit real-time, on-site sampling of metal ions would constitute a critical enabling advance in the field.*

Fluorosensors based on fluorescently-labeled organic chelators, proteins or peptides have emerged as powerful tools toward achieving the above goals (42-44). While remarkable progress has been made in developing fluorosensors for metal ions such as  $\text{Ca}^{2+}$  and  $\text{Zn}^{2+}$ , designing and synthesizing sensitive and selective metal ion fluorosensors remains a significant challenge. Perhaps the biggest challenge in fluorosensor research is the design and synthesis of a sensor capable of specific and strong metal-binding. Since our knowledge about the construction of metal-binding sites is limited, searching for sensors in a combinatorial way can drastically reduce the research effort required to identify effective fluorescently-active chelating agents. In this regard, *in vitro* selection of DNA/RNA from a library of  $10^{14}$ - $10^{15}$  random DNA/RNA sequences offers considerable opportunity (38,39). Compared with combinatorial searches of chemo- and peptidyl-sensors, *in vitro* selection of DNA/RNA is capable of sampling a larger pool of sequences, amplifying the desired sequences by the polymerase chain reaction (PCR), and introducing mutations to improve performance by mutagenic PCR. For example, the *in vitro* selection method has been used to obtain DNA/RNA aptamers (45,46) and aptazymes (47,48) that are responsive to small organic molecules. Similarly, catalytic DNA/RNAs that are highly specific for  $\text{Pb}^{2+}$  (38,49),  $\text{Ca}^{2+}$  (50,51) and  $\text{Zn}^{2+}$  (52,53) have been obtained. These results set the stage for the utilization of catalytic DNAs with hydrolytic cleavage activity for detection of metal ions.

**Microfabricated analysis systems.** A trend throughout the last two decades has been towards miniaturized analytical methods to achieve unique capabilities as well as better performance specifications. The development of microelectro-mechanical systems (MEMS) and the related concept of miniaturizing a total analytical system,  $\mu$ -TAS, started with the work of Terry *et al.* (54) in 1979, who fabricated a complete gas chromatography system on a silicon wafer. Manz

and coworkers reached another milestone with liquid phase separations (55), followed rapidly by pioneering work by Harrison and Manz (56), Ramsay (57), and Mathies (58). Since then, there has been an exponential growth in this field, including advances in fabrication methods from silicon (55), optically transparent materials (59,60), and exciting advances in polymer substrates (61,62). Besides analytical microfluidics, a tremendous effort has gone into the development of mixers, valves, interconnects, filters and other elements required for a complete microfluidics system (63). Recent reviews describe the important milestones in this research area (64).

### Summary of PIs' previous work.

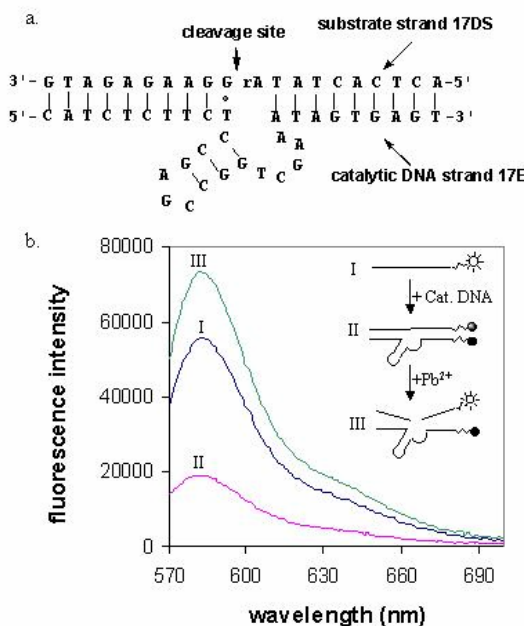


Figure 1. (a) Structure of the Pb-sensing catalytic DNA. (b) Fluoresensing mechanism and results.

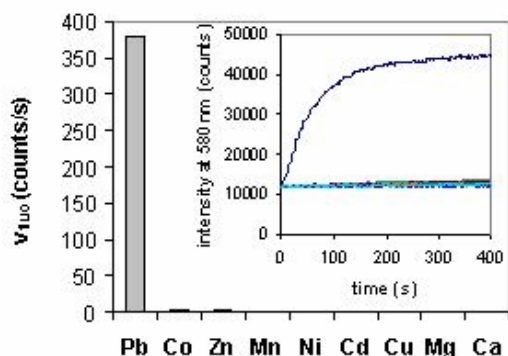


Figure 2. Sensor selectivity.

Recently, Li and Lu reported a new application for catalytic DNAs as biosensors for metal ions, specifically  $Pb^{2+}$  (15). This application is based on the observation that catalytic DNA, obtained through *in vitro* selection, can be used to bind metal ions with high affinity and specificity (38,52,53). Therefore, the activity of a selected catalytic DNA can be used to measure the identity and quantity of the specific metal ion. The biosensor consists of a catalytic DNA capable of base-pairing to a DNA substrate containing a single ribonucleotide residue (labeled rA in Fig. 1a). When a fluorophore, *e.g.* carboxytetramethylrhodamine (TAMRA), is attached to the 5'-end of the DNA substrate, the fluorescence signal at 580 nm is quenched by its proximity to a fluorescence quencher, *e.g.* 4-(((4-dimethylamino)-phenyl)azo)benzoic acid (Dabcyl), at the nearby 3'-end of the catalytic DNA. In the presence of  $Pb^{2+}$ , the fluorescence emission of TAMRA increases dramatically ( $\sim 400\%$ ), due to the cleavage of the substrate DNA and subsequent separation of the fluorophore from the quencher (Fig. 1b inset). This is followed by the release of substrate DNA fragments and  $Pb^{2+}$ . This system represents a new class of metal ion sensors and is the first example of using the powerful tools of combinatorial molecular biology to identify a cation-specific catalytic DNA for sensing of metal ions. It combines the high selectivity of catalytic DNA ( $> 80$  fold for  $Pb^{2+}$  over other divalent metal ions, see Fig. 2) with the ultralow background and resulting high sensitivity of fluorescence detection, and it can be applied to quantitative detection of  $Pb^{2+}$  over a concentration range of three orders of magnitude. The sensitivity and selectivity of the

system can be altered by using different fluorescence/quencher pairs for different sensors. The system is easily regenerated by washing away the cleaved products and adding new substrate

DNA to the catalytic DNA strand -- a fact that will be exploited to regenerate active material in the proposed sensor. Finally, catalytic DNA specific for other metal ions and with various detection ranges can be isolated by varying the catalytic DNA selection conditions in the combinatorial search, making this approach extensible to other metal ions and small organic molecules. Thus, the approach outlined here is targeted not only at the development of a specific sensor for  $\text{Pb}^{2+}$  but also toward *rapid development of a whole class of highly specific sensors*.

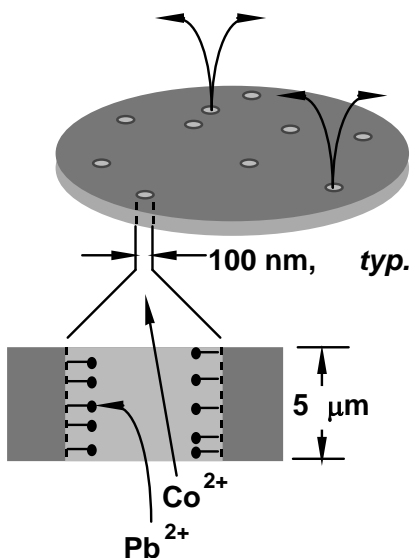


Figure 3. Schematic diagram of the molecular gate used as an intelligent nanofluidic processor.

Bohn *et al.* have developed a new approach to fluidic control, in which a ‘molecular gate’ is constructed from a thin (typically  $5\ \mu\text{m}$ ) polymeric membrane perforated with a number ( $\sim 10^8\ \text{cm}^{-2}$ ) of long narrow (typical aspect ratios of 25-250) channels, *viz.* Figure 3. These structures exhibit unique and tunable electrokinetic flow properties, because the product of the channel diameter,  $a$ , and the inverse Debye length,  $\kappa$ , is  $\sim 1$ . When  $\kappa a < 1$  the electric double layer extends throughout the pore (65-67) and the mobile counterions filling the channel determine transport. At the other limit,  $\kappa a > 1$ , the electrical double layer is mostly collapsed, and normal ion migration effects dominate. Thus, flow can be controlled by (a) direction of the applied bias, (b) sign and surface density of the immobile charge on the wall, *i.e.*, pH and chemical derivatization, and (c) the magnitude of  $\kappa a$ . Because  $\kappa$  is controlled by solution ionic strength, control of flow in these nanometer channels is

exceptionally versatile (68,69). These nanoscale porous materials with well-defined cross-sectional geometry are an excellent choice for fluidic handling at low levels due to several related factors. (a) The separations capacity factor,  $k'$ , which scales like the surface-to-volume ratio, is huge. Comparing a  $20\ \mu\text{m}$  i.d. wall-coated open tubular column with a  $10\ \text{nm}$  thick coating to a  $200\ \text{nm}$  i.d. nanopore with the same coating, the increase in capacity factor is a factor  $> 10^2$ . (b) Nanopores have fundamentally different properties than their larger  $\mu\text{m}$ -scale analogs, because characteristic length scales that describe important physico-chemical phenomena are approximately equal to the dimensions of the nanochannels. (c) Nanopores are ideally suited to making intelligent interconnects between microfluidic elements, because the interconnect itself can be made to be integral to the intelligent movement of biomolecules, and it is simple to integrate and to interface with existing microfluidic technologies. Combining catalytic DNA with molecular gates to achieve a Nanofluidic Intelligent Processor (NIP) will exploit all three of these important characteristics.

This work will produce a prototype sensor having all desired characteristics of a remote field sensor. Several key operating characteristics make this sensor modality stand apart. Repetitive analyte delivery cycles can be realized, meaning that the catalytic DNA can react with analyte for as long as is needed to generate a usable signal, increasing sensitivity. Second, the substrate DNA can be released and regenerated, allowing repeated unattended use in the field. Third, unlike other chemically based sensors, the waste stream produced from operation of this device is exceedingly small, (mL/year) and only non-toxic DNA fragments are added. Finally,

the sensor can be extremely rugged -- in particular it is insensitive to episodic loss of liquid analyte stream, so it can survive periods without liquid input, such as might be encountered with groundwater sources that periodically dry up. Finally, the strategy outlined here is completely general and a sensor can be constructed for *any* analyte for which a combinatorial binding sequence can be identified.

Successful sensor design includes the use of the electrophoresis to introduce the lead containing solution to the catalytic DNA within a microfluidic channel. Our desire is a prototype device that demonstrates the ability to quantitate lead within a clean sample and within a complex sample with detection limits near EPA drinking water action limits of 15 ppb. With this limit of detection, the device would clearly be usable for determining hazardous waste according to the EPA Toxicity Characteristic Leaching Procedure with a lead limit of 5 ppm. It can also be field-portable to become the analytical device for determination of action limits of lead in paint (5000 ppm) or lead in soil (400 ppm on a playground) when accompanied by an extraction technique.

## Materials and Methods

Over the course of this project, the numerous tasks required copious supplies, however, the critical items for this work are the DNA sequences, the molecular gate membranes, and the electroplating sludge. All DNA is purchased from Integrated DNA Technologies (IDT) (Coralville, IA) or from Trilink BioTechnologies, Inc. (San Diego, CA). Prepolymer and curing agent (Sylgard 184, Dow Corning Corp. Midland, MI) and polycarbonate nuclear track-etched (PCTE) membranes with a hydrophilic wetting layer of poly(vinylpyrrolidone) (Osmonics, Minnetonka, MN) were used in the PDMS (poly(dimethylsiloxane)) chip. These PCTE membranes are 10 microns thick with 200 nm diameter pores at a pore density of  $3 \times 10^8$  pores /  $\text{cm}^2$  and are used as the molecular gate membranes. The electroplating sludge sample was purchased from Resource Technology Corporation (Laramie, WY). The methods for each part of the project will be described as the results are discussed.

## Results and Discussion

The accomplishments of this work divided into two areas: 1) Manipulation of the lead sensitive catalytic DNA and 2) Creation and characterization of the microfluidic device that brings together the lead with the catalytic DNA sensing molecules. These accomplishments are described in large part in our publications that are provided in the Appendix.

**Catalytic DNA – Thiolation, Immobilization, and Regeneration.** The behavior of the  $\text{Pb}^{2+}$ -specific DNAzyme has been illustrated in Figure 1b above. The hybridized substrate / enzyme construct is free in solution, permitting uninhibited conformation for reactions with lead cations. The  $\text{Pb}^{2+}$ -specific DNAzyme sensor has been limited to bulk solution reactions. There are two inherent advantages associated with moving to a surface-immobilized sensor. First, since hybridization of enzyme and substrate strands is never complete, background fluorescence is observed, even in the absence of a specific cleavage reaction due to free substrate in the solution. Because noise in the background fluorescence is a fundamental limitation when working at low analyte concentrations, efforts to reduce the background can produce lower limits of detection.

To this end, reducing background levels due to higher hybridization efficiency and elimination of free substrate can be accomplished with immobilization. Second, the surface-immobilized DNAzyme may be regenerated and used multiple times, a possibility that is not straightforward in solution-based sensors. Hybridization of surface-bound DNA has been shown to be reversible, suggesting the possibility of reusing the surface for successive measurements (70). For example, Ramachandran *et al.* produced a surface-immobilized DNAzyme that exhibited 75 % of the original activity after one regeneration (71).

Though many strategies for immobilization exist, exploiting Au-thiol chemisorption is the most attractive due to ease of preparation and broad applicability. Organothiols readily self-assemble on Au surfaces, forming densely packed monolayers (SAMs) with the distal end of the thiol solution-accessible (72-74). DNA can be tethered to Au in a straightforward manner by thiolating one end of the DNA (75-79). However, DNA does not typically form densely packed monolayers, the detailed packing structure of DNA SAMs depending on several factors, including, importantly, oligonucleotide length. Due to the propensity of Lewis bases, especially nitrogen-based moieties, to chemisorb to Au, bases along the DNA backbone also interact with the surface (80). Tarlov and coworkers have developed a unique method to combat multivalent adsorption of thiolated DNA by mixing monolayers of DNA with mercaptohexanol (MCH) (70,80,81). In this process, the DNA-modified substrate is soaked in MCH after formation of the DNA SAM, effectively displacing N-Au bonds, leaving DNA bound only at the S headgroup. In addition, this increases the average distance between adjacent DNA molecules, producing an environment more conducive to physical access of complementary strands for hybridization. Mixed monolayers have also been shown to be stable through sensor regeneration, with no loss of specificity (81).

Planar Au surfaces were produced by vapor deposition onto glass microscope slides. Assembly of thiolated-DNA on Au and hybridization of complementary DNA followed previously reported methods (70,81,82). The DNA sequences used are shown in Table 1.

Table 1. DNA labels and sequences.

<b>17E</b>	5'-CATCTCTTCTCCGAGCCGGTCGAAATAGTGAGT-3'
<b>17DS</b>	5'-ACTCACTATrAGGAAGAGATG-3'
<b>HS-17E-FI</b>	5'-(C <sub>6</sub> Thiol)-TTTTTAAAGAGACATCTCTTCTCCGAGCCGGTCGAAATAGTGAGT-Fluorescein-3'
<b>HS-17E-Dy</b>	5'-(C <sub>6</sub> Thiol)-TTTTTAAAGAGACATCTCTTCTCCGAGCCGGTCGAAATAGTGAGT-Dabcyl-3'
<b>17DS-FI</b>	5'-Fluorescein-ACTCACTATrAGGAAGAGATGTCTCTTT-3'

Immobilization of HS-17E-Dy (or HS-17E-FI) on Au was achieved by soaking piranha-cleaned Au surfaces (*ca.* 0.5 x 0.5 cm<sup>2</sup>) in 1 M potassium phosphate buffer for 90 min. Hybridization was accomplished by soaking in 1 μM 17DS-FI in 50 mM tris acetate buffer (pH=7.2) and 1 M NaCl in a 70 °C water bath for 60 min. The bath was then allowed to cool to room temperature over 60 min, cooled to 4 °C for 30 min, and again allowed to come to room temperature.

Solution assays of DNAzyme were performed with 10 nM HS-17E-Dy and 10 nM 17DS-FI in 50

mM tris acetate buffer (pH=7.2) and 50 mM NaCl. Hybridization was accomplished by heating in a 70°C water bath for 60 min and cooling to room temperature over 60 minutes. The solution was then cooled to 4°C for 30 min, and again allowed to come to room temperature. Fluorescence spectra was recorded using a 0.5 by 0.5 cm<sup>2</sup> quartz cell in a Jobin Yvon Fluoromax-P fluorimeter ( $\lambda_{\text{ex}} = 491 \text{ nm}$  and  $\lambda_{\text{em}} = 500\text{-}575 \text{ nm}$ ). 10  $\mu\text{M}$   $\text{Pb}^{2+}$  was then added, and after five minutes of reaction time, fluorescence spectra again documented.

Prior to using the substrate-immobilized DNAzyme for  $\text{Pb}^{2+}$  sensing, it was soaked in 50 mM tris acetate buffer (pH=7.2) and 50 mM NaCl solution for 5 min in an effort to remove any remaining physisorbed substrate strand and to rinse away any dissociated substrate strand at the lower NaCl concentration. Measurements were made by placing the assembled DNAzyme-MCH SAM in a  $\text{Pb}^{2+}$ -containing solution in 50 mM tris acetate buffer (pH=7.2) and 50 mM NaCl. The DNAzyme surface was allowed to react with the Pb solution for 60 min, after which it was removed and then rinsed with the reaction solution. Fluorescence intensity of the cleaved DNA portion in the solution was determined with  $\lambda_{\text{ex}} = 491 \text{ nm}$  and  $\lambda_{\text{em}} = 518 \text{ nm}$ .

For determination of regeneration, the surface-immobilized DNAzyme was first prepared as described above. After an initial reaction of the sensor with  $\text{Pb}^{2+}$ , the activity was determined by fluorescence measurements. The reacted sensors were subsequently soaked, individually, in Millipore water for 18 hours in closed sample vials. The samples were then rinsed with Millipore water for 5 minutes. Hybridization of 17DS-FI was repeated by soaking the reacted sensors in 50 mM tris acetate buffer at pH=7.2 and 1 M NaCl with 1  $\mu\text{M}$  17DS-FI with the same heating and cooling described above. Non-regenerated control samples were soaked in identical buffer solutions and heating conditions, without 17DS-FI. The controls and regenerated substrates were reacted with 10  $\mu\text{M}$   $\text{Pb}^{2+}$  in 50 mM tris acetate buffer (pH=7.2) and 50 mM NaCl for 60 minutes. The reaction solution was rinsed over the surface of the sensor and fluorescence intensity determined.

Since the DNAzyme used is slightly modified from that used in previous publications (13,15), *i.e.* with addition of a thiol group and linker T's, the DNAzyme activity in solution was first assessed. As seen in Figure 4, when 17DS-FI is hybridized with HS-17E-Dy in solution, fluorescence

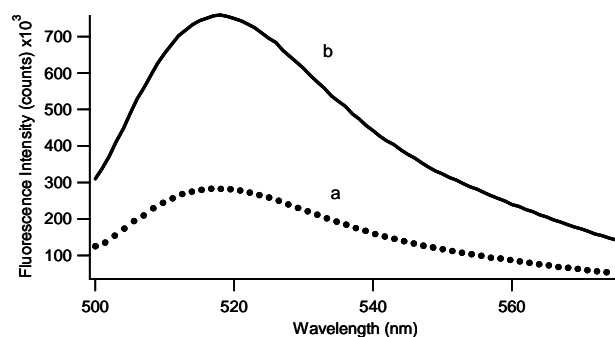


Figure 4: Fluorescence spectra for (a) background and (b) solution after addition of lead.

intensity is relatively low. After addition of 10  $\mu\text{M}$   $\text{Pb}^{2+}$ , fluorescence intensity increases by 269% after only 5 minutes of reaction time, indicating that the thiolated-DNAzyme behaves similarly to previously reported  $\text{Pb}^{2+}$ -specific DNAzymes (13,15). Specifically, the addition of a sulfhydryl headgroup and polyT linker has no adverse effect on Pb-induced cleavage and generation of luminescence.

Figure 5 illustrates the basic immobilization and reaction protocol used throughout this work.

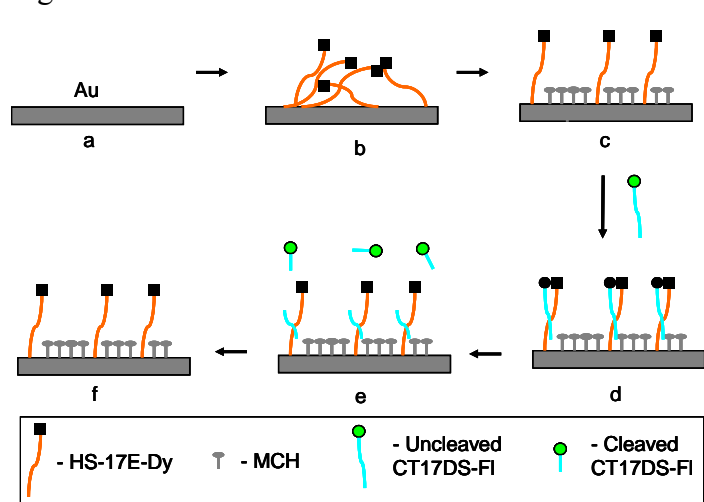


Figure 5: Immobilization and lead reaction schematic.

Thiolated-enzyme strand is immobilized on Au via thiol chemisorption; the surface is back-filled with MCH; and substrate strand is hybridized onto enzyme strand to prepare the DNAzyme surface for  $Pb^{2+}$  detection. Upon reaction with  $Pb^{2+}$ , the fluorophore-containing portion is released into solution where it can subsequently be detected. The goal of this work is to establish the activity and figures of merit for the fluorogenic  $Pb^{2+}$ -DNAzyme reaction, when the DNAzyme is initially immobilized on a planar Au substrate.

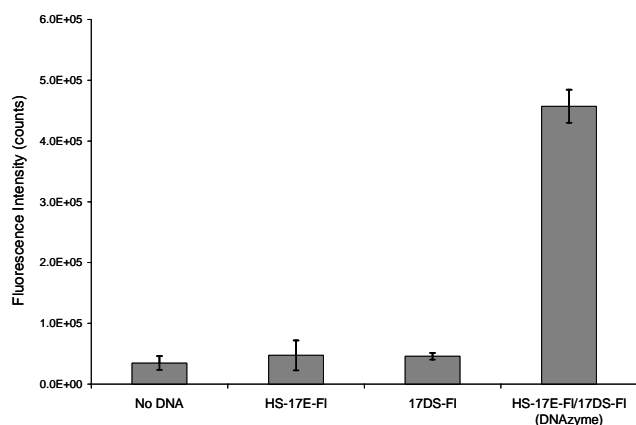


Figure 6: Fluorescence intensities produced from reactions of immobilized DNA on Au surfaces.

Control experiments were carried out that proved that the DNAzyme is actually immobilized, rather than simply physisorbed on the Au surface. These data demonstrate two points: 1) thiolated enzyme strands are not released to a significant extent after chemisorption to Au, and 2) any non-specific adsorption of substrate strands on the Au surface containing MCH is minor. Figure 6 shows the fluorescence intensities from reactions of lead solution with different surfaces. The first three bars show the fluorescence from gold surfaces with no DNA present, with only the enzyme strand present, and with only the substrate strand

present. All show equivalent background fluorescence. The final bar shows the fluorescence resulting from the reaction of lead solution with the enzyme / substrate construct. The relatively high fluorescence intensity ( $457,184 \pm 27,390$ ) for the DNAzyme positive control compared to the negative controls indicates that the sensor is responding to  $Pb^{2+}$  as anticipated. In fact, the increase for the DNAzyme is  $> 700\%$  upon addition of  $10 \mu M Pb^{2+}$ , indicating that  $Pb^{2+}$  specifically cleaves the hybridized substrate DNA, just as it

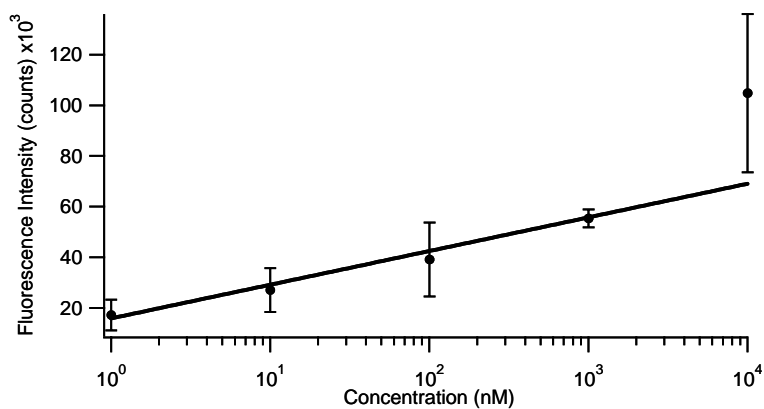


Figure 7: Calibration curve for immobilized DNAzyme on Au surfaces for fluorescence versus lead solution concentration.

does in solution.

A critical figure-of-merit for molecular recognition chemistry to be exploited in a functional sensor is its ability to determine the analyte of interest in a useful concentration range. A calibration curve for  $\text{Pb}^{2+}$  activity on the DNAzyme immobilized sensor is shown in Figure 7. A linear response can be achieved over a wide range,  $10 \mu\text{M} > [\text{Pb}^{2+}] > 1 \text{ nM}$ , though this linearity deviates at higher  $\text{Pb}^{2+}$  concentrations. The error associated with these measurements, as characterized by the  $\pm\sigma$  error bars on the points in Fig. 7, is due partially to variations in the physical dimensions of Au substrates that are linked directly to uncertainties in surface coverage. A major advantage of utilizing a surface-immobilized DNAzyme for analyte recognition is the ability to regenerate the surface, so that the DNAzyme can be reused. To test the possibility of regenerating previously cleaved DNAzyme molecules, an experiment was performed in which DNAzyme was initially reacted with  $\text{Pb}^{2+}$ . Following the  $\text{Pb}^{2+}$  recognition reaction the surface was soaked in deionized  $\text{H}_2\text{O}$  for 18 h to remove the substrate strands (both cleaved and uncleaved). The remaining immobilized enzyme strands were then rehybridized with 17DS-F1,

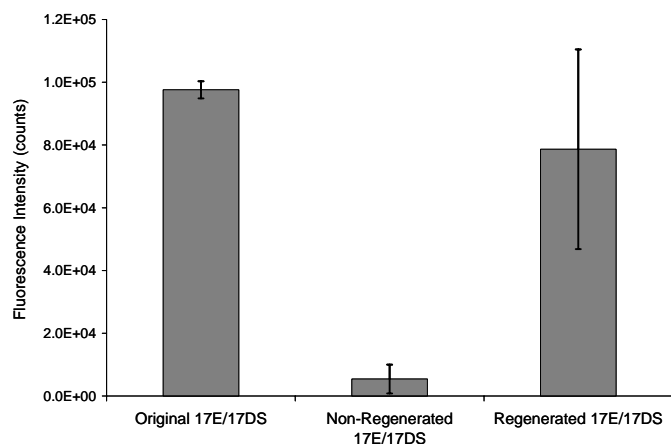


Figure 8: Fluorescence intensities from reactions with lead solutions with immobilized DNAzymes, non-regenerated surfaces, and regenerated surfaces.

and the DNAzyme surface was again reacted with  $10 \mu\text{M} \text{ Pb}^{2+}$ . The regenerated DNAzyme surface elicited a fluorescence intensity 81% of the original upon exposure to  $\text{Pb}^{2+}$ , *viz.* Figure 8. In contrast, exposure of non-regenerated DNAzyme to  $\text{Pb}^{2+}$  produced fluorescence only 6% of the intensity produced by the original reaction, a value comparable to that produced by the negative controls, *cf.* Fig. 6.

**Membrane gold plating and subsequent reactions.** We have demonstrated that DNAzymes retain their activity after immobilization onto gold surfaces. This indicates that incorporation of gold surfaces within sensor designs provides an avenue to bind the thiolated DNAzyme in the path of lead containing solution. Furthermore, the enzyme surface can be regenerated with substrate DNA after a reaction to prepare the sensor for subsequent analyses. We examined the ability to use the molecular gate membrane pores as the sensing surface.

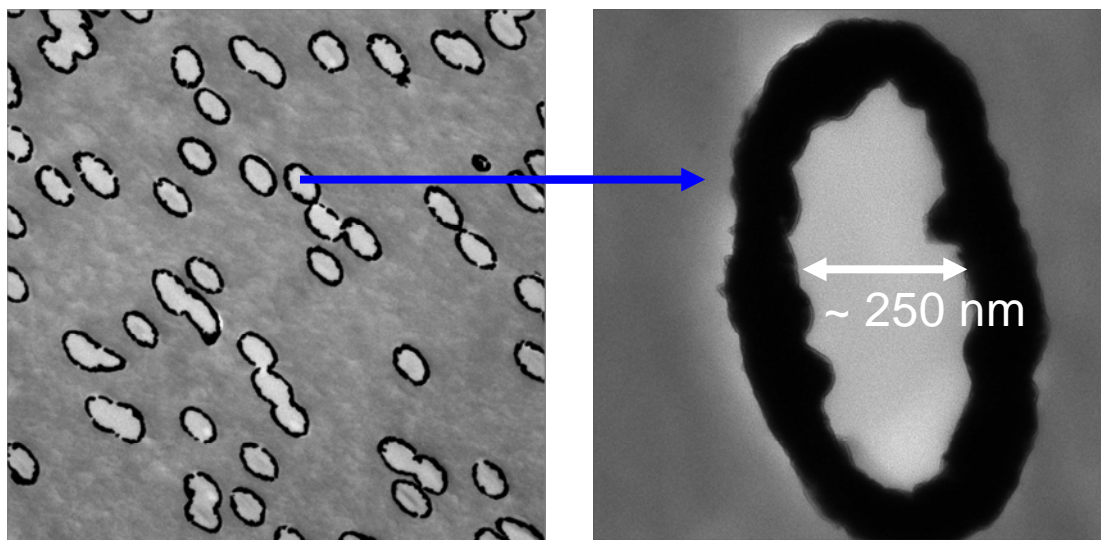


Figure 9: Transmission electron micrograph of the molecular gate membrane after electroless deposition of gold.

Figure 9 shows the micrographs for the molecular gate membrane with pore interiors coated with gold by an electroless deposition process. The dark interior surfaces are the gold layers within the pores. These pores can be used as reaction surfaces for lead detection as the thiolated DNAzyme will react and bind at this point.

Soaking these membranes in a solution of DNAzyme followed by the substrate DNA created active molecular beacons within the pores. Figure 10 shows the fluorescence intensities for a reaction of lead solution with either a DNAzyme on a planar gold coated glass surface or in the membrane pores. We have shown the pores ( $\sim 250\text{nm}$  after electroless deposition of Au) are accessible to the 40-mer DNAzyme chain ( $\sim 12\text{nm}$ ) which is determined by comparing the overall fluorescence intensity of assembled membranes versus planar gold surfaces after complete reaction with  $\text{Pb}^{2+}$ . The membrane creates a fluorescence intensity  $9.2 \pm 3.1$  times higher than that of planar gold (Figure 10) despite the fact that we used identical geometric sizes for glass and membrane. Two variables can contribute to this increased intensity. The first, surface roughness, can constitute up to a two-fold increase while the second, pore accessibility, makes up the remainder of the coverage.

The validity of the Au-coated membranes as usable sensor surfaces has been accomplished and to some extent, optimized. The current range of detection shown possible has an upper limit of  $10 \mu\text{M Pb}^{2+}$ , where fluorescence of  $4.85 \pm 1.15$  times control signal was detected (Figure 11). This upper limit is not due to the DNAzyme sensitivity, but is currently due to precipitation of  $\text{Pb}^{2+}$  at the reaction pH, preventing more concentrated  $\text{Pb}^{2+}$  solutions from being used. The lower limit of detection has been demonstrated as low as  $10 \text{nM Pb}^{2+}$ , where a total of  $2.33 \pm 0.98$  times the control was observed after one hour reaction time (Figure 11).

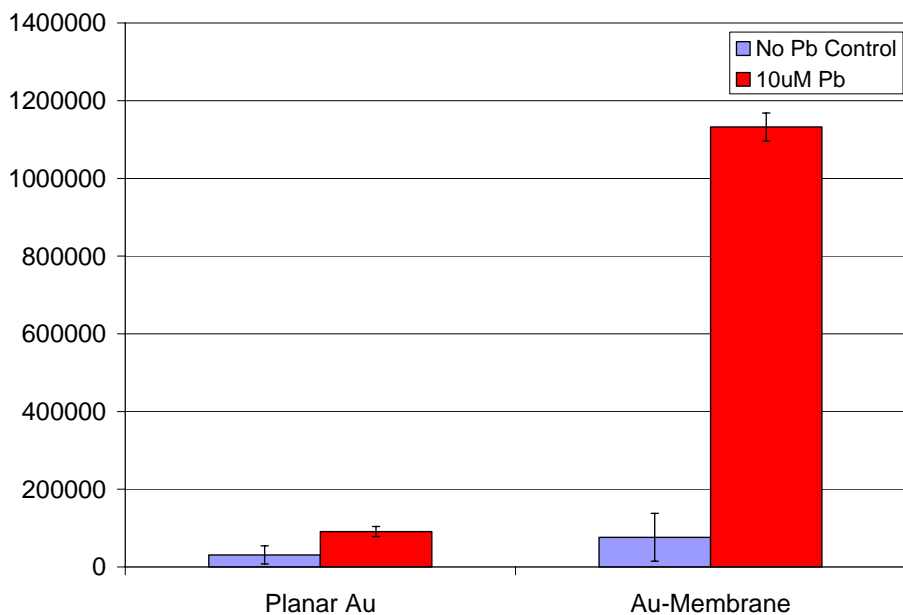


Figure 10: Comparison of total fluorescent intensities for DNAzyme sensors assembled on planar gold-coated glass and gold-coated polycarbonate membranes with identical geometric size after complete reaction with 10  $\mu\text{M}$   $\text{Pb}^{2+}$ . Access to  $\sim 250\text{nm}$  pores through the membrane allows for  $9.2 \pm 3.1$  times higher intensity attributed to the higher surface area.

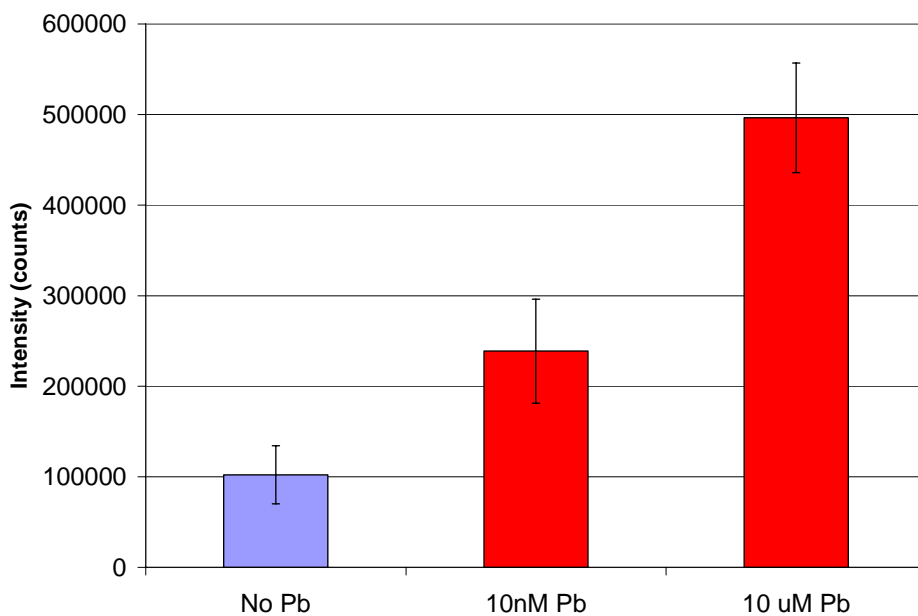
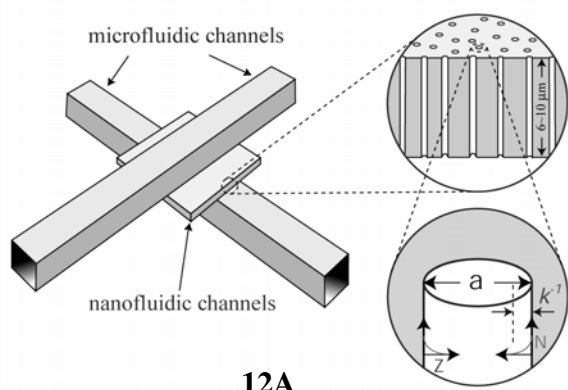
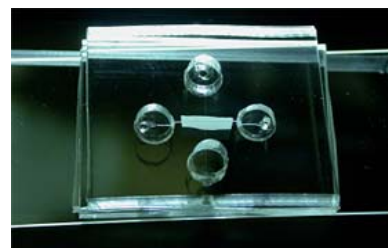


Figure 11: Intensities of fluorescence after reaction with 10 nM and 10  $\mu\text{M}$   $\text{Pb}^{2+}$  for 60 minutes compared to the intensity of the solution without reaction with  $\text{Pb}^{2+}$  after the same time interval. Values of  $2.33 \pm 0.98$  times and  $4.85 \pm 1.15$  times the control were calculated for 10 nM and 10  $\mu\text{M}$   $\text{Pb}^{2+}$ , respectively.

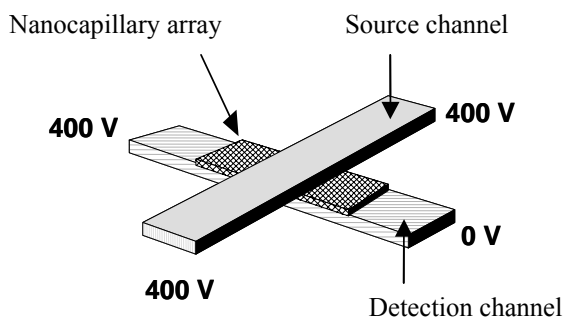
**Chip design.** We designed two types of chips for these experiments. Figure 12 shows the simpler design that contains two channels, a source channel and a detection channel. For this transport device, the general chip design consists of the thin PCTE nanocapillary array layer sandwiched between two crossed PDMS microfluidic channels (Figure 12A). Crossed microfluidic channels were fabricated from poly(dimethylsiloxane) (PDMS) using standard rapid prototyping protocols for PDMS (83). Channels used in this experiment were 100  $\mu\text{m}$  wide, 60  $\mu\text{m}$  deep and 1.4 cm long for the transport devices. A reservoir PDMS layer was sealed on the top of the sandwiched device and fluidic connection to the various channel layers was accomplished by punching small holes through the PDMS channel layers. Figure 12B shows a photograph of the transport device. The small rectangle is the PCTE membrane containing 200-nm diameter cylindrical pores. This device was used for lead calibration and characterization of a complex electroplating sludge waste described later in this report. Figure 12C describes one possible arrangement of applied voltages across the channel arms that force solution to flow from one reservoir to another along the channels, in this case, positively charged species would move from the source channel through the membrane to the detection channel.



12A



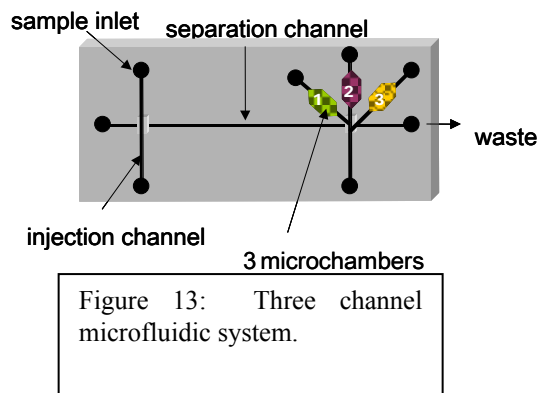
12B



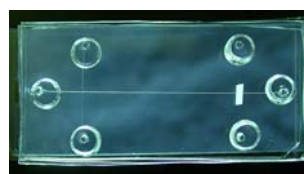
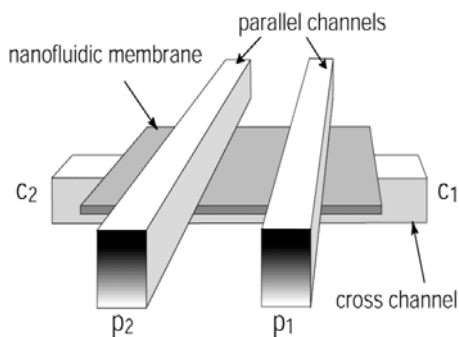
12C

Figure 12: (A) Schematic of two crossed microfluidic channels with a nanocapillary array interconnect. (B) Optical image of the PDMS gated injection and transport device. (C) Electrical bias configuration for electrokinetic injection and electrophoretic transport of  $\text{Pb}^{2+}$ .

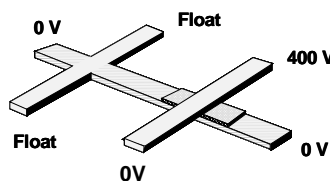
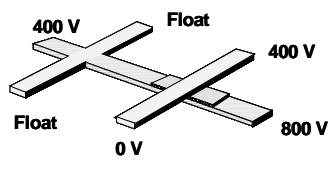
A second design is shown in Figure 13. A three channel design allows more flexibility. The injection channel can be constantly replenished with sample from an environmental source, such as river water. For analysis, voltages are altered to inject a portion of the injection channel volume onto the separation channel. This channel is designed for electrophoretic separation of analytes. When the analyte of interest is at the intersection of the detection channel with the microchambers, voltage switching sends the analyte band into the microchamber of choice where the catalytic DNA is immobilized.



When the analyte of interest is at the intersection of the detection channel with the microchambers, voltage switching sends the analyte band into the microchamber of choice where the catalytic DNA is immobilized. In this configuration, three microchambers are shown, each with its own specific DNAzyme for multianalyte detection. Figure 14 shows the three channel chip. Figure 14A shows a schematic where the channels can be isolated from one another using the molecular gate membrane as well as a photograph of an actual device. Solutions can be moved from one area of the chip to another by proper application of voltages across the reservoir ends as shown in Figure 14B.



14A



14B

Figure 14: Three channel microfluidic sensors.

**Electrophoretic control of solution movement.** Using a two channel sensor (Figure 12B), we demonstrated the movement of  $Pb^{2+}$  from a reservoir, through the source channel, through the molecular gate membrane, and into the detection channel. The injection channel was filled with background electrolyte solution (BGE) and the reservoirs were filled with  $Pb^{2+}$  in BGE. The

detection channel was filled with DNAzyme system (hybridized system with enzyme strand (17E) and a substrate strand (17DS)) in BGE. Microfluidic transport was achieved by applying bias across different reservoir. The electrical bias pathway for the sequences of injection and collection modes for  $Pb^{2+}$  are illustrated in Figure 12C. To inject  $Pb^{2+}$  solution into the detection channel, a positive high voltage were applied to the two reservoirs at the ends of the source channel while grounding the waste reservoir of the detection channel. With 200 nm pore diameter nanocapillary array interconnections, this forward bias condition causes flow from the injection channel through the nanocapillary array to the collection channel. The sequential images in Figure 3 captures injection band at the intersection of the two cross-channels. The fluorescence steadily increases with time as the  $Pb^{2+}$  band moves through the channel.

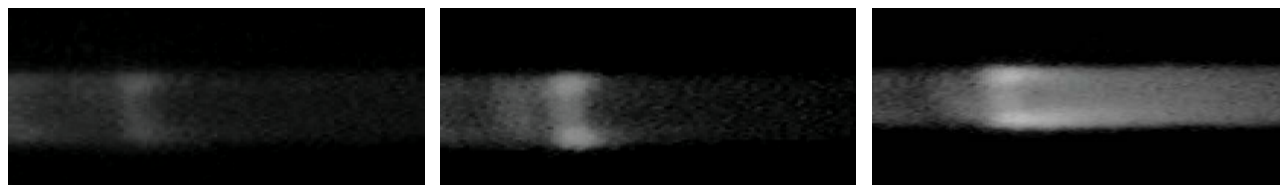


Figure 15. Fluorescence image series for gated injection of  $Pb^{2+}$  band across the array of 200 nm diameter capillaries.

As soon as high bias was applied (the on state),  $Pb^{2+}$  was brought into contact with the DNAzyme in the nanocapillary array and emission occurred since the fluorescently tagged substrate DNA cleaves from the DNAzyme upon contact with  $Pb^{2+}$ . Because only the detection waste reservoir is grounded, flow is directed from both arms of the source channel toward the end of right arm of detection channel. The  $Pb^{2+}$  migration was monitored by fluorescence microscopy performed on an inverted Olympus (Melville, NY) epi-illumination microscope as shown in Figure 16.

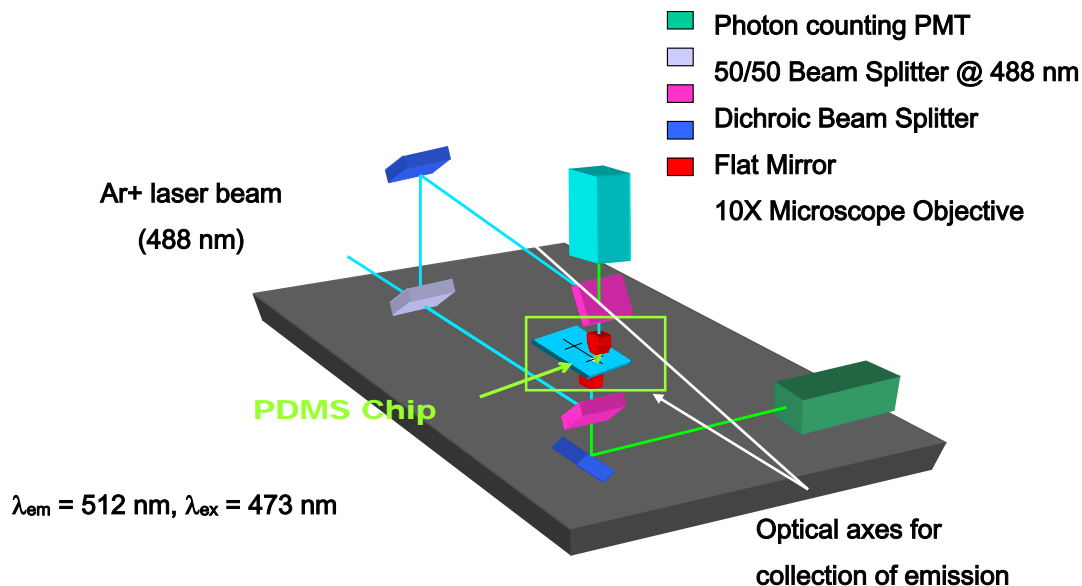


Figure 16: Experimental set up for detection of fluorescent emission from the detection channel. A three channel chip is shown.

Figure 17 shows results from using the three channel chip (Figure 14). With the electrical biases from Fig 14B, we were able to prove controlled movement of solutions along multiple channels. By switching the voltage bias configurations, a versatile fluidic manipulation was demonstrated. The injection and separation channel (Fig. 13) were filled with BGE and the collection channel was filled with 500 nM DNAzyme. After verifying complete filling, one of the reservoirs of the injection channel was replaced with 10  $\mu\text{M}$   $\text{Pb}^{2+}$ . Figure 17A shows a sequence of fluorescence images of electrokinetically injected  $\text{Pb}^{2+}$  forced into the collection (detection) channel containing the DNAzyme. The first picture is the background state where slight fluorescence is observed due to substrate DNA adhesion to the membrane. The second picture shows the migration and injection of the lead solution into the detection channel whereupon the DNAzyme reacts to cleave the substrate DNA and release fluorophores. We note that the negatively charged cleaved DNA moves toward the highest positive bias. The off state shows the eventual clear out of the fluorescent fragments after injection is stopped. The images show the electrophoretic control of  $\text{Pb}^{2+}$  and cleaved DNA through the microchannels via nanocapillary array. These results were obtained using the laser induced fluorescence detection scheme (Figure 16). Future control of the migration and collection of the fluorescent substrate fragments will further enhance our detection limits. If we monitor the fluorescence increase over multiple injections of the lead solution, the trace shown in Figure 17B is obtained. This figure shows three separate injections of lead, indicating very reproducible performance.

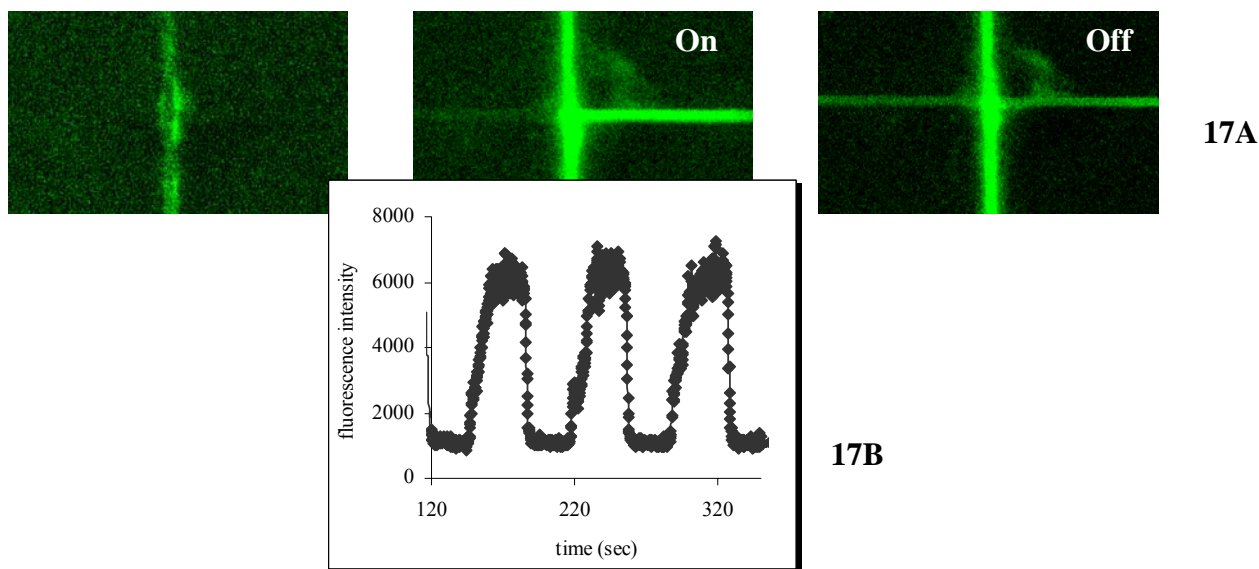


Figure 17: Fluorescent images of lead injections into the collection channel from background to the on (inject) state to the off state (17A). Results from multiple injections show the system reproducibility.

**Calibration Curve with Lead Solution.** Using the two channel system (Figure 12), additional experiments were performed to investigate the reproducibility of low lead concentrations and the quantitative behavior of the chip. Figure 18 (left) shows the reproducibility of transfer

experiments in which 100 nM  $\text{Pb}^{2+}$  is transferred from the source channel to the detection channel across a PCTE molecular gate membrane under the same bias conditions used in Figure 12C. The source channel was filled with 100 nM  $\text{Pb}^{2+}$  in BGE and the detection channel was filled with 500 nM DNAzyme. Fluorescence was detected by laser-induced fluorescence (LIF) excited with 488-nm radiation from an argon ion laser (Fig. 16). Excellent reproducibility was obtained using this low lead concentration. The detection limit was evaluated by repetitive injection of 50 nM  $\text{Pb}^{2+}$  standard solution. From the baseline noise during the off state and the fluorescence intensity of 50 nM  $\text{Pb}^{2+}$  at during the on state, the detection limit (signal-to-noise ratio of 3:1) was determined to be 11 nM (2.2 ppb) which is lower than the 72 nM (15 ppb) action level in drinking water recommended by the U.S. Environmental Protection Agency (84). These results demonstrate that the combination of electrokinetically actuated measurement cycles on a microfluidic device and a  $\text{Pb}^{2+}$ -selective DNAzyme produce a device sensitive enough to monitor lead in drinking water or ground water. A calibration curve (Figure 18 (right)) was constructed by measuring fluorescence intensities using 7 different concentrations  $\text{Pb}^{2+}$  solutions varying in concentration from 100 nM to 200  $\mu\text{M}$ . The plot of fluorescence intensity versus  $[\text{Pb}^{2+}]$  agreed well with the response rate versus  $[\text{Pb}^{2+}]$  curve using a conventional spectrofluorometer (13) suggesting reliable performance of on-chip DNAzyme assays for  $\text{Pb}^{2+}$ .

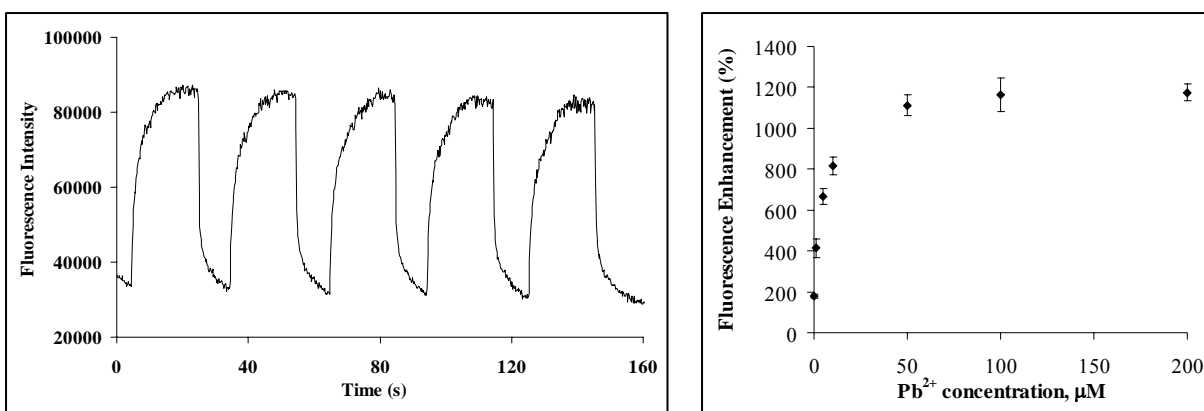
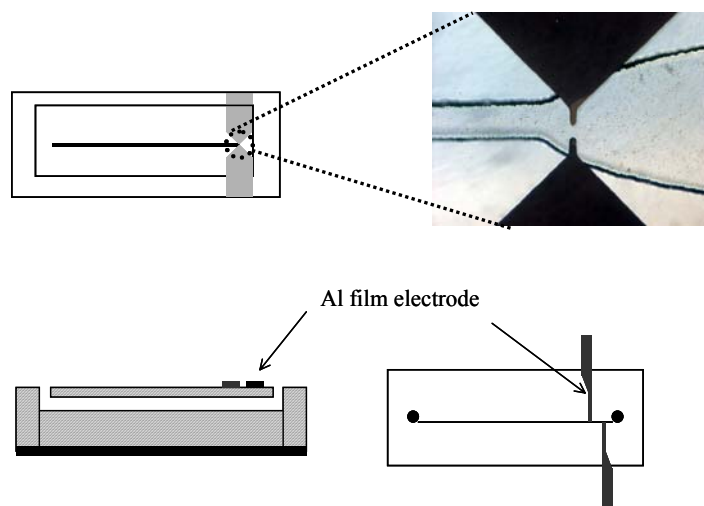


Figure 18: (Left) Migration of a probe across PCTE nano-capillary arrays with 200 nm-diameters connecting to PDMS channels. Fluorescence intensity to monitor the transport of  $\text{Pb}^{2+}$  in Lactate/HEPES BGE, pH7.2. (Right) Calibration curve of the DNAzyme-based  $\text{Pb}^{2+}$  detection system.

**Electrophoretic Cation Separation.** In future generations of these microfluidic devices, the separation channel will be used to isolate the desired analyte band from other analytes and interferents. To this end, we began investigating the use of conductivity detection to prove the metal separation on column. The microfabricated capillary electrophoresis channel is used to

separate  $\text{Pb}^{2+}$  from other common divalent metal ions. The separated  $\text{Pb}^{2+}$  is then selectively brought into contact with the DNAzyme contained in the detection channel via the nanocapillary array. Knowing the velocity of  $\text{Pb}^{2+}$  migration in the separation channel and its arrival at the nanocapillary gate allows timing of the voltage biases to move this  $\text{Pb}^{2+}$  band into the detection channel. Conductivity detection (CD) has been studied to evaluate the migration time of  $\text{Pb}^{2+}$  as well as the separation of alkali, alkaline earth and heavy metal ions in the microchannel. In this study, two different CD methods have been tested as shown in Figure 19; (A) the contact approach, based on electrodes embedded in the chip that are in direct contact with the solution and measuring resistances of the contacting solutions, and (B) capacitively coupled contactless CD, based on placing two planar sensing aluminum film electrodes on the outer side of the  $\sim 50$   $\mu\text{m}$ -thick (PDMS) layer (without contacting the solution) and measuring the impedance of the solution in the separation channel. Preliminary work has shown that the contact approach has the greatest sensitivity to changes in solution conductivity with the sensing electrodes in contact with the separation solution, but presented a significant design problem because the detection circuits must be isolated from the high voltage. In this study, the optimized BGE itself has very high conductance with high concentrations of lactate and HEPES ions and the method sensitivity was considered as significant issue. The end-column detection was adopted to decouple the separation voltage from the electrochemical detector unit. The electrodes were fabricated from sputter coated Au electrodes ( $30 \mu\text{m} \times 50 \mu\text{m}$ ) separated by a gap of  $26 \mu\text{m}$  on a glass aligned PDMS channel. The electrodes were just outside, yet as close as possible to the exit of the separation channel. Figure 19A shows an optical picture of the end of separation channel, illustrating the alignment of the working electrode with the microchannel. Recently, the contactless detection method has been shown to have several advantages over the contact mode, including the absence of problems such as electrode degradation, bubble formation, the effective isolation from high separation voltage, and a simplified construction and work will continue with this method. A commercially available LCR meter was used for the detection of impedance of



the passing solution. An 8-relay system (Chemistry Electronics Shop, UIUC) was used to switch electrical contact between electrode and voltage source (Bertan High Voltage, Hicksville, NY,) at different configurations for microfluidic manipulation. Control of the relay system, LCR meter and data collection were achieved through USB-GPIB interface (Agilent Technologies) with Labview programs and data acquisition cards (National Instruments). Figure 19: Microchip electrophoretic system with conductivity detection. (A) contact gold electrode chip and (B)

contactless aluminum film electrode chip.

Results for the contact electrode approach are shown in Figure 20. The contact electrode approach showed better sensitivity for both conductivity standard solutions and standard lead solutions than the contactless electrode approach. Figure 20 presents the resistance responses for the sputter coated electrode based chip when different standard solutions were injected showing sufficient method sensitivity under optimized detection electronics. These results show that this conductivity measurement approach will work to show the presence of metal ion analyte bands as they pass the electrodes. We can use this approach to optimize our ability to separate metal ions on the separation channel and characterize the migration behavior of analytes on our microfluidic devices.

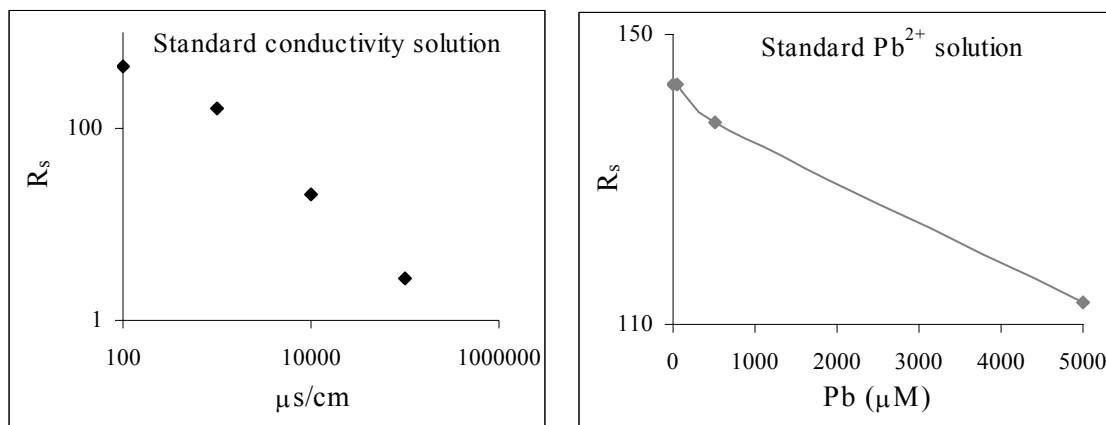


Figure 20: Resistance (conductivity) measurements for different standard conductivity solutions (left) and standard lead concentrations (right) at an operation frequency of 100 kHz and an excitation voltage of 1V.

We have worked to optimize the composition of the background electrolyte (BGE) since its composition will affect separation ability, DNAzyme performance, and detection efficiency. The electrolyte must allow controllable fluidic transfer of lead-containing analyte solution, delivery of the hybridized DNA strands (DNAzyme) and sample to the detection site, while also enabling high efficiency cleavage of the DNA substrate in the presence of  $\text{Pb}^{2+}$ . Because the future goal was to optimize DNAzyme performance while retaining the possibility of separating a metal ion mixture by capillary ion analysis in the microfluidic device, the lactate system by Fritz *et al.* was adopted (85). Using the 12 mM lactate system at pH 4, pH 5 and pH 7,  $\text{Pb}^{2+}$  was separated from other divalent metal ions such as  $\text{Mn}^{2+}$ ,  $\text{Cd}^{2+}$ ,  $\text{Co}^{2+}$ ,  $\text{Ni}^{2+}$ , and  $\text{Cu}^{2+}$  in a laboratory capillary electrophoresis (CE) (P/ACE, Beckman Coulter Inc., Fullerton, CA) system equipped with indirect UV detection as shown in Figure 21A. For the CE study, 8 mM 4-methylbenzylamine was used as a UV reagent, the separation voltage was 30 kV, and a 75  $\mu\text{m}$  ID and 60 cm long capillary was used. Unfortunately, the DNAzyme was not active in the presence of  $\text{Pb}^{2+}$  in these lactate system. In an effort to improve the DNA cleavage reaction performance, 50 mM HEPES with 50 mM NaCl (15) was selected as a potential electrolyte. Addition of 50 mM NaCl was found to play a critical role in stabilizing the substrate and enzyme strand hybridization reaction, resulting in improved sensitivity. But CE separation was not optimal in the HEPES buffer. Finally, the BGE was optimized by a combination of lactate and HEPES at 25 mM with 50 mM NaCl. Under this condition,  $\text{Pb}^{2+}$  was separated from other metal ions on the laboratory CE (Figure 21B) and the DNA cleavage reaction was efficient with

a 700% fluorescence enhancement in the presence of 5  $\mu\text{M}$   $\text{Pb}^{2+}$  (Figure 21C). The use of higher NaCl concentrations was not pursued in order to prevent generation of excess current within the microchannels where Joule heating degrades performance and can eventually cause bubble formation. This lactate/HEPES background electrolyte was used for all experiments with these chips.

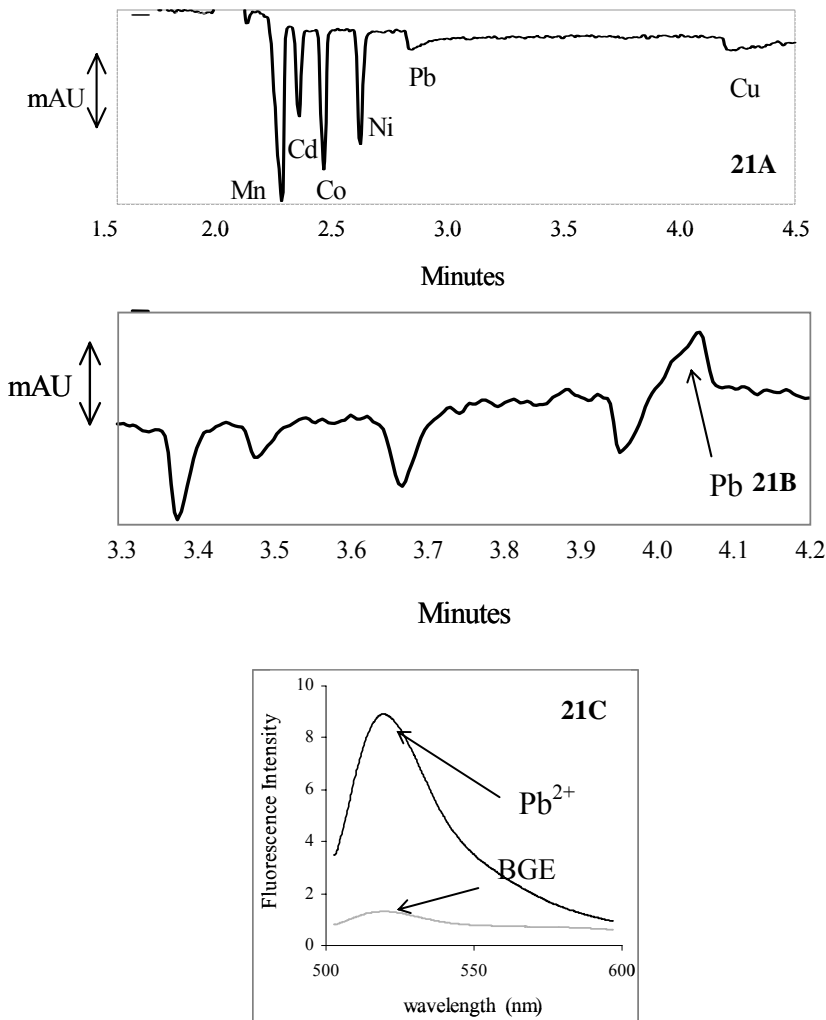


Figure 21: (A) Separation of metal ions using lactate. Carrier electrolyte, 15 mM lactate, 8 mM 4-methylbenzylamine (pH 7.2 adjusted with ammonium hydroxide); Applied separation voltage, 30 kV; capillary, fused-silica, 75  $\mu\text{m}$  ID, 60 cm long. (B) Separation of metal ions using lactate/HEPES. Carrier electrolyte, 25 mM lactate, 25 mM HEPES, 50 mM NaCl, 8 mM 4-methylbenzylamine (pH 7.2 adjusted with ammonium hydroxide); (C) Fluorescence enhancement of the cleaved strand in the presence of  $\text{Pb}^{2+}$  using the lactate/HEPES buffer system.

**Characterization of a Complex Electroplating Sludge Sample.** The electroplating sludge sample was purchased from Resource Technology Corporation (Laramie, WY) and prepared for analysis by USEPA Method 3050B (86). The sludge sample was thoroughly mixed, dried and ground immediately before use. For the digestion, 2.5 mL of concentrated  $\text{HNO}_3$  and 10 mL of concentrated HCl were added to 0.1 g sample and refluxed for 15 min. on a hot plate. The digestate was filtered through filter paper (Whatman No. 41) and the filtrate was collected in a volumetric flask. The filter paper and the residue were both washed with 5 mL of hot HCl. These washings were collected in the same flask. The filter paper and residue were removed and placed back in the reflux beaker. 5 mL of concentrated HCl was added and heated at  $95 \pm 5$   $^\circ\text{C}$  until the filter paper dissolved. The residue was filtered and the filtrate was collected in the same flask. The cover and sides of the reflux beaker were washed with HCl and this solution was also added to the flask. A control sample was prepared by following the entire sample preparation procedure without sludge. The sample was diluted 1:1 using concentrated ammonium hydroxide followed by a 1000-fold dilution with background electrolyte before injecting on the microchip. The lead concentration was determined based on the actual weight

of the dried sludge sample and the final dilution volumes.

The two channel sensor shown in Figure 12 was used in this analysis. Fluorescence signals were detected using the experimental arrangement from Figure 16. To challenge the microfluidic DNAzyme sensor against a complex matrix, it was used for Pb<sup>2+</sup> determination in an electroplating sludge standard reference material. The certified metal contents in this material are shown in Table 2.

Table 2. Certified metal content in electroplating sludge reference material.

element	concn, <sup>a</sup> mg/kg	element	concn, mg/kg	element	concn, mg/kg
Al	692.5 ± 82.5	Ba	173.3 ± 23.5	Ca	562.7 ± 33.0
Cr	79.5 ± 14.1	Cu	63,169.3 ± 2410.0	Fe	2,698.7 ± 814.5
Pb	119,344.0 ± 27453.0	Mg	(80.0)	Mn	17.5 ± 2.1
Hg	(1.4)	Ni	193.6 ± 15.0	Ag	56.4 ± 6.3
Na	(1,576.2)	Zn	182.6 ± 41.0		

<sup>a</sup> Certified and noncertified values (87), values in parentheses are not certified; certified values are determined on a dry weight basis; uncertainties are one standard deviation of the measurement; the uncertainty is obtained from 95% Confidence Intervals.

For this assay, the standard addition method was used to account for matrix effects. In this electroplating sludge sample, it was also observed that copper (at a two-fold higher molar concentration) partially quenched the fluorescence of cleaved DNA, resulting in a systematic error in the quantitative detection of Pb<sup>2+</sup>. Since the solubility constant of Pb(OH)<sub>2</sub> ( $K_{sp} = 2.5 \times 10^{-16}$ ) is three orders of magnitude larger than that of Cu(OH)<sub>2</sub> ( $K_{sp} = 1.6 \times 10^{-19}$ ) (88), it was possible to effect quantitative removal of copper in the sludge digestate as a copper hydroxide precipitate at the electrolyte pH of  $\geq 8$ . We confirmed that copper ion was removed to an undetectable level using the laboratory CE instrument. The lead ion, on the other hand, gave a quantitative recovery at pH 8 and the enzymatic DNA reaction was even more efficient than at pH 7, showing faster reaction times in the microfluidic device. Other metal ions did not interfere in the quantitative determination of lead.

The sludge digestate was prepared as described earlier but four aliquots were spiked with a 50

mM  $\text{Pb}^{2+}$  standard solution to make final added concentrations of 7, 12, 52 and 102  $\mu\text{M}$   $\text{Pb}^{2+}$  producing a five point calibration including the non-spiked sludge sample. The experiments were conducted in the same manner as the calibration using the lead standard in buffer solution. The calibration plot had a correlation coefficient of 0.9993. The concentration of lead in the standard electroplating sludge reference material was determined to be  $[\text{Pb}^{2+}] = 125,200 \pm 3,756$  mg/kg, a value within 4.9% of the certified value of 119,344 mg/kg, indicating the potential for excellent accuracy of this microfluidic / DNAzyme system for  $\text{Pb}^{2+}$  determination.

## Conclusions

As detection limits for  $\text{Pb}^{2+}$  determinations have pushed lower, the toxicity levels have fallen accordingly. Not surprisingly, there is a push for robust, sensitive and selective methods to detect  $\text{Pb}^{2+}$  *in situ*, especially because of the well-known detrimental effects to children. Field-usable methods for  $\text{Pb}^{2+}$  determinations must possess the analytical figures of merit possessed by laboratory methods, and be rugged and regenerable, to enable long-time unattended use. Working toward this goal, this work demonstrates the applicability of a molecular beacon approach based on a Au surface-immobilized DNAzyme that is specifically cleaved in the presence of  $\text{Pb}^{2+}$ . The cleavage reaction frees a fluorophore-containing fragment, effectively removing it from vicinal region near a quencher on the complementary strand. Subsequent fluorescence measurements are related to  $\text{Pb}^{2+}$  concentration in the range  $10 \mu\text{M} > [\text{Pb}^{2+}] > 1 \text{ nM}$ . Additionally, the intact DNAzyme can be regenerated after use for subsequent measurement cycles. The immobilized DNAzyme may also be dried after assembly with little loss of activity indicating that the immobilized system is robust. All these results suggest that the Au surface-based DNAzyme-Pb recognition event leading to molecular beacon operation is suitable for incorporation into a portable  $\text{Pb}^{2+}$  detection device. Furthermore, detection limit estimates indicate that this device, even in its current embryonic state, is capable of lead detection below drinking water action limits, drastically increasing its utility. Since the rate-limiting step is diffusion to and away from the Au surface, incorporation into a flow-through device is expected to dramatically improve reaction times.

Although this DNAzyme is selective for  $\text{Pb}^{2+}$  compared to its response for other divalent cations, higher selectivities are required in some applications. This microfluidic device will be further developed so that the sample analytes are separated using on-chip capillary electrophoresis, allowing user selectable fractions of the sample flow to be introduced to the DNAzyme. For such a system, the selectivity for particular ions would be enhanced, since it will be determined by the product of the ability to separate the desired metal cation from interfering metal ions and the selectivity of the DNAzyme molecular recognition agent itself. The sensitivity and robust nature of the DNAzyme can also be improved by immobilizing the DNA within the molecular gate pores or even within the detection channel, instead of using it in solution. This platform offers the possibility of incorporating multiple sensing locations in one device; thus, by incorporating different metal ion selective DNAzymes into a single microfluidic device, multiple species can be determined simultaneously. Successful creation of this microfluidic device leads to creation of a sensor for any analyte that a DNAzyme can react with. Other research is engaged in finding sequences that are selective for other heavy metal species.

The direction of this research focuses on the desired characteristics in the evolution of sensing

modalities. The trend toward miniaturization continues here and, when combined with lab-on-a-chip technology, the resultant product has improved selectivity and sensitivity. The reaction chemistry for sensing is regenerable and produces no additional toxic waste. Operation can be geared for unattended use during remote and long term monitoring. Highly controlled flows equals a high degree of user-defined and user-selectable operation parameters, i.e., data can be collected in a manner relevant to complement and augment other measurement devices. The greatest benefit, however, may derive from the immediate applicability of this research toward the development of other metal or organic molecule sensors -- with the goal that *a battery of complementary sensors can be arranged for full and simultaneous characterization of all desired chemical content.*

## References

- (1) Air Quality Criteria for Lead; U.S. Environmental Protection Agency, Office of Research and Development: Research Triangle Park, NC, 1986; EPA/600/8-83/028bF.
- (2) Reay, R. J.; Flannery, A. F.; Storment, C. W.; Kounaves, S. P.; Kovacs, G. T. A. *Sens. Actuators, B* **1996**, *34*, 450-455.
- (3) Tsukagoshi, K.; Hashimoto, M.; Nakajima, R.; Arai, A., *Anal. Sci.* **2000**, *16*, 1111-1112.
- (4) Jacobson, S. C.; Moore, A. W.; Ramsey, J. M., *Anal. Chem.*, **1995**, *67*, 2059-2063.
- (5) Kutter, J. P.; Ramsey, R. S.; Jacobson, S. C.; Ramsey, J. M., *J. Microcolumn Sep.*, **1998**, *10*, 313-319.
- (6) Collins, G.; Lu, Q., *Sens. Actuators, B* **2001**, *76*, 244-249.
- (7) Collins, G.; Lu, Q., *Analytica Chimica Acta* **2001**, *436*, 181-189.
- (8) Lu, Q.; Collins, G. *Analyst* **2001**, *126*, 429-432.
- (9) Deng, G.; Collins, G. E. *J. Chromatogr. A* **2003**, *989*, 311-316.
- (10) Tauriainen, S.; Karp, M.; Chang, W.; Virta, M. *Biosensors Bioelectron*, **1998**, *13*, 931-938.
- (11) Deo, S.; Godwin, H. A., *J. Am. Chem. Soc.*, **2000**, *122*, 174-175.
- (12) Babkina, S. S.; Ulakhovich, N. A., *Bioelectrochem.*, **2004**, *63*, 261-265.
- (13) Liu, J.; Lu, Y., *J. Am. Chem. Soc.*, **2003**, *125*, 6642-6643.
- (14) Lu, Y.; Liu, J.; Li, J.; Bruesehoff, P. J.; Pavot, C. M.-B.; Brown, A. K., *Biosensors Bioelectron*, **2003**, *18*, 529-540.
- (15) Li, J., Lu, Y. *J. Am. Chem. Soc.*, **2000**, *122*, 10466-10467.
- (16) Kuo, T.-C.; Cannon, D. M., Jr; Shannon, M. A.; Bohn, P. W.; Sweedler, J. V. *Sens. Actuators, A* **2003**, *102*, 223-233.
- (17) Kuo, T.-C.; Cannon, D. M., Jr; Chen, Y.; Tulock, J. J.; Shannon, M. A.; Sweedler, J. V.; Bohn, P. W., *Anal Chem.*, **2003**, *75*, 1861-1867.
- (18) Cannon, D. M., Jr.; Kuo, T.-C.; Bohn, P. W.; Sweedler, J. V., *Anal Chem.*, **2003**, *75*, 2224-2230.
- (19) Bannon, D. L.; Murashchic, C.; Zapf, C. R.; Farfel, M. R.; Chisolm, J. J., Jr. *Clin. Chem.* **1994**, *40*, 1730-1734.
- (20) Parsons P. J.; Slavin, W. *Spectrochim. Acta Part B*, **1993**, *48*, 925-939.
- (21) Tahan, J. E.; Granadillo, V. A.; Romero R. A., *Anal. Chim. Acta*, **1994**, *295*, 187-197.
- (22) Aggawal, S. K.; Kinter, M.; Herold, D. A., *Clin. Chem.*, **1994**, *40*, 1494-1502.
- (23) Liu, H. W.; Jiang, S. J.; Lie, S. H., *Spectrochim. Acta Part B*, **1999**, *54B*, 1367-1375.
- (24) Bowins, R. J.; Mcnutt, R. H. *J. Anal. At. Spectrom.* **1994**, *9*, 1233.
- (25) Ivanova, E.; Van Mol, W.; Adams, F. *Spectrochim. Acta Part B*, **1998**, *53*, 1041-1048.

- (26) Braco-Sánchez, L. R.; De la Riva, B. S. V.; Costa-Fernández, J. M.; Pereiro, R.; Sanz-Medel, A. *Talanta*, **2001**, *55*, 1071-1078.
- (27) Wang, J.; Hansen, E. H.; Gammelgaard, B. *Talanta*, **2001**, *55*, 117-126.
- (28) Li, J.; Lu, F.; Umemmura, T.; Tsunoda, K. *Anal. Chim. Acta.* **2000**, *419*, 65-72.
- (29) Luconi, M.; Silva, M. F.; Olsina, R. A.; Fernandez, L. *Talanta*, **2001**, *54*, 45-52.
- (30) Schneider, J. A.; Hornig, J. F. *Analyst*, **1993**, *118*, 933-936.
- (31) Peper, S.; Qin, Y.; Almond, P.; Mckee, M.; Telting-Diaz, M.; Albrecht-Schmitt, T.; Bakker, E. *Anal. Chem*, **2003**, *75*, 2131-2139.
- (32) Yang, X.; Hibbert, D. B.; Alexander, P.W. *Anal. Chim. Acta.* **1998**, *372*, 387-398.
- (33) Masawat, P.; Liawruangrath, S.; Slater, J. M. *Sens. Actuators B* **2003**, *91*, 52-59.
- (34) Mourzina, Y. G.; Schubert, J.; Zander, W.; Legin, A.; Vlasov, Y. G.; Lüth, H.; Schöning, M. J., *Electrochimica Acta*, **2001**, *47*, 251-258.
- (35) Ding, X.; Mou, S.; Lie, K.; Yan, Y. *J. Chromatogr. A* **2000**, *883*, 127-136.
- (36) Lu, H.; Mou, S.; Riviello, J. M., *J. Chromatogr. A* **1999**, *857*, 343-349.
- (37) Chen, Z.; Naidu, R. *J. Chromatogr. A* **2002**, *996*, 245-251.
- (38) Breaker, R. R.; Joyce, G. F. *Chem. Biol.* **1994**, *1*, 223-229.
- (39) Breaker, R. R. *Nat. Biotechnol.* **1997**, *15*, 427-431.
- (40) Parsons, P. J.; Slavin, W. *Spectrochim. Acta, Part B* **1993**, *488*, 925-939.
- (41) Jagner, D.; Renman, L.; Wang, Y. *Electroanalysis* **1994**, *6*, 285-291.
- (42) Tsien, R. Y. *Fluorescent and photochemical probes of dynamic biochemical signals inside living cells*; Czarnik, A. W., Ed.; American Chemical Society: Washington, DC, **1993**; 538, 130-146.
- (43) Czarnik, A. W. *Chem. Biol.* **1995**, *2*, 423-428.
- (44) Oehme, I.; Wolfbeis, O. S. *Mikrochim. Acta* **1997**, *126*, 177-192.
- (45) Potyrailo, R. A.; Conrad, R. C.; Ellington, A. D.; Hieftje, G. M. *Analyt. Chem.* **1998**, *70*, 3419-3425.
- (46) Jhaveri, S. D.; Kirby, R.; Conrad, R.; Maglott, E. J.; Bowser, M.; Kennedy, R. T.; Glick, G.; Ellington, A. D. *J. Am. Chem. Soc.* **2000**, *122*, 2469-2473.
- (47) Robertson, M. P.; Ellington, A. D. *Nat. Biotechnol.* **1999**, *17*, 62-66.
- (48) Koizumi, M.; Kerr, J. N. Q.; Soukup, G. A.; Breaker, R. R. *Nucleic Acids Symp. Ser.* **1999**, *42*, 275-276.
- (49) Pan, T.; Uhlenbeck, O. C. *Nature* **1992**, *358*, 560-563.
- (50) Cuenoud, B.; Szostak, J. W. *Nature* **1995**, *375*, 611-614.
- (51) Carmi, N.; Shultz, L. A.; Breaker, R. R. *Chem. Biol.* **1996**, *3*, 1039-1046.
- (52) Li, J.; Zheng, W.; Kwon, A. H.; Lu, Y. *Nucleic Acids Res.* **2000**, *28*, 481-488.
- (53) Santoro, S. W.; Joyce, G. F.; Sakhivel, K.; Gramatikova, S.; Barbas, C. F., III *J. Am. Chem. Soc.* **2000**, *122*, 2433-2439.
- (54) Terry, S. C.; Jermann, J. H.; Angell, J. B. *IEEE Trans. Electron Devices* **1979**, *ED-26*, 1880-1886.
- (55) Christel, L. A.; Petersen, K.; McMillan, W.; Kovacs, G. T. A. *Transducer Res. Found.* **1998**, 363-366.
- (56) Harrison, D. J.; Fluri, K.; Seiler, K.; Fan, Z.; Effenhauser, C. S.; Manz, A. *Science* **1993**, *261*, 895-897.
- (57) Jacobson, S. C.; Hergenroder, R.; Koutny, L. B.; Warmack, R. J.; Ramsey, J. M. *Analyt. Chem.* **1994**, *66*, 1107-1113.
- (58) Woolley, A. T.; Mathies, R. A. *Proc. Natl. Acad. Sci. U. S. A.* **1994**, *91*, 11348-11352.

- (59) Ruano, J. M.; Ortega, D.; Bonar, J. R.; McLaughlin, A. J.; Jubber, M. G.; Cooper, J. M.; Aitchison, J. S. *Microelec. Eng.* **1999**, *46*, 419-422.
- (60) Backhouse, C.; Caamano, M.; Oaks, F.; Nordman, E.; Carrillo, A.; Johnson, B.; Bay, S. *Electrophoresis* **2000**, *21*, 150-156.
- (61) Folch, A.; Ayon, A.; Hurtado, O.; Schmidt, M. A.; Toner, M. J. *Biomech. Eng.* **1999**, *121*, 28-34.
- (62) McDonald, J. C.; Duffy, D. C.; Chio, D. T.; Wu, H.; Schueller, O. J. A.; Whitesides, G. M. *Electrophoresis* **2000**, *21*, 27-40.
- (63) Koch, M.; Schabmueller, C. G. S.; Evans, A. G. R.; Brunnschweiler, A. *Sensors & Actuators A* **1999**, *74*, 207-210.
- (64) Kricka, L. J. *Nature Biotech.* **1998**, *16*, 513-514.
- (65) Saksena, S.; Zydney, A. L. *J. Membr. Sci.* **1995**, *105*, 203-215.
- (66) Basu, S.; Sharma, M. M. *J. Membr. Sci.* **1997**, *124*, 77-91.
- (67) Kim, K. J.; Stevens, P. V. *J. Membr. Sci.* **1997**, *123*, 303-314.
- (68) Kemery, P. J.; Steehler, J. K.; Bohn, P. W. *Langmuir* **1998**, *14*, 2884-2889.
- (69) Steehler, J. K.; Kemery, P. J.; Bohn, P. W. *J. Membr. Sci.* **1998**, *139*, 243-257.
- (70) Levicky, R.; Herne, T. M.; Tarlov, M. J.; Satija, S. K. *J. Am. Chem. Soc.* **1998**, *120*, 9787-9792.
- (71) Ramachandran, A.; Flinchbaugh, J.; Ayoubi, P.; Olah, G. A.; Malayer, J. R. *Biosens. Bioelectron.* **2004**, *19*, 727-736.
- (72) Porter, M. D.; Bright, T. B.; Allara, D. L.; Chidsey, C. E. D. *J. Am. Chem. Soc.* **1987**, *109*, 3559-3568.
- (73) Nuzzo, R. G.; Allara, D. L. *J. Am. Chem. Soc.* **1983**, *105*, 4481-4483.
- (74) Nuzzo, R. G.; Fusco, F. A.; Allara, D. L. *J. Am. Chem. Soc.* **1987**, *109*, 2358-2368.
- (75) Kelley, S. O.; Barton, J. K.; Jackson, N. M.; McPherson, L. D.; Potter, A. B.; Spain, E. M.; Allen, M. J.; Hill, M. G. *Langmuir* **1998**, *14*, 6781-6784.
- (76) Hegner, M.; Wagner, P.; Semenza, G. *FEBS Lett.* **1993**, *336*, 452-456.
- (77) Du, H.; Disney, M. D.; Miller, B. L.; Krauss, T. D. *J. Am. Chem. Soc.* **2003**, *125*, 4012-4013.
- (78) Nakamura, F.; Ito, E.; Sakao, Y.; Ueno, N.; Gatuna, I. N.; Ohuchi, F. S.; Hara, M. *Nano Lett* **2003**, *3*, 1083-1086.
- (79) Marie, R.; Jensenius, H.; Thaysen, J.; Christensen, C. B.; Boisen, A. *Ultramicroscopy* **2002**, *91*, 29-36.
- (80) Petrovykh, D. Y.; Kimura-Suda, H.; Whitman, L. J.; Tarlov, M. J. *J. Am. Chem. Soc.* **2003**, *125*, 5219-5226.
- (81) Herne, T. M.; Tarlov, M. J. *J. Am. Chem. Soc.* **1997**, *119*, 8916-8920.
- (82) Aqua, T.; Naaman, R.; Daube, S. S. *Langmuir* **2003**, *19*, 10573-10580.
- (83) Duffy, D.C.; McDonald, J.C.; Chueller, O.J.A.; Whitesides, G.M. *Anal. Chem.* **1998**, *70*, 4974-4984.
- (84) Lead and Copper Rule Minor Revision; EPA 815-F-899-010; Environmental Protection Agency, 1999.
- (85) Shi, Y.; Fritz, J. S. *J. Chromatogr.* **1993**, *640*, 473-479.
- (86) Method 3050B; *Acid Digestion of Sediments, Sludges and Soils*; Environmental Protection Agency, 1996; available at <http://www.epa.gov/sw-846/pdfs/3050b.pdf>.
- (87) Certificate of Analysis; CRM 010-100 Electroplating Sludge No. 2; Resource Technology Corp., Laramie, WY, 2003.

- (88) Skoog, D. A.; West, D. M. *Analytical Chemistry*, 3rd ed.; Holt, Rinehart and Winston Press, New York, 1979.

## Appendix

Attached below are the two peer-review journal articles resulting from this project. Paper 1 has been accepted and published in *Analytical Chemistry*. Paper 2 has been reviewed and revised and is in press at *Environmental Science and Technology*.

# Immobilization of a Catalytic DNA Molecular Beacon on Au for Pb(II) Detection

*Carla B. Swearingen<sup>†</sup>, Daryl P. Wernette<sup>†</sup>, Donald M. Cropek<sup>‡</sup>, Yi Lu<sup>†\*</sup>, Jonathan V.  
Sweedler<sup>†\*</sup>, and Paul W. Bohn<sup>†\*</sup>*

<sup>†</sup>Beckman Institute for Advanced Science and Technology and Department of Chemistry  
University of Illinois at Urbana-Champaign  
405 N. Mathews Ave.  
Urbana, IL 61801

<sup>‡</sup>Construction Engineering Research Lab  
Interstate Research Park  
2902 Newmark Drive  
Champaign, IL 61822

\*Authors to whom correspondence should be addressed. [yi-lu@uiuc.edu](mailto:yi-lu@uiuc.edu), [jweedle@uiuc.edu](mailto:jweedle@uiuc.edu),  
[p-bohn@uiuc.edu](mailto:p-bohn@uiuc.edu)

## ABSTRACT

A Pb(II)-specific DNAzyme fluorescent sensor has been modified with a thiol moiety in order to immobilize it on a Au surface. Self-assembly of the DNAzyme is accomplished by first adsorbing the single thiolated-enzyme strand (HS-17E-Dy) followed by adsorption of mercaptohexanol (MCH), which serves to displace any Au-N interactions and ensure that DNA is bound only through the S-headgroup. The pre-formed self-assembled monolayer (SAM) is then hybridized with the complementary fluorophore-containing substrate strand (17DS-FI). Upon reaction with Pb(II), the substrate strand is cleaved, releasing a fluorescent fragment for detection. Fluorescence intensity may be correlated with original Pb(II) concentration, and a linear calibration was obtained over nearly four decades:  $10 \mu\text{M} \geq [\text{Pb(II)}] \geq 1 \text{ nM}$ . The immobilized DNAzyme is a robust system; it may be regenerated after cleavage, allowing multiple sensing cycles. In addition, drying of fully assembled DNAzyme before reaction with Pb(II) does not significantly affect analytical performance. These results demonstrate that, in comparison with solution-based schemes, immobilization of the DNAzyme sensor onto a Au surface lowers the detection limit (from 10 nM to 1 nM), maintains activity and specificity, allows sensor regeneration and long-term storage. Realization of Pb(II) detection through an immobilized DNAzyme is the first important step toward creation of a stand-alone, portable Pb(II) detection device such as those immobilizing DNAzyme recognition motifs in the nanofluidic pores of a microfluidic-nanofluidic hybrid multilayer device.

Lead has historically been, and remains today, a persistent contaminant in the environment. Environmentally available Pb may originate from lead-based paints, soil and dust generated from gasoline and industrial pursuits, and water from pipes with lead-containing connectors or joints.<sup>1</sup> Regulatory improvements have been made, with bans on Pb additives in paints and reduction of Pb(C<sub>2</sub>H<sub>5</sub>)<sub>4</sub> levels in gasoline both occurring in the 1970's. However, because Pb is not biodegradable, it is still present in the environment today. Compounding the problem is the reality that lead use remains legal in many military and industrial settings.

Lead is particularly harmful to children because of their small size and developing bodies. Although known to affect every system, Pb has uniquely deleterious effects on the brain and central nervous system. At high blood levels (> 18  $\mu$ M), coma and death can occur.<sup>1</sup> While incidence of Pb poisoning at this level is rare, a worrisome percentage of school-aged children still have Pb levels in blood that are considered harmful. Indeed, the blood Pb level considered harmful has itself fallen dramatically over the past four decades. A level above 3  $\mu$ M was considered toxic in the 1960's. However, by the 1990's, blood concentrations as low as 500 nM had been associated with decreased intelligence, behavioral problems, and impaired growth.<sup>1</sup> Given the environmental availability of Pb and the dire consequences of accidental exposure, especially on the young, it is not surprising that a push is being made to develop sensitive and robust analytical approaches for sensing of Pb in the field.

The most commonly used detection techniques for laboratory-scale Pb determinations have been

atomic absorption spectroscopy and ICP, due mainly to their high sensitivity for Pb and relative simplicity.<sup>2-6</sup> Analytical advancements have provided a detection limit of approximately 1 nM.<sup>7,8</sup> Electrochemical methods have better sensitivity and correspondingly lower detection limits, though interference from a wide range of ions can compromise the selectivity.<sup>9-12</sup> Colorimetric tests for Pb(II) based on sulfide or rhodizonate have been widely used for decades due to their portability and cost-effectiveness.<sup>13,14</sup> Nanoparticle-based sensors are also being developed for Pb detection providing additional colorimetric methods with detection limits of ~100 nM.<sup>15,16</sup> New optical sensors have been developed and exhibit high sensitivity but are currently expensive to produce.<sup>17-20</sup> It would be advantageous to develop a sensor that combines the desirable properties of these sensors; that is portable and that is capable of detecting Pb with both high sensitivity and high selectivity at reasonable cost.

*In-vitro* selection is a powerful technique that has been used to isolate deoxyribozymes (DNAzymes) that are cleaved by a variety of analytes, including metal ions.<sup>21-23</sup> Specifically, a DNAzyme that is cleaved selectively by Pb(II) has been developed in our laboratories.<sup>24</sup> Briefly, the *in vitro* selection process involves using a large random sequence pool of DNA (~10<sup>14</sup> sequences), with each sequence containing a single ribonucleic adenosine (rA) base. The random sequence pool of modified DNAzyme is immobilized on a column, then reacted with Pb(II)-containing eluent. The DNAzyme is cleaved upon exposure to Pb(II) at the rA base, because rA is susceptible to hydrolytic cleavage. The fragmented DNAzyme is eluted after cleavage in quantities determined by the efficiency of the Pb(II)-induced

cleavage reaction for each specific sequence. The most abundant fragments are amplified with PCR, reconstructed to contain rA, and the corresponding sequences are reapplied to the column, followed by another exposure to Pb(II), but under more stringent conditions. Specificity can be further increased by incorporating a negative selection criterion in which DNAzymes that are reactive with analytes other than Pb(II) are eliminated, until only a small number of reactive sequences remain.<sup>25</sup> The process is repeated many times, until the single sequence which is most efficient and selective for recognizing Pb(II) is identified. At this point, the DNAzymes are sequenced. This DNA sequence is strategically divided to create an enzyme strand that contains the random base sequence and a complementary substrate strand that contains the rA base and cleaves in the presence of Pb(II).

In order to create an effective sensor, detection of small amounts of the DNAzyme-Pb(II) reaction product must be possible. To this end, a molecular beacon strategy is implemented by fluorescence labeling of the original Pb(II)-specific DNAzyme.<sup>26</sup> In this case, the substrate strand (17DS) is labeled with a fluorophore at the 5' end, while the enzyme strand (17E) is labeled with a corresponding quencher at the 3' end. When the strands are hybridized, fluorescence is effectively quenched, and little signal is observed. The principal background fluorescence arises due to incomplete hybridization. Upon reaction with Pb(II), the substrate strand is cleaved, releasing the fluorescent portion for detection. Solution-based operation elicits a linear working curve in the range  $4 \mu\text{M} \geq [\text{Pb(II)}] \geq 10 \text{ nM}$ , indicating a sensitivity that rivals that of atomic absorption.<sup>26</sup> In addition, selectivity was greatly enhanced over other divalent metal ions with several thousand-fold selectivity over Mn(II), Ni(II), Cd(II), Cu(II), Mg(II), and

Ca(II), and ~ 80-fold selectivity over the next best competitor Co(II).

Until now the Pb(II)-specific DNAzyme sensor has been limited to bulk solution reactions. There are two inherent advantages associated with moving to a surface-immobilized sensor. First, since hybridization of enzyme and substrate strands is never complete, background fluorescence is observed, even in the absence of a specific cleavage reaction. Because noise in the background fluorescence is a fundamental limitation when working at low analyte concentrations, efforts to reduce the background can produce lower limits of detection. Immobilization of DNAzymes on a surface can overcome limited hybridization efficiency making it feasible to wash away un-hybridized fluorescent substrate DNA, thus reducing the background fluorescence, a task not easily achievable when DNAzymes are in bulk solution. Second, the surface-immobilized DNAzyme may be regenerated and used multiple times, a possibility that is not straightforward in solution-based sensors. Hybridization of surface-bound DNA has been shown to be reversible, suggesting the possibility of reusing the surface for successive measurements.<sup>27</sup> For example, Ramachandran *et al.* produced a surface-immobilized DNA molecular beacon that exhibited 75 % of the original signal intensity after one regeneration.<sup>28</sup>

Despite the above benefits, transforming DNAzyme sensors from bulk solution to planar surfaces is not trivial, because surface interactions may interfere with the DNAzymes' activity. Therefore biotin-avidin has been used for immobilization of DNAzyme on planar gold surfaces to prevent direct interaction between the DNAzyme and the gold surface.<sup>30</sup> Detection methods used for hybridization and activity in this scheme are based on surface plasmon resonance. While DNAzyme does retain its activity using

this method, it was desirable to find a simpler and less expensive way to immobilize the DNAzyme as well as a more sensitive method of detection, such as fluorescence.

Though many strategies for immobilization exist, exploiting Au-thiol chemisorption is attractive due to ease of preparation and broad applicability. Thiol-gold chemistry for DNAzyme immobilization has been demonstrated for Au nanoparticle functionalization,<sup>15,16,31,32</sup> but the different surface termination chemistry and the drastically different diffusion properties of planar surfaces mean that utilizing Au-thiol chemistry for immobilization of DNAzyme on planar surfaces is a non-trivial undertaking.

Organothiols readily self-assemble on Au surfaces, forming densely packed monolayers (SAMs) with the distal end of the thiol solution-accessible.<sup>33-35</sup> DNA can be tethered to Au in a straightforward manner by thiolating one end of the DNA<sup>36-40</sup>. However, DNA does not typically form densely packed monolayers, the detailed packing structure of DNA SAMs depending on several factors, including, importantly, oligonucleotide length. Due to the propensity of Lewis bases, especially nitrogen-based moieties, to chemisorb to Au, bases along the DNA backbone also interact with the surface.<sup>41</sup> Tarlov and coworkers have developed a unique method to combat multivalent adsorption of thiolated DNA by mixing monolayers of DNA with mercaptohexanol (MCH).<sup>27, 42, 43</sup> In this process, the DNA-modified substrate is soaked in MCH after formation of the DNA SAM, effectively displacing N-Au bonds, leaving DNA bound only at the S headgroup. In addition, this increases the average distance between adjacent DNA molecules, producing an environment more conducive to physical access of complementary strands for hybridization. Mixed monolayers have also been shown to be stable through sensor regeneration,

with no loss of specificity.<sup>42</sup>

In the present work, MCH-DNA mixed monolayers are utilized to immobilize the DNAzyme on a Au surface with the goal of creating a surface-based Pb(II) sensor. Conditions for optimum surface immobilization and hybridization are defined, and the resulting structures are characterized with respect to their ability to detect Pb(II) sensitively and selectively. Sensor regeneration is also explored.

## EXPERIMENTAL SECTION

### Oligonucleotide sequences

DNA enzyme strand, 17E, with modifications was purchased from Integrated DNA Technologies (IDT) or from Trilink Bio Technologies, Inc., while the DNA/RNA chimeric substrate strand, 17DS, with modifications was purchased from IDT. All oligonucleotides and abbreviations are shown in Table 1. All reagents were purchased from Aldrich, Inc., and were used without additional purification, with the exception of buffer solutions, which were chelated for divalent metal ions using Chelex 100 beads.

### Planar Au surfaces

Planar Au surfaces were produced by vapor deposition onto glass microscope slides. Glass microscope slides were first cleaned in piranha solution (70% H<sub>2</sub>SO<sub>4</sub>, 30% H<sub>2</sub>O<sub>2</sub>) for 30 min followed by thorough rinsing with deionized (18 MΩ cm) water. (*CAUTION: Piranha is a vigorous oxidant and should be used with extreme caution!*) After cleaning, the glass slides were rinsed with isopropyl alcohol

and dried with a dry N<sub>2</sub> stream. Prior to Au film deposition, Cr was deposited as an adhesion layer at a rate of 0.1 Å/s to a final thickness of 50 Å. Au was then deposited at a rate of 1 Å/s to a final thickness of 500 Å. Freshly prepared Au films were stored in a dry N<sub>2</sub> atmosphere until ready for use. Before use, Au surfaces were cleaned with piranha solution for 20 min and rinsed with deionized water for 5 min.

### **Assembly of DNA SAMs on Au**

Assembly of thiolated-DNA on Au and hybridization of complementary DNA followed previously reported methods.<sup>27, 42, 44</sup> Immobilization of HS-17E-Dy (or HS-17E-FI) on Au was achieved by soaking piranha-cleaned Au surfaces (*ca.* 0.5 x 0.5 cm<sup>2</sup>) in a solution comprised of 1 M potassium phosphate buffer (pH = 6.9), 100 μM tris(2-chloroethyl) phosphate (TCEP), and 1 μM HS-17E-Dy (or HS-17E-FI) for 90 min. TCEP was added in order to reduce disulfide bonds or oxidized thiols that may have formed.<sup>44</sup> Surfaces were then thoroughly rinsed in deionized water and immediately soaked in 1 mM mercaptohexanol for 5 min. Subsequently, surfaces were thoroughly rinsed in 50 mM tris acetate buffer (pH=7.2) and 1 M NaCl. Hybridization was accomplished by soaking in 1 μM 17DS-FI in 50 mM tris acetate buffer (pH=7.2) and 1 M NaCl in a 70°C water bath for 60 min. The bath was then allowed to cool to room temperature over 60 min, cooled to 4°C for 30 min, and again allowed to come to room temperature.

### **Detection of Pb(II) by DNAzyme in solution**

Solution assays of DNAzyme were performed with 10 nM HS-17E-Dy and 10 nM 17DS-FI in 50 mM tris acetate buffer (pH=7.2) and 50 mM NaCl. 100 μM TCEP was also added. Hybridization was

accomplished by heating in a 70°C water bath for 60 min and cooling to room temperature over 60 minutes. The solution was then cooled to 4°C for 30 min, and again allowed to come to room temperature. Fluorescence spectra was recorded using a 0.5 by 0.5 cm<sup>2</sup> quartz cell in a Jobin Yvon Fluoromax-P fluorimeter ( $\lambda_{\text{ex}} = 491 \text{ nm}$  and  $\lambda_{\text{em}} = 500\text{-}575 \text{ nm}$ ). 10  $\mu\text{M}$  Pb(II) was then added and, after 5 min reaction time, fluorescence spectra again documented.

### **Detection of Pb(II) by immobilized DNAzyme**

Prior to using the substrate-immobilized DNAzyme for Pb sensing, it was soaked in 50 mM tris acetate buffer (pH=7.2) and 50 mM NaCl solution for 5 min in an effort to remove any remaining physisorbed substrate strand, which was minimized by MCH-passivation, and to rinse away any dissociated substrate strand at the lower NaCl concentration. Measurements were made by placing the assembled DNAzyme-MCH SAM in a Pb(II)-containing solution in 50 mM tris acetate buffer (pH=7.2) and 50 mM NaCl. The DNAzyme surface was allowed to react with the Pb solution for 60 min, after which it was removed and then rinsed with the reaction solution. Single wavelength fluorescence intensity of the cleaved DNA portion in the solution was determined with  $\lambda_{\text{ex}} = 491 \text{ nm}$  and  $\lambda_{\text{em}} = 518 \text{ nm}$ . Since no fluorescence peak shift nor shape change was observed under varying experimental conditions, the

measurement of peak integrated areas and peak maxima produced similar values (within 5 %). Thus, fluorescence peak intensities have been used for simplicity and because they allow real-time monitoring and rapid measurements during kinetic experiments.

### **Regeneration of active DNAzyme substrates**

For determination of regeneration, the surface-immobilized DNAzyme was first prepared as described above. After an initial reaction of the sensor with Pb(II), the activity was determined by fluorescence measurements. The reacted sensors were subsequently soaked, individually, in Millipore water for 18 hours in closed sample vials. The samples were then rinsed with Millipore water for 5 minutes. Hybridization of 17DS-FI was repeated by soaking the reacted sensors in 50 mM tris acetate buffer at pH=7.2 and 1 M NaCl with 1  $\mu$ M 17DS-FI with the same heating and cooling described above. Non-regenerated control samples were soaked in identical buffer solutions and heating conditions, without 17DS-FI. The controls and regenerated substrates were reacted with 10  $\mu$ M Pb(II) in 50 mM tris acetate buffer (pH=7.2) and 50 mM NaCl for 60 minutes. The reaction solution was rinsed over the surface of the sensor and fluorescence intensity determined.

## **RESULTS AND DISCUSSION**

### **Activity of DNAzyme in solution**

The DNAzyme used is slightly modified from that used in previous publications,<sup>26,45</sup> and thus its solution activity was first assessed. The enzyme strand has been modified by addition of a thiol group

via a (CH<sub>2</sub>)<sub>6</sub> linker to a 5-T linker and extension of the arm nearest the thiol modification. The substrate strand has had its complementary arm extended to match that of the enzyme strand up to the polyT linker.

While previously reported DNA array techniques employ a longer polyT linker (10-15 bases), a 5-T linker was chosen for two reasons. First, previous work has shown that 100% hybridization efficiency is achieved using this MCH backfilling methodology in the absence of any polyT linker, i.e., the (CH<sub>2</sub>)<sub>6</sub> chain between the thiol headgroup and the complementary portion of the nucleotide sequence is sufficient for extending the DNA above the MCH layer for complete hybridization.<sup>27,42</sup> Second, single molecule fluorescence resonance energy transfer work in our laboratories has shown that a 5-T linker is sufficient for DNAzyme activity (unpublished observation).

As seen in Figure 1, when 17DS-FI is hybridized with HS-17E-Dy in solution, fluorescence intensity is relatively low. After addition of 10 μM Pb(II), fluorescence intensity increases by 270% after only 5 min reaction time at 300K, compared to a 60% increase observed for the previously reported sequence.<sup>46</sup> The increased ratio is attributed to the extension of the tethering arm, thereby increasing hybridization efficiency at room temperature. Spectra show no peak shift or shape change after cleavage. It is also inferred that the addition of a sulfhydryl headgroup and polyT linker has no discernible effect on Pb-induced cleavage and generation of luminescence.

### **Activity of DNAzyme on Au surfaces**

Figure 2 illustrates the basic immobilization and reaction protocol used throughout this work.

Thiolated-enzyme strand is immobilized on Au via thiol chemisorption; the surface is back-filled with MCH; and substrate strand is hybridized onto enzyme strand to prepare the DNAzyme surface for Pb detection. Upon reaction with Pb(II), the fluorophore-containing portion is released into solution, where it can subsequently be detected. The goal of this work is to establish the activity and figures of merit for the fluorogenic Pb(II)-DNAzyme reaction, when the DNAzyme is initially immobilized on a planar Au substrate.

The choice of sampling time is important in this experiment. In order to determine the optimal time of reaction, a kinetic experiment was performed. The surface immobilized DNAzyme was reacted with 10  $\mu$ M Pb(II) in quiescent solution, and fluorescence intensities were collected at 10 min intervals. Figure 3 shows fluorescence intensity versus time for an active, Au-bound DNAzyme upon addition of Pb(II). The solid line shows a fit to a second order reaction with fluorescence intensity proportional to  $t^{1/2}$ , typical of a diffusion-limited process. A mechanism in which the rate limiting step is diffusion of species to and away from the Au surface, rather than the reaction of DNAzyme with Pb(II), is consistent with the rapid DNAzyme cleavage observed in solution. Clearly the fluorescence intensity nears saturation at times  $t > 1$ h, from which it was determined that 1 h is an appropriate reaction time for quantitative Pb(II) determinations.

A control experiment was carried out to ensure that the DNAzyme is actually immobilized, rather than simply physisorbed on the Au surface. For this experiment, both 17E and 17DS strands were labeled with fluorescein. With both strands labeled, if either DNA strand is removed from the surface in the absence of specific cleavage, it can be detected by fluorescence. Figure 4 shows the steady state fluorescence intensity after addition of Pb(II) to a

series of four Au-DNA SAMs: DNAzyme and three negative controls consisting of no DNA, 17E only, and 17DS only. Clearly, fluorescence intensities are comparable for all three of the controls ( $43,000 \pm 7,000$ ), even in the absence of any fluorophore, as in the no DNA condition. These data demonstrate two points: 1) thiolated enzyme strands are not released to a significant extent after chemisorption to Au, and 2) any non-specific adsorption of substrate strands on the Au surface containing MCH is minor. The comparable fluorescence intensities from all three negative controls indicate that the reaction buffer used for the Pb(II) recognition reaction, not liberation of either fluorescent strand from the Au surface, is responsible for the observed background fluorescence. The relatively high fluorescence intensity ( $460,000 \pm 30,000$ ) for the DNAzyme positive control, compared to the negative controls, indicates that the sensor is responding to Pb(II) as anticipated. In fact, the increase for the DNAzyme is  $>700\%$  upon addition of  $10\ \mu\text{M}$  Pb(II), indicating that Pb(II) specifically cleaves surface-bound DNAzyme, just as it does in solution.

For the Pb(II) specific DNAzyme sensor on Au it was necessary to verify that selectivity is maintained in the immobilized state. An experiment was conducted to compare the activity of the DNAzyme with Pb(II) to that of its previously identified most strongly interfering divalent metal ions Zn(II) and Co(II), and the biologically relevant ion, Mg(II).<sup>26</sup> Detection was performed as previously described, independently reacting  $5\ \mu\text{M}$  of each of the above listed metal ions with the surface-bound DNAzyme, and additional control samples with no added metal ion. Figure 5 shows the fluorescence intensity of the interfering ions to be within error of the control intensity. The Pb(II) reacted samples, however, show  $\sim 300\%$  the intensity observed for the control. This demonstrates that the Au-thiol immobilization has not lowered the specificity of the Pb(II) DNAzyme.

A critical figure-of-merit for molecular recognition chemistry to be exploited in a functional sensor is its ability to determine the analyte of interest in a useful concentration range. A calibration curve for Pb(II) activity on the DNAzyme immobilized sensor is shown in Figure 6. A linear response can be achieved over a wide range,  $10 \mu\text{M} > [\text{Pb(II)}] > 1 \text{ nM}$ , though linearity deviates at higher Pb(II) concentrations. The error associated with these measurements, as characterized by the  $\pm\sigma$  error bars on the points in Fig. 6, is due partially to variations in the physical dimensions of Au substrates that are linked directly to uncertainties in surface coverage. In addition, the self-assembly of biological molecules, with its inherent dependence on local structure, can also contribute to the statistical variation.<sup>47</sup>

A major advantage of utilizing a surface-immobilized DNAzyme for analyte recognition is the ability to regenerate the surface, so that the DNAzyme can be reused. To test the possibility of regenerating previously cleaved DNAzyme molecules, an experiment was performed in which DNAzyme was initially reacted with Pb(II). Following the Pb(II) recognition reaction the surface was soaked in deionized H<sub>2</sub>O for 18 h to remove the substrate strands (both cleaved and uncleaved). The remaining immobilized enzyme strands were then rehybridized with 17DS-FI, and the DNAzyme surface was again reacted with  $10 \mu\text{M}$  Pb(II). The regenerated DNAzyme surface elicited a fluorescence intensity 81% of the original upon exposure to Pb(II), *viz.* Fig. 7. In contrast, exposure of non-regenerated, DNAzyme to Pb(II) produced fluorescence only 6% of the intensity produced by the original reaction, a value comparable to that produced by the negative controls, *cf.* Fig. 4.

Since the surface-bound DNAzyme can be regenerated, the possibility exists of storing the

DNAzyme surfaces for later use and/or reuse. This is a necessity, if they are to be incorporated as the active elements of microfluidic-based sensor structures for field use. Preliminary results indicate that this is possible. DNAzyme surfaces were completely assembled with mixed monolayers of thiolated-enzyme strand and MCH on Au, followed by hybridization with substrate strand. A portion of the DNAzyme structures were reacted with Pb(II) immediately, while the remaining structures were stored dry for a period of 1 day followed by reaction with Pb(II). The stored substrates produced a Pb(II)-induced fluorescence intensity indistinguishable ( $0.98 \pm 0.08$ ) from that of substrates used immediately after preparation. Unfortunately, significant fluorescence intensity ( $0.14 I_{control}$ ) is also observed in the absence of Pb(II) as well. The increased background most likely arises from non-specific dissociation upon drying, loss of orientation of the enzyme strand, and non-specific cleavage when moisture is not completely removed.

### **CONCLUSIONS**

As biological experiments test lead toxicity on ever lower concentrations of lead, the acceptable exposure levels have fallen, requiring improved detection limits for Pb(II) determinations. Not surprisingly, there is a push for robust, sensitive and selective methods to detect Pb(II) *in situ*, especially because of the well-known detrimental effects to children. Field-useable methods for Pb determinations must possess the analytical figures of merit possessed by laboratory methods, and be rugged and regenerable, to enable long-time unattended use. Working toward this goal, this work demonstrates the applicability of a molecular beacon approach based on a Au surface-immobilized DNAzyme that is

specifically cleaved in the presence of Pb(II). The cleavage reaction frees a fluorophore-containing fragment, effectively removing it from the vicinal region near a quencher on the complementary strand. Subsequent fluorescence measurements are linear in Pb(II) concentration in the range  $10 \mu\text{M} > [\text{Pb(II)}] > 1 \text{ nM}$ . Additionally, the intact DNAzyme can be regenerated after use for subsequent measurement cycles. The immobilized DNAzyme may also be dried after assembly with little loss of activity indicating that the immobilized system is robust. All these results suggest that the Au surface-based DNAzyme-Pb recognition event leading to molecular beacon operation is suitable for incorporation into a portable Pb(II) detection device.

What else is needed for a practical DNAzyme-Pb-based sensor? The selectivity of currently available Pb detection schemes is relatively high, with a selectivity between two and three orders of magnitude over other divalent metal ions.<sup>26</sup> However, this may not be sufficient in some applications. Incorporating the DNAzyme into a microfluidic device offers a convenient package and the ability to include capillary ion analysis on selected analyte bands prior to the Pb determination for greatly improved selectivity. We expect that the combination of immobilized DNAzyme inside the nanopores of a hybrid nanofluidic/microfluidic device will offer a convenient method of accomplishing this.<sup>48-53</sup> Although all of the experiments discussed here were performed on planar Au, there is every reason to believe the molecular beacon chemistry can be ported to other Au-coated surfaces, such as the electrolessly deposited Au on the interior of nanocapillaries, to yield a flow-through device compatible with a prepreparation. Since the rate-limiting step is diffusion to and away from the Au surface, incorporation

into a flow-through device is expected to improve reaction times dramatically. Research en route to this goal is on-going.

## **Acknowledgment**

This work was supported by the National Science Foundation Science and Technology Center for Advanced Materials for Water Purification, the Strategic Environmental Research and Development Program, and by the Department of Energy through grant 99ER62797. Juewen Liu is acknowledged for helpful discussions on DNAzyme hybridization.

## REFERENCES

- (1) Centers for Disease Control (U.S.) *Preventing lead poisoning in young children : a statement*, [4th revision] ed.; The Centers: Atlanta, GA, 1991.
- (2) Ma, R.; Mol, W. V.; Adams, F. *Anal. Chim. Acta* **1994**, *285*, 33-43.
- (3) Liu, J.; Chen, H.; Mao, X.; Jin, X. *Int. J. Environm. Analyt. Chem.* **2000**, *76*, 267-282.
- (4) Ochsenkuhn-Petropoulou, M.; Ochsenkuhn, K. M. *Fresenius' J. Analyt. Chem.* **2001**, *369*, 629-632.
- (5) Elfering, H.; Andersson, J. T.; Poll, K. G. *Analyst (Cambridge, United Kingdom)* **1998**, *123*, 669-674.
- (6) Fang, Z.; Sperling, M.; Welz, B. *J. Analyt. Atomic Spec.* **1991**, *6*, 301-306.
- (7) Wuilloud, R. G.; Acevedo, H. A.; Vazquez, F. A.; Martinez, L. D. *Analyt. Lett.* **2002**, *35*, 1649-1665.
- (8) Di Nezio, M. S.; Palomeque, M. E.; Band, B. S. F. *Talanta* **2004**, *63*, 405-409.
- (9) Crowley, K.; Cassidy, J. *Electroanalysis* **2002**, *14*, 1077-1082.
- (10) Ganjali, M. R.; Rouhollahi, A.; Mardan, A. R.; Hamzeloo, M.; Mogimi, A.; Shamsipur, M. *Microchem. J.* **1998**, *60*, 122-133.
- (11) Sokalski, T.; Ceresa, A.; Zwickl, T.; Pretsch, E. *J. Am. Chem. Soc.* **1997**, *119*, 11347-11348.
- (12) Sussell, A.; Ashley, K. *J. Envir. Mon.* **2002**, *4*, 156-161.

- (13) Schmehl, R. L.; Cox, D. C.; Dewalt, F. G.; Haugen, M. M.; Koyak, R. A.; Schwemberger, J. G., Jr.; Scalera, J. V. *Am. Ind. Hyg. Assoc. J.* **1999**, *60*, 444-451.
- (14) Ashley, K.; Hunter, M.; Tait, L. H.; Dozier, J.; Seaman, J. L.; Berry, P. F. *Field Analyt. Chem. Technol.* **1998**, *2*, 39-50.
- (15) Liu, J.; Lu, Y. *J. Am. Chem. Soc.* **2003**, *125*, 6642-6643.
- (16) Liu, J. W.; Lu, Y. *J. Fluoresc.* **2004**, *14*, 343-354.
- (17) Yusof, N. A.; Ahmad, M. *Talanta* **2002**, *58*, 459-466.
- (18) Blake, D. A.; Blake, R. C., II; Khosraviani, M.; Pavlov, A. R. *Analyt. Chim. Acta* **1998**, *376*, 13-19.
- (19) Wilson, R.; Schiffrin, D. J.; Luff, B. J.; Wilkinson, J. S. *Sens. Actuat. B* **2000**, *B63*, 115-121.
- (20) Reese, C. E.; Asher, S. A. *Analyt. Chem.* **2003**, *75*, 3915-3918.
- (21) Breaker, R. R.; Joyce, G. F. *Chem. Biol.* **1994**, *1*, 223-229.
- (22) Li, Y.; Breaker, R. R. *Curr. Op. Struct. Biol.* **1999**, *9*, 315-323.
- (23) Lu, Y. *Chem. Eur. J.* **2002**, *8*, 4588-4596.
- (24) Li, J.; Zheng, W.; Kwon, A. H.; Lu, Y. *Nucleic Acids Res.* **2000**, *28*, 481-488.
- (25) Bruesehoff, P. J.; Li, J.; Augustine, I. A. J.; Lu, Y. *Combinat. Chem. High Throughput Screening* **2002**, *5*, 327-335.
- (26) Li, J.; Lu, Y. *J. Am. Chem. Soc.* **2000**, *122*, 10466-10467.
- (27) Levicky, R.; Herne, T. M.; Tarlov, M. J.; Satija, S. K. *J. Am. Chem. Soc.* **1998**, *120*, 9787-9792.
- (28) Ramachandran, A.; Flinchbaugh, J.; Ayoubi, P.; Olah, G. A.; Malayer, J. R. *Biosens. Bioelectron.*

- 2004**, *19*, 727-736.
- (29) Sugimoto, N. *J. Inorg. Biochem.* **2001**, *86*, 102-102.
- (30) Okumoto, Y.; Ohmichi, T.; Sugimoto, N. *Biochemistry* **2002**, *41*, 2769-2773.
- (31) Ito, Y.; Hasuda, H. *Biotechnol. Bioeng.* **2004**, *86*, 72-77.
- (32) Liu, J.; Lu, Y. *Analyt. Chem.* **2004**, *76*, 1627-1632.
- (33) Porter, M. D.; Bright, T. B.; Allara, D. L.; Chidsey, C. E. D. *J. Am. Chem. Soc.* **1987**, *109*, 3559-3568.
- (34) Nuzzo, R. G.; Allara, D. L. *J. Am. Chem. Soc.* **1983**, *105*, 4481-4483.
- (35) Nuzzo, R. G.; Fusco, F. A.; Allara, D. L. *J. Am. Chem. Soc.* **1987**, *109*, 2358-2368.
- (36) Kelley, S. O.; Barton, J. K.; Jackson, N. M.; McPherson, L. D.; Potter, A. B.; Spain, E. M.; Allen, M. J.; Hill, M. G. *Langmuir* **1998**, *14*, 6781-6784.
- (37) Hegner, M.; Wagner, P.; Semenza, G. *FEBS Lett.* **1993**, *336*, 452-456.
- (38) Du, H.; Disney, M. D.; Miller, B. L.; Krauss, T. D. *J. Am. Chem. Soc.* **2003**, *125*, 4012-4013.
- (39) Nakamura, F.; Ito, E.; Sakao, Y.; Ueno, N.; Gatuna, I. N.; Ohuchi, F. S.; Hara, M. *Nano Letters* **2003**, *3*, 1083-1086.
- (40) Marie, R.; Jensenius, H.; Thaysen, J.; Christensen, C. B.; Boisen, A. *Ultramicroscopy* **2002**, *91*, 29-36.
- (41) Petrovykh, D. Y.; Kimura-Suda, H.; Whitman, L. J.; Tarlov, M. J. *J. Am. Chem. Soc.* **2003**, *125*, 5219-5226.

- (42) Herne, T. M.; Tarlov, M. J. *J. Am. Chem. Soc.* **1997**, *119*, 8916-8920.
- (43) Steel, A. B.; Herne, T. M.; Tarlov, M. J. *Analyt. Chem.* **1998**, *70*, 4670-4677.
- (44) Aqua, T.; Naaman, R.; Daube, S. S. *Langmuir* **2003**, *19*, 10573-10580.
- (45) Liu, J. W.; Lu, Y. *J. Am. Chem. Soc.* **2003**, *125*, 6642-6643.
- (46) Liu, J.; Lu, Y. *Analyt. Chem.* **2003**, *75*, 6666-6672.
- (47) Steel, A. B.; Levicky, R. L.; Herne, T. M.; Tarlov, M. J. *Biophys. J.* **2000**, *79*, 975-981.
- (48) Kuo, T.-C.; Sloan, L. A.; Sweedler, J. V.; Bohn, P. W. *Langmuir* **2002**, *17*, 6298-6303.
- (49) Yang, H. C.; Kuo, P. F.; Lin, T. Y.; Chen, Y. F.; Chen, K. H.; Chen, L. C.; Chyi, J.-I. *Appl. Phys. Lett.* **2000**, *76*, 3712.
- (50) Spencer, M. G.; Flachsbar, B. R.; Yasunaga, T.; Kuo, T.-C.; Sweedler, J. V.; Bohn, P. W.; Shannon, M. A., *MicroTotal Analysis Systems 2001*, Monterey, CA 2001; Kluwer Academic; 195-196.
- (51) Kuo, T. C.; Cannon, D. M.; Chen, Y. N.; Tulock, J. J.; Shannon, M. A.; Sweedler, J. V.; Bohn, P. W. *Analyt. Chem.* **2003**, *75*, 1861-1867.
- (52) Kuo, T. C.; Cannon, D. M.; Shannon, M. A.; Bohn, P. W.; Sweedler, J. V. *Sens. Actuat. A* **2003**, *102*, 223-233.
- (53) Cannon, D. M., Jr.; Kuo, T.-C.; Bohn, P. W.; Sweedler, J. V. *Analyt. Chem.* **2003**, *75*, 2224-2230.

## FIGURE CAPTIONS

**Figure 1.** Fluorescence spectra for: (a) 10 nM 17DS-FI + 10 nM HS-17E-Dy, and (b) after addition of 10  $\mu$ M Pb(II).

**Figure 2.** Schematic of the immobilization and Pb(II) reaction process: (a) piranha-cleaned Au surface, (b) assembly of HS-17E-Dy, (c) subsequent assembly of MCH, (d) hybridization with 17DS-FI, (e) reaction with Pb(II) cleaves 17DS-FI, and (f) water soak removes the 17-DS-FI fragment remaining from cleavage, prior to regeneration.

**Figure 3.** Fluorescence intensities for Pb(II) reaction double-stranded DNAzyme on Au surface as a function of time. 10  $\mu$ M Pb(II) added at time  $t = 0$ . Error bars represent the standard deviation obtained from replicate measurements on three distinct surfaces, and the solid line is a fit to  $I(t) = I_0 + kt^{1/2}$ , with  $I_0 = 15889$  and  $k = 13288 \text{ min}^{-1/2}$ .

**Figure 4.** Fluorescence intensities produced by exposure of four surfaces to 10  $\mu$ M Pb(II). Three negative controls: no DNA, HS-17E-FI, HS-17DS-FI, and a positive control: DNAzyme. Error bars represent the standard deviation obtained from replicate measurements on at least two distinct surfaces.

**Figure 5.** Fluorescence intensities for DNAzyme assembled on Au surface after reaction with various interfering divalent metal ions. Standard deviation represents measurements on three distinct surfaces.

**Figure 6.** Fluorescence intensities for DNAzyme assembled on Au surface at various Pb(II) concentrations. Standard deviation represents three distinct surfaces.

**Figure 7.** Fluorescence intensities for DNAzyme, a non-regenerated surface, and regenerated surface in the presence of Pb(II). Error bars represent the standard deviation obtained from replicate measurements on at least two distinct surfaces.

**TABLE 1.** DNA labels and sequences.

<b>17E</b>	5'-CATCTCTTCTCCGAGCCGGTCGAAATAGTGAGT-3'
<b>17DS</b>	5'-ACTCACTATrAGGAAGAGATG-3'
<b>HS-17E-FI</b>	5'-(C <sub>6</sub> Thiol)-TTTTTAAAGAGACATCTCTTCTCCGAGCCGGTCGAAATAGTGAGT-Fluorescein-3'
<b>HS-17E-Dy</b>	5'- (C <sub>6</sub> Thiol)- TTTTTAAAGAGACATCTCTTCTCCGAGCCGGTCGAAATAGTGAGT-Dabcyl-3'
<b>17DS-FI</b>	5'-Fluorescein-ACTCACTATrAGGAAGAGATGTCTCTTT-3'

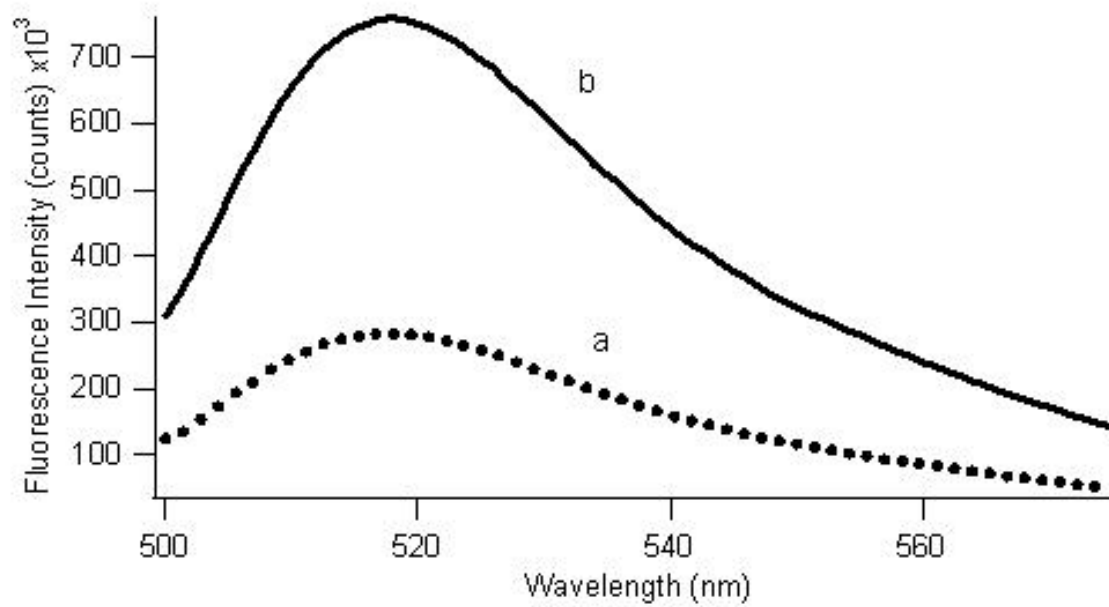


Figure 1

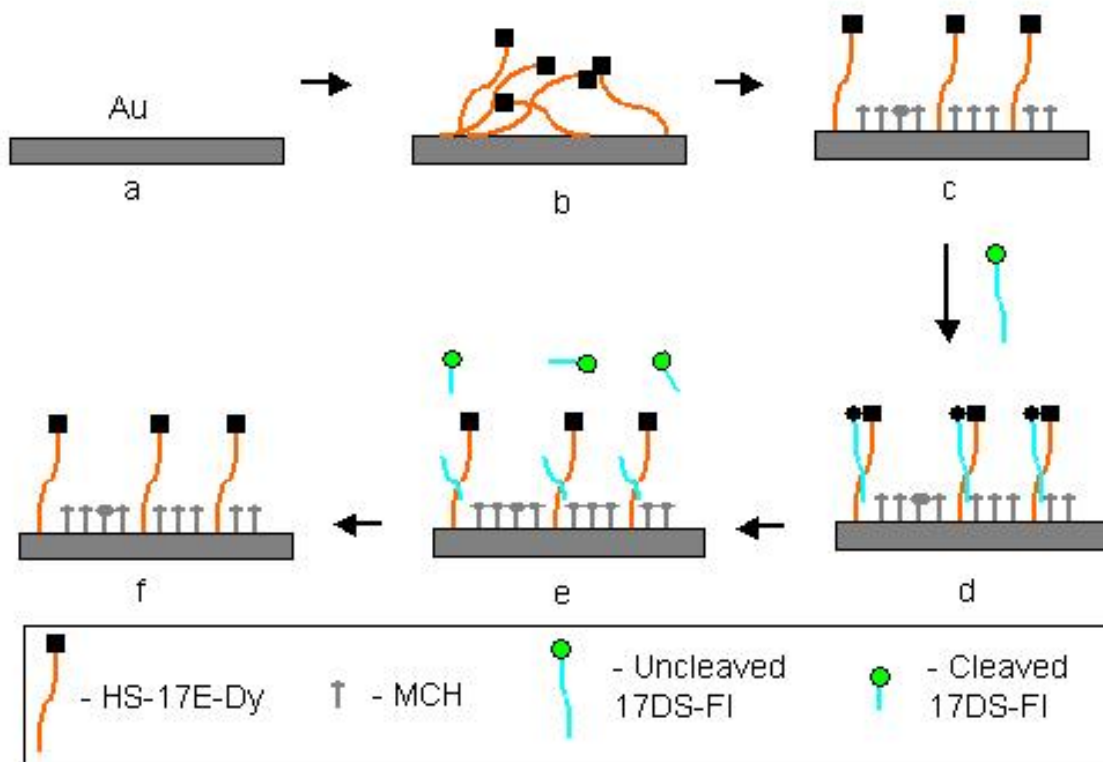


Figure 2

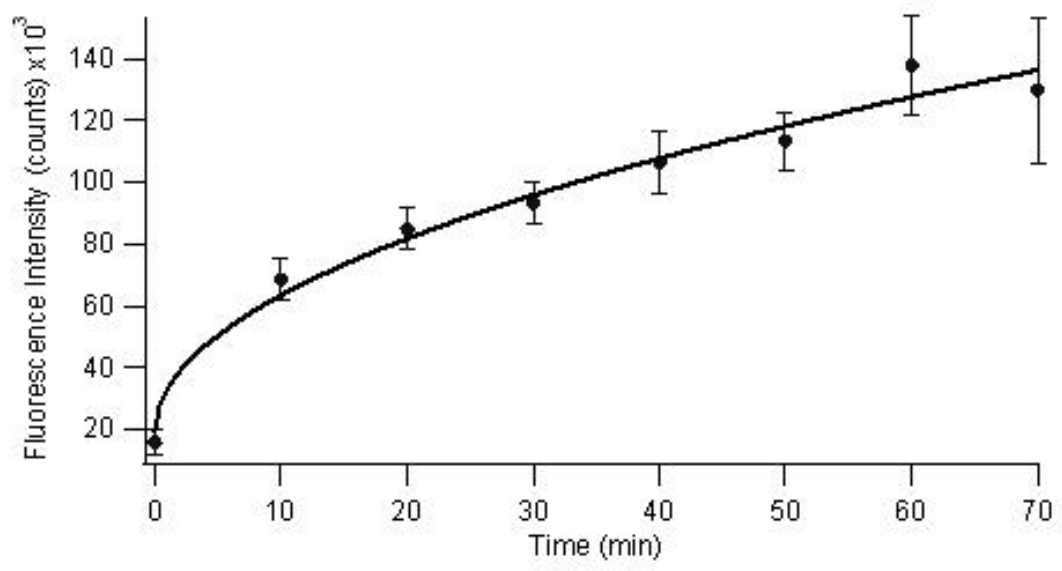


Figure 3

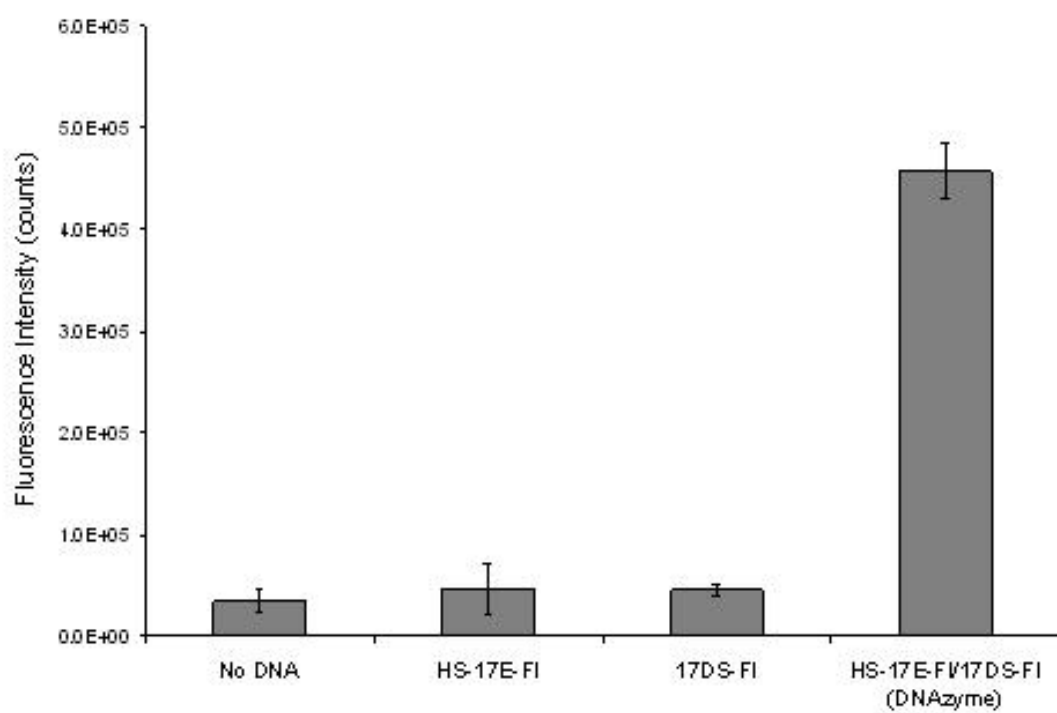


Figure 4

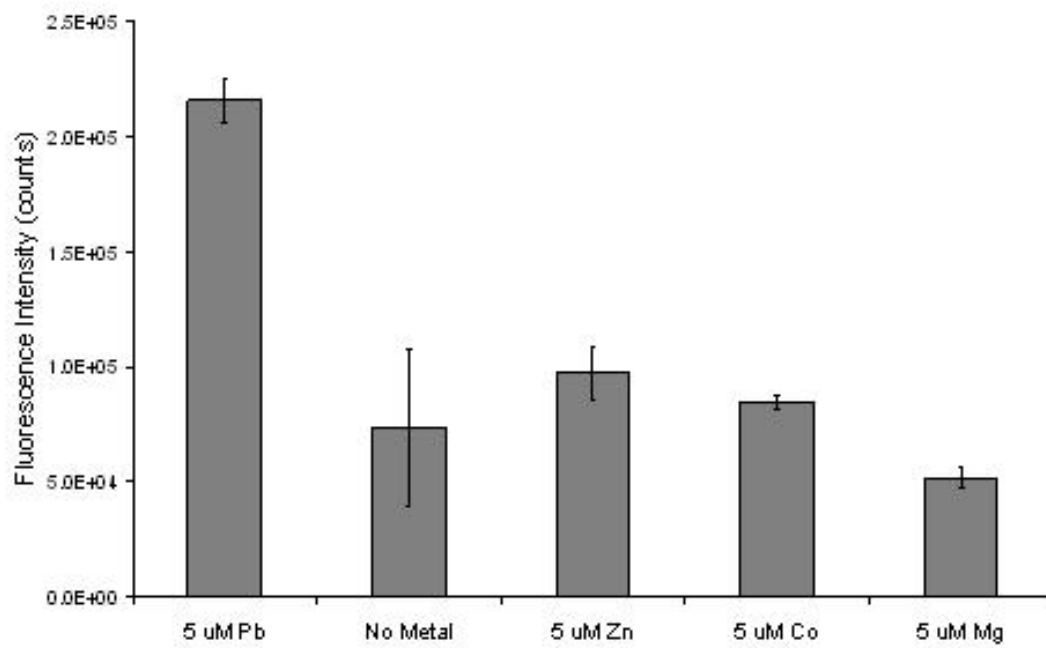


Figure 5

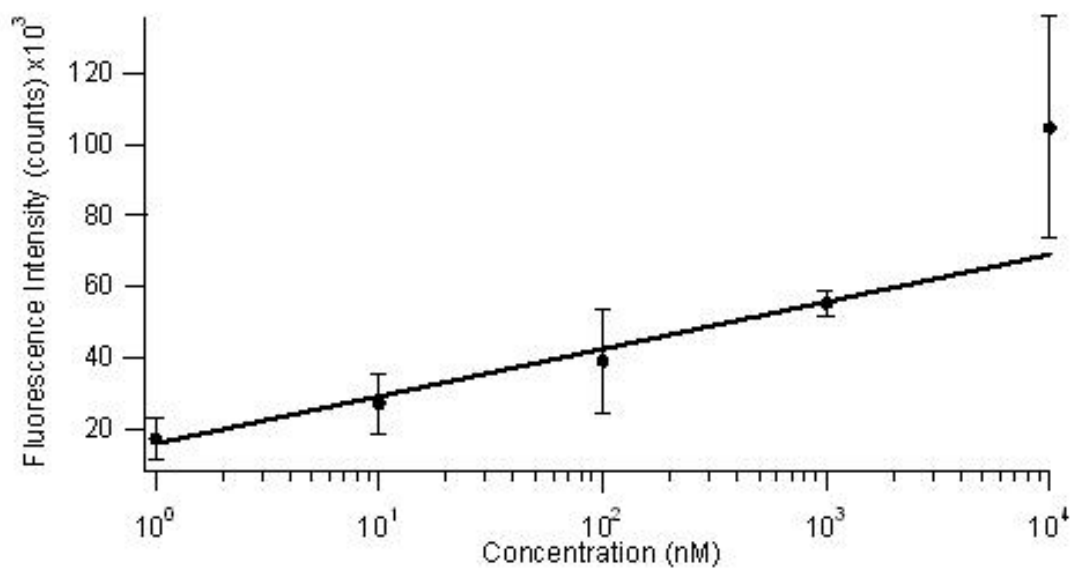


Figure 6

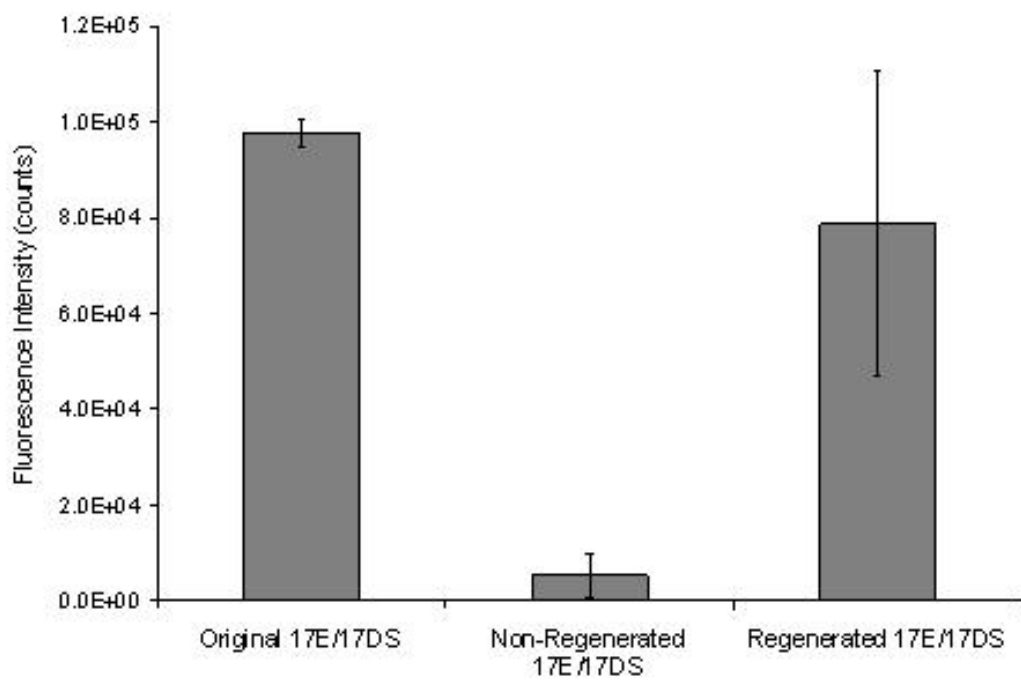


Figure 7



# Miniaturized Lead Sensor Based on Lead-Specific DNAzyme in a Nanocapillary Interconnected Microfluidic Device

IN-HYOUNG CHANG<sup>†</sup>, JOSEPH J. TULLOCK<sup>†</sup>, JUEWEN LIU<sup>†</sup>, WON-SUK KIM<sup>†</sup>, DONALD M. CANNON, JR.<sup>†</sup>, YI LU<sup>†</sup>, PAUL W. BOHN<sup>‡</sup>, JONATHAN V. SWEEDLER<sup>†</sup>, AND DONALD M. CROPEK<sup>\*‡</sup>

*Department of Chemistry and the Beckman Institute for Advanced Science and Technology, University of Illinois at Urbana-Champaign, 600 S. Mathews Avenue, Urbana, IL 61801, and U.S. Army Engineer Research and Development Center, Construction Engineering Research Laboratory, Champaign, IL 61822*

\*Corresponding author telephone: (217) 373-6737; fax: (217) 373-7222; e-mail: Donald M. Cropek@erdc.usace.army.mil

<sup>†</sup>Department of Chemistry and the Beckman Institute for Advanced Science and Technology, University of Illinois

<sup>‡</sup>U.S. Army Engineer Research and Development Center, Construction Engineering Research Laboratory

## ABSTRACT

A miniaturized lead sensor has been developed by combining a lead-specific DNAzyme with a microfabricated device containing a network of microfluidic channels that are fluidically coupled via a nanocapillary array interconnect. A DNAzyme construct, selective for cleavage in the presence of Pb<sup>2+</sup> and derivatized with fluorophore (quencher) at the 5' (3') end of the substrate and enzyme strand, respectively, forms a molecular beacon, that is used as the recognition element. The nanocapillary array membrane interconnect is used to manipulate fluid flows and deliver the small volume sample to the beacon in a spatially confined detection window where the DNAzyme is interrogated using laser induced fluorescence (LIF) detection. A transformed log plot of the fluorescent signal exhibits a linear response ( $r^2 = 0.982$ ) over a Pb<sup>2+</sup> concentration range of 0.1 – 100  $\mu$ M, and a detection limit of 11 nM. The sensor has been applied to the determination of Pb<sup>2+</sup> in an electroplating sludge reference material, the result agreeing with the certified value within 4.9%. Quantitative measurement of Pb<sup>2+</sup> in this

complex sample demonstrates the selectivity of this sensor scheme and points favorably to the application of such technologies to analysis of environmental samples. The unique combination of a DNAzyme with a microfluidic-nanofluidic hybrid device makes it possible to change the DNAzyme to select for other compounds of interest, and to incorporate multiple sensing systems within a single device for greater flexibility. This work represents the initial steps toward creation of a robust field sensor for lead in ground water or drinking water.

## **Introduction**

Bioavailable lead is a toxic element, linked to a variety of adverse health effects (1-3). Since lead is not biodegradable, it accumulates in the environment and produces toxic effects in plants and animals, even at low concentrations (4-6). With growing understanding of the health effects of lead, the US government has increasingly become involved in addressing the lead threat, and new regulations have been created for lead. In the Clean Air Act Amendment of 1990, the EPA designated  $Pb^{2+}$  as an “air toxic”, meaning that it may cause serious health and environmental hazards when present as an airborne pollutant (3-7). Also, new guidance from the Department of Defense Directive 4715 (8) requires a high degree of management and monitoring of impact areas on test firing ranges where lead accumulates due to use of lead containing munitions. In addition, lead has been listed as a pollutant of concern in EPA’s Great Water Program (9) due to its persistence in the environment, potential for bioaccumulation, and toxicity to humans and the environment. These examples demonstrate that the focus of lead monitoring has been extended from high-dose effects for workers in an industrial environment to potential health and ecological hazards in the global habitat and ecosystem. It is therefore essential that sensitive, reliable and cost-effective analytical methods are developed for the remote monitoring of lead.

Miniaturization is currently an important trend in environmental monitoring due to its potential to reduce cost, provide portability and increase analysis speed. In recent years, considerable interest has been focused on the development of miniaturized microfluidic (lab-on-a-chip) systems (10-13) offering improved analytical performance metrics such as inducing fast and efficient chemical reactions within small volumes and low manufacturing costs. A further benefit of miniaturization is the reduction in reagent and sample consumption and a subsequent reduction in the quantity of waste produced. Several approaches have been published for the

separation and simultaneous determination of metal ions based on microfluidic devices (14-21). For example, Jacobson *et al.* have demonstrated a successful separation of Zn, Cd, and Al with detection limits in the 10 - 100 ppb range using a capillary electrophoresis (CE) microchip (16). Deng and Collins utilized colorimetric detection, and six heavy metals including  $\text{Pb}^{2+}$  were effectively separated and simultaneously determined on a CE microchip with sub ppb detection limits after preconcentration by solid-phase extraction (21).

The use of biosensors for environmental pollution monitoring has been another growing area, as these devices provide rapid, simple and reliable determination of pollutants at trace levels. Novel lead specific biosensors have been developed (22-27). Lu *et al.* (22, 26-28) developed a new biosensor for lead by combining the high selectivity of a DNAzyme with a molecular beacon strategy to achieve sensitive and quantitative fluorescent detection of  $\text{Pb}^{2+}$  over a wide concentration range from 10 nM to 10  $\mu\text{M}$ .

This study demonstrates the combination of a  $\text{Pb}^{2+}$ -specific DNAzyme biosensor with a multi-level nanofluidic-microfluidic hybrid device, in which a nanocapillary array membrane is used to control motion of pL-volume fluid voxels from the analyte-containing sample stream to the biosensor compartment. These devices employ a membrane containing an array of nanocapillaries located between multilayered microfluidic channels, allowing for the convenient and efficient control of fluids in the device (29-31). In this paper, methods for adapting this lead-selective DNAzyme to the nanofluidic device are explored, an optimal protocol is identified, and the analytical figures of merit including dynamic range, limit of detection, accuracy, and precision are determined. Finally, the microfluidic / DNAzyme molecular beacon is successfully applied to analysis of  $\text{Pb}^{2+}$  in an electroplating sludge certified reference material.

## **Experimental Section**

**Materials.** Lactic acid and ammonium hydroxide were obtained from Fisher Scientific (Fair Lawn, NJ). HEPES (N-[2-hydroxyethyl]piperazine-N'-[2-ethanesulfonic acid]), sodium chloride and sodium hydroxide were purchased from Aldrich (Milwaukee, WI). Prepolymer and curing agent (Sylgard 184, Dow Corning Corp. Midland, MI) and polycarbonate nuclear track-etched (PCTE) membrane with a hydrophilic wetting layer of poly(vinylpyrrolidone) (Osmonics, Minnetonka, MN) were used in the PDMS (poly(dimethylsiloxane)) chip. These PCTE membranes are 10 microns thick with 200 nm diameter pores at a pore density of  $3 \times 10^8$  pores /  $\text{cm}^2$ . The lead stock solutions (1000 mg/L) were purchased from Fisher Scientific as an atomic absorption standard solution in 2%  $\text{HNO}_3$ . Working solutions of lower concentration were prepared by serial dilution of the stock solution with a background electrolyte (BGE). The BGE (25 mM lactate, 25 mM HEPES, and 50 mM NaCl) was prepared by dissolving lactic acid, HEPES and NaCl in deionized water (18.2 M $\Omega$ , Milli-Q UV-plus system, Millipore, Bedford, MA). The pH of the electrolyte was adjusted to 7 with ammonium hydroxide. Calibration of the chip sensor was performed using seven different lead concentrations. All reagents were analytical grade or higher.

**Preparation of DNAzyme.** The fluorescently labeled oligonucleotides were purchased from Integrated DNA Technology Inc. (Coralville, IA). The design of lead DNAzymes is described in detail by Lu *et al.* (28). Briefly, 3' end Dabcyl (4-(4'-dimethylaminophenylazo)benzoic acid)-labeled enzyme strand, termed 17E-Dy, and 5' end FAM (6-carboxyfluorescein) and 3' end Dabcyl-labeled cleavable DNA substrate, termed 17DS-FD, were chosen (Figure 1). The DNAzyme enzyme-substrate complex was prepared with 500 nM of both 17E-Dy and 17DS-FD for LIF measurements and 2.5  $\mu\text{M}$  of both enzyme and substrate for fluorescence microscopy studies. A sample of enzyme and substrate was heated at 90  $^\circ\text{C}$  for

2 min and slowly cooled to 5 °C for 2 hr. to anneal the strands together and create the complex.

**Sample Preparation.** The electroplating sludge sample was purchased from Resource Technology Corporation (Laramie, WY) and prepared for analysis by USEPA Method 3050B (32). The sludge sample was thoroughly mixed, dried and ground immediately before use. For the digestion, 2.5 mL of concentrated HNO<sub>3</sub> and 10 mL of concentrated HCl were added to 0.1 g sample and refluxed for 15 min. on a hot plate. The digestate was filtered through filter paper (Whatman No. 41) and the filtrate was collected in a volumetric flask. The filter paper and the residue were both washed with 5 mL of hot HCl. These washings were collected in the same flask. The filter paper and residue were removed and placed back in the reflux beaker. 5 mL of concentrated HCl was added and heated at 95 ± 5 °C until the filter paper dissolved. The residue was filtered and the filtrate was collected in the same flask. The cover and sides of the reflux beaker were washed with HCl and this solution was also added to the flask. A control sample was prepared by following the entire sample preparation procedure without sludge. The sample was diluted 1:1 using concentrated ammonium hydroxide followed by a 1000-fold dilution with background electrolyte before injecting on the microchip. The lead concentration was determined based on the actual weight of the dried sludge sample and the final dilution volumes.

**Microfluidic Device and Measurement System.** Details of the channel layout and fabrication of multilevel microfluidic-nanofluidic hybrid architectures have been provided previously (29). A three-dimensional transport device is depicted schematically in Figure 2. Two identical channels (50 μm wide, 30 μm deep and 14 mm long) were orthogonally oriented on a PDMS microchip and separated at the intersection by a nanocapillary array interconnect (NAI); the PCTE membrane with 200 nm diameter cylindrical pores. Platinum wires (250 μm

diameter, Goodfellow Corp., Berwyn, PA), mounted into reservoirs at the distal ends of the microchannels, were used to apply bias voltages. An 8-relay system, designed to switch electrical contacts between Pt electrodes and high voltage power supplies (Bertan High Voltage, Hicksville, NY) for different configurations and magnitudes of microfluidic manipulation, was computer controlled via a multifunction data acquisition card (DAQ, National Instruments Corp., Austin, TX) and Labview software (National Instruments Corp.).

Fluorescence microscopy was used for signal acquisition using an inverted Olympus epi-illumination microscope (Melville, NY). The CCD camera (Javelin Ultrichip Hi Res, Torrance, CA) output was recorded with a videocassette recorder and a computer-controlled video capture device (ATI Technologies, Markham, Ontario, Canada). Fluorescence was excited with 488 nm radiation from an Ar<sup>+</sup> ion laser (Innova 300, Coherent Inc., Santa Clara, CA) which is very close to the FAM 492 nm excitation maximum. The laser light was passed through a set of irises and a neutral density filter (Newport, Irvine, CA) before reaching a dichroic mirror (505DCLP, Chroma Technology Corp., Brattleboro, VT). The excitation light was focused by a 10x objective for a 50 μm diameter area of interrogation. Fluorescence signals were collected by the same lens and dichroic mirror assembly and optically filtered through a 100 μm pinhole and bandpass filter (HQ525/50m, Chroma Technology Corp.) that permits passage of the 518 nm FAM emission maximum before being detected by a photomultiplier tube (PMT) (HC124, Hamamatsu Corp., Bridgewater, NJ). Control of the PMT data collection was achieved through computer with a Labview program and data acquisition card (DAQ, National Instruments Corp.). All fluorescence signals were collected at the intersection of the crossed channels, *i.e.* just below the nanocapillary array interconnect membrane.

## **Results and Discussion**

The goal of this study is to adapt the  $\text{Pb}^{2+}$ -specific DNAzyme concept to a nanofluidic reagent delivery and detection scheme to realize a robust, sensitive, regenerable platform for sensing of  $\text{Pb}^{2+}$ . The specific recognition of  $\text{Pb}^{2+}$  by the DNAzyme is a necessary, but not sufficient condition to realize a biosensor. For sensing, the necessary elements of reagent delivery, signal generation and recording must be added. Achieving these objectives requires several advances over the macroscale homogeneous DNAzyme assays, including (a) using solutions compatible with electrokinetic control of fluid motion, (b) accomplishing the molecular recognition reaction efficiently within a small ( $< 100$  pL) volume, and (c) regenerating the analytical reagent, *i.e.* active form of the DNAzyme. After optimizing composition and device geometry, the overall system is characterized in terms of common analytical figures of merit and validated using a standard reference material.

**$\text{Pb}^{2+}$ -specific DNAzyme and Electrolyte Optimization.** The synthesis and characterization of the  $\text{Pb}^{2+}$ -specific DNAzyme was described earlier in detail (28). The enzyme DNA strand is a 33 base oligomer and the substrate DNA strand is a 20 base DNA/RNA chimer with a single RNA base whose specific sequences have been previously determined (22,28). Briefly, the molecular beacon is constructed by labeling the 5' end of the cleavable substrate with the fluorophore FAM and the 3' end with a fluorescence quencher Dabcyl and labeling the 3' end of the enzyme strand with Dabcyl as shown in Figure 1. When the substrate (17DS-FD) is hybridized to the enzyme strand (17E-Dy), the fluorescence of FAM is quenched by inter- and intramolecular Dabcyl. The melting temperature of the uncleaved substrate is designed to be above the room temperature ( $\sim 34$  °C) so that the substrate will not melt from the enzyme strand in this hybridized state. On addition of  $\text{Pb}^{2+}$  (the right hand side of Figure 1), the substrate is cleaved at the RNA base site. Upon cleavage, the melting temperatures of the

shorter parts of the substrate are designed to be below room temperature so that it will melt and dissociate from the enzyme strand (28). Thus, FAM is no longer in close proximity to the Dabcyl quenchers and the fluorescence increases with the concentration of  $\text{Pb}^{2+}$ . In a previous report, the substrate cleavage reaction was monitored using fluorescence spectroscopy that illustrated the excellent sensitivity, dynamic range (quantifiable detection in the range of  $10 \text{ nM} < [\text{Pb}^{2+}] < 10 \text{ }\mu\text{M}$ ), and selectivity (at least an 80-fold selectivity enhancement over other divalent metals) for  $\text{Pb}^{2+}$  (22).

Optimizing the composition of the background electrolyte (BGE) is critical, because the composition affects biosensor performance and detection efficiency. The electrolyte must allow controllable fluidic transfer of lead-containing analyte solution, delivery of the hybridized DNA strands (DNAzyme) and sample to the detection window, while also enabling high efficiency cleavage of the DNA substrate in the presence of  $\text{Pb}^{2+}$ . Future generations of the device shown in Figure 2 may include four fluidic channels; an injection channel that has a continually refreshed sample stream, a separation channel that can act as a capillary electrophoresis column to isolate the analyte from other matrix components, the nanofluidic gate PCTE membrane, and a detection channel containing the DNAzyme. Solution flow along any channel can be controlled via potential bias application. Injection of a sample band onto the separation (source) channel merely requires the application of the correct bias along the ends of the injection and separation channels. The migration rate of the analyte must be characterized to know its movement along the separation channel and the time interval when the analyte is present at the NAI. Another bias change will divert solution flow through the PCTE membrane and thus introduce the analyte into the detection channel. The analyte is simultaneously removed from potential matrix interferences and established in the appropriate detection electrolyte. Clearly, this proposed

device may require one electrolyte for optimal electrophoretic separation and a second electrolyte for effective DNAzyme cleavage. Current research is investigating the ability of the NAI to segregate these cross channel solutions. While electrophoretic separation is not occurring on the device described in this report, the future goal is to optimize DNAzyme performance while retaining the possibility of pre-separating a metal ion mixture by capillary ion analysis in the microfluidic device. Therefore, the lactate system, developed by Fritz *et al.* (33) for the separation of metal ions and lanthanides by capillary electrophoresis, became the starting electrolyte. Using the 12 mM lactate system at pH 4, pH 5 and pH 7,  $\text{Pb}^{2+}$  was separated from other divalent metal ions such as  $\text{Mn}^{2+}$ ,  $\text{Cd}^{2+}$ ,  $\text{Co}^{2+}$ ,  $\text{Ni}^{2+}$ , and  $\text{Cu}^{2+}$  in a laboratory capillary electrophoresis (CE) (P/ACE, Beckman Coulter Inc., Fullerton, CA) system equipped with indirect UV detection. For the CE study, 8 mM 4-methylbenzylamine was used as a UV reagent, the separation voltage was 30 kV, and a 75  $\mu\text{m}$  ID and 60 cm long capillary was used. Unfortunately, the DNAzyme was not active in the presence of  $\text{Pb}^{2+}$  in these lactate system. In an effort to improve the DNA cleavage reaction performance, 50 mM HEPES with 50 mM NaCl (22) was selected as a potential electrolyte. Addition of 50 mM NaCl was found to play a critical role in stabilizing the substrate and enzyme strand hybridization reaction, resulting in improved sensitivity. But CE separation was not optimal in the HEPES buffer. Finally, the BGE was optimized by a combination of lactate and HEPES at 25 mM with 50 mM NaCl. Under this condition,  $\text{Pb}^{2+}$  was separated from other metal ions on the laboratory CE and the DNA cleavage reaction was efficient (700% fluorescence enhancement in the presence of 5  $\mu\text{M}$   $\text{Pb}^{2+}$ ). The use of higher NaCl concentrations was not pursued in order to prevent generation of excess current within the microchannels where Joule heating degrades performance and can eventually cause bubble formation.

**Transport Control and Measurement.** The function of the microfluidic device is to introduce and reactively mix the lead-containing sample with the  $\text{Pb}^{2+}$ -selective DNAzyme. NAI provides a controllable mechanism for fluidic metering and rapid mixing (29-31, 34). In essence, the PCTE membrane acts as an electronically gateable valve with voltage-controlled fluid transport rates, preventing fluid flow between vertically separated microchannels in the off-state, and electrokinetically driving fluid flow across the membrane when the proper voltage scheme is applied to the four terminal device. In the off-state, any diffusion of analyte across the NAI is below our detection limit as shown by the use of fluorescent probes under reverse bias conditions (29, 30).

The electrical bias pathways for the sequence of on and off states on the microfluidic device are defined in Figure 3a and b. The source channel (horizontal) was filled with  $1\ \mu\text{M}\ \text{Pb}^{2+}$  solution in BGE and the receiving channel (vertical) was filled with  $2.5\ \mu\text{M}$  hybridized DNA in BGE. The sequential images in Figure 3c-h capture the fluorescence from repeated injections of  $\text{Pb}^{2+}$  at the intersection of the cross-channels. Figure 3c shows the background fluorescence of the two channel system. The dotted white lines indicate the position of the horizontal channel and fluorescence from the vertical channel is barely observable. In the on state (Fig. 3d-e),  $\text{Pb}^{2+}$ -containing solution is electrostatically driven from the horizontal channel across the NAI to the vertical channel containing the DNAzyme. To accomplish this transfer, positive high voltages were applied to the reservoirs at the two ends of the source channel and the upper reservoir of the receiving channel while grounding the bottom reservoir of the receiving channel. The transfer efficiency of  $\text{Pb}^{2+}$  is proportional to the magnitude of applied bias on either end of the source channel (Figure 3a) up to 400 V, showing larger transfer ratios at higher voltages. However, bubble generation due to electrolysis/heating was observed after several repetitive

injections at voltages higher than 400 V, thereby establishing an upper limit on the voltage applied to any of the channel arms. With a 200 nm pore diameter NAI, the bias condition illustrated in Figure 3a causes  $\text{Pb}^{2+}$  flow from both arms of the source channel through the nanocapillary array toward the bottom reservoir of the receiving channel.

As soon as the on state bias is applied (Fig. 3d), the  $\text{Pb}^{2+}$  plug moves through the NAI toward the ground end of the receiving channel and starts to cleave the substrate DNA, resulting in a significant fluorescence increase. The cleaved, fluorescently tagged DNA has a slight negative charge and is thus transported toward the positively biased upper reservoir, giving rise to fluorescence on both sides of the channel intersection. The off state switches the positive bias on the source channel to ground, stopping the injection of  $\text{Pb}^{2+}$  into the receiving channel and flushing the cleaved DNA strand to the upper reservoir (Fig. 3f) until all cleaved DNA is removed from the viewing image (Fig. 3g). Repetitive injections of  $\text{Pb}^{2+}$  solution (Fig. 3h) show that this microfluidic chip can be used repeatedly.

**Calibration, Precision, and Detection Limit.** Calibration of the DNA biosensor coupled microfluidic system was accomplished by measuring fluorescence intensity (DNAzyme substrate strand cleavage efficiency) as a function of  $\text{Pb}^{2+}$  concentration in the range of  $100 \text{ nM} < [\text{Pb}^{2+}] < 200 \text{ }\mu\text{M}$ . A plot of fluorescence enhancement vs. lead concentration is shown in Figure 4. At each measurement, electrical bias was cycled four times between on and off states. Each datum in the plot represents the average fluorescence enhancement of these four trials as a function of  $\text{Pb}^{2+}$  concentration and the error bars represent  $\pm \sigma$ . The expression of best fit for the plot is described as  $\ln(I_{max}-I) = -0.0436 [\text{Pb}^{2+}] + 4.2072$ , where  $I_{max}$  and  $I$  are maximum fluorescence enhancement (%) and fluorescence enhancement (%) at the lead concentration, respectively. The microfluidic system response has a linear correlation using the above expression over the

100 nM to 100  $\mu$ M concentration range with a correlation coefficient ( $r^2$ ) of 0.98. This range likely encompasses  $\text{Pb}^{2+}$  concentration levels for most environmental samples. Repetitive detection of 100 nM  $\text{Pb}^{2+}$  is illustrated in Figure 5. During repetitive injection sequences, signals were reproducible with a coefficient of variation of 3.5% ( $n=5$ ) and the baseline consistently returned to a constant level. The detection limit was evaluated by repetitive injection of 50 nM  $\text{Pb}^{2+}$  standard solution. From the baseline noise during the off state and the fluorescence intensity of 50 nM  $\text{Pb}^{2+}$  at during the on state, the detection limit (signal-to-noise ratio of 3:1) was determined to be 11 nM (2.2 ppb) that is lower than the 72 nM (15 ppb) action level in drinking water recommended by the U.S. Environmental Protection Agency (35). These results demonstrate that the combination of electrokinetically actuated measurement cycles on a microfluidic device and a  $\text{Pb}^{2+}$ -selective DNAzyme produce a device sensitive enough to monitor lead in drinking water or ground water.

**Determination of Lead in an Electroplating Sludge Standard Reference Material.** To challenge the microfluidic DNAzyme sensor against a complex matrix, it was used for  $\text{Pb}^{2+}$  determination in an electroplating sludge standard reference material. The certified metal contents in this material are shown in Table 1. For this assay, the standard addition method was used to account for matrix effects. In this electroplating sludge sample, it was also observed that copper (at a two-fold higher molar concentration) partially quenched the fluorescence of cleaved DNA, resulting in a systematic error in the quantitative detection of  $\text{Pb}^{2+}$ . Since the solubility constant of  $\text{Pb}(\text{OH})_2$  ( $K_{\text{sp}} = 2.5 \times 10^{-16}$ ) is three orders of magnitude larger than that of  $\text{Cu}(\text{OH})_2$  ( $K_{\text{sp}} = 1.6 \times 10^{-19}$ ) (37), it was possible to effect quantitative removal of copper in the sludge digestate as a copper hydroxide precipitate at the electrolyte pH of  $\geq 8$ . We confirmed that copper ion was removed to an undetectable level using the laboratory CE instrument. The

lead ion, on the other hand, gave a quantitative recovery at pH 8 and the enzymatic DNA reaction was even more efficient than at pH 7, showing faster reaction times in the microfluidic device. Other metal ions did not interfere in the quantitative determination of lead.

Figure 6 shows the standard addition curve for the determination of lead in the sludge sample. The sludge digestate was prepared as described earlier but four aliquots were spiked with a 50 mM  $\text{Pb}^{2+}$  standard solution to make final added concentrations of 7, 12, 52 and 102  $\mu\text{M}$   $\text{Pb}^{2+}$  producing a five point calibration including the non-spiked sludge sample. The experiments were conducted in the same manner as the calibration using the lead standard in buffer solution. The calibration plot had a correlation coefficient of 0.9993. The concentration of lead in the standard electroplating sludge reference material was determined to be  $[\text{Pb}^{2+}] = 125,200 \pm 3,756$  mg/kg, a value within 4.9% of the certified value of 119,344 mg/kg, indicating the potential for excellent accuracy of this microfluidic / DNAzyme system for  $\text{Pb}^{2+}$  determination.

Although this DNAzyme is selective for  $\text{Pb}^{2+}$  compared to its response for other divalent cations, higher selectivities are required in some applications. This microfluidic device will be further developed so that the sample analytes are separated using on-chip capillary electrophoresis, allowing user selectable fractions of the sample flow to be introduced to the DNAzyme (30, 38). For such a system, the selectivity for particular ions would be enhanced, since it will be determined by the product of the ability to separate the desired metal cation from interfering metal ions and the selectivity of the DNAzyme molecular recognition agent itself. The sensitivity and robust nature of the DNAzyme can also be improved by immobilizing the DNA within the NAI pores, instead of using it in solution (39). This platform offers the possibility of incorporating multiple sensing locations in one device; thus, by incorporating different metal ion selective DNAzymes into a single microfluidic device, multiple species can

be determined simultaneously.

### **Acknowledgements**

This work was supported by the Strategic Environmental Research and Development Program, the Department of Energy under grant FG02 88ER13949, and the Engineering Research and Development Center Long Term Monitoring Focus Area.

## Literature Cited

- (1) Needleman, H. Lead poisoning. *Annu. Rev. Med.* **2004**, *55*, 209-222.
- (2) Fassett, J. D.; MacDonald, B. S. The development and certification of standard reference materials<sup>®</sup> (SRMs) to assess and ensure accurate measurement of Pb in the environment. *Fresenius J. Anal. Chem.* **2001**, *370*, 838-842.
- (3) Control of Emissions of Hazardous Air Pollutants from Motor Vehicles and Motor Vehicle Fuels; EPA-420/R-00-023; Environmental Protection Agency, 2000.
- (4) Rodriguez, B. B.; Bolbot, J. A.; Tohill, I. E. Development of urease and glutamic dehydrogenase amperometric assay for heavy metals screening in polluted samples. *Biosens. Bioelectron.* **2004**, *19*, 1157-1167.
- (5) Shetty, R. S.; Deo, S. K.; Shah, P.; Sun, Y.; Rosen, B. P.; Daunert, S. Luminescence-based whole-cell-sensing systems for cadmium and lead using genetically engineered bacteria. *Anal. Bioanal. Chem.* **2003**, *376*, 11-17.
- (6) Blake, D. A.; Jones, R. M.; Blake II, R. C.; Pavlov, A. R.; Darwish, I. A.; Yu, H. Antibody-based sensors for heavy metal ions. *Biosens. Bioelectron.* **2001**, *16*, 799-809.
- (7) Taking Toxics Out of the Air; EPA/451/K-98-001; Environmental Protection Agency, 1998; available at <http://www.epa.gov/ttnatw01/brochure/brochure.html>.
- (8) DoD Directive 4715.1-Environmental Security; Department of Defense, 1996; available at [http://www.dtic.mil/whs/directives/corres/pdf/d47151\\_022496/d47151p.pdf](http://www.dtic.mil/whs/directives/corres/pdf/d47151_022496/d47151p.pdf).
- (9) Deposition of Air Pollutants to the Great Waters; EPA-453/R-00-005; Environmental Protection Agency, 2000.
- (10) Eijkel, J. C. T.; Mello, A. J. D.; Manz, A. A miniaturized total chemical analysis system:  $\mu$ -TAS. In *Organic Mesoscopic Chemistry*; Masuhara, H.; Shuryver, F.C.D., Eds.; Blackwell Science: New York, 1999, pp 185-219.
- (11) Jacobson, S. C.; Ramsey, J. M. Microfabricated Chemical Separation Devices: Theory, Techniques and Applications. In *High Performance Capillary Electrophoresis*; Khaledi, M.G., Ed.; John Wiley & Sons: New York, 1998, pp 613-633.
- (12) Kopp, M. U.; Crabtree, H. J.; Manz, A. Developments in technology and applications of microsystems. *Curr. Op. Chem. Biol.* **1997**, *1*, 410-419.
- (13) Effenhauser, C. S.; Bruin, G. J. M.; Paulus, A. Integrated chip-based capillary electrophoresis. *Electrophoresis* **1997**, *18*, 2203-2213.
- (14) Reay, R. J.; Flannery, A. F.; Storment, C. W.; Kounaves, S. P.; Kovacs, G. T. A. Microfabricated electrochemical analysis system for heavy metal detection. *Sens. Actuators, B* **1996**, *34*, 450-455.
- (15) Tsukagoshi, K.; Hashimoto, M.; Nakajima, R.; Arai, A. Application of microchip capillary electrophoresis with chemiluminescence detection to an analysis for transition-metal ions. *Anal. Sci.* **2000**, *16*, 1111-1112.
- (16) Jacobson, S. C.; Moore, A. W.; Ramsey, J. M. Fused quartz substrates for microchip electrophoresis. *Anal. Chem.* **1995**, *67*, 2059-2063.
- (17) Kutter, J. P.; Ramsey, R. S.; Jacobson, S. C.; Ramsey, J. M. Determination of metal cations in microchip electrophoresis using on-chip complexation and sample stacking. *J. Microcolumn Sep.* **1998**, *10*, 313-319.
- (18) Collins, G. E.; Lu, Q. Radionuclide and metal ion detection on a capillary electrophoresis microchip using LED absorbance detection. *Sens. Actuators, B* **2001**, *76*, 244-249.
- (19) Collins, G. E.; Lu, Q. Microfabricated capillary electrophoresis sensor for uranium (VI).

- Analytica Chimica Acta* **2001**, 436, 181-189.
- (20) Lu, Q.; Collins, G. E. Microchip separations of transition metal ions via LED absorbance detection of their PAR complexes. *Analyst* **2001**, 126, 429-432.
  - (21) Deng, G.; Collins, G. E. Nonaqueous based microchip separation of toxic metal ions using 2-(5-bromo-2-pyridylazo)-5-(*N*-propyl-*N*-sulfopropylamino)phenol. *J. Chromatogr. A* **2003**, 989, 311-316.
  - (22) Li, J.; Lu, Y. A highly sensitive and selective catalytic DNA biosensor for lead ions. *J. Am. Chem. Soc.* **2000**, 122, 10466-10467.
  - (23) Tauriainen, S.; Karp, M.; Chang, W.; Virta, M. Luminescent bacterial sensor for cadmium and lead. *Biosens. Bioelectron.* **1998**, 13, 931-938.
  - (24) Deo, S.; Godwin, H. A. A selective, ratiometric fluorescent sensor for Pb<sup>2+</sup>. *J. Am. Chem. Soc.* **2000**, 122, 174-175.
  - (25) Babkina, S. S.; Ulakhovich, N. A. Amperometric biosensor based on denatured DNA for the study of heavy metals complexing with DNA and their determination in biological, water and food samples. *Bioelectrochemistry* **2004**, 63, 261-265.
  - (26) Liu, J.; Lu, Y. A colorimetric lead biosensor using DNAzyme-directed assembly of gold nanoparticles. *J. Am. Chem. Soc.* **2003**, 125, 6642-6643.
  - (27) Lu, Y.; Liu, J.; Li, J.; Brueshoff, P. J.; Pavot, C. M.-B.; Brown, A. K. New highly sensitive and selective catalytic DNA biosensors for metal ions. *Biosens. Bioelectron.* **2003**, 18, 529-540.
  - (28) Liu, J.; Lu, Y. Improving fluorescent DNAzyme biosensors by combining inter- and intramolecular quenchers. *Anal. Chem.* **2003**, 75, 6666-6672.
  - (29) Kuo, T.-C.; Cannon, D. M., Jr; Shannon, M. A.; Bohn, P. W.; Sweedler, J. V. Hybrid three-dimensional nanofluidic/microfluidic devices using molecular gates. *Sens. Actuators, A* **2003**, 102, 223-233.
  - (30) Kuo, T.-C.; Cannon, D. M., Jr.; Chen, Y.; Tulock, J. J.; Shannon, M. A.; Sweedler, J. V.; Bohn, P. W. Gateable nanofluidic interconnects for multilayered microfluidic separation systems. *Anal. Chem.* **2003**, 75, 1861-1867.
  - (31) Cannon, D. M., Jr.; Kuo, T.-C.; Bohn, P. W.; Sweedler, J. V. Nanocapillary array interconnects for gated analyte injections and electrophoretic separations in multilayer microfluidic architectures. *Anal. Chem.* **2003**, 75, 2224-2230.
  - (32) Method 3050B; *Acid Digestion of Sediments, Sludges and Soils*; Environmental Protection Agency, 1996; available at <http://www.epa.gov/sw-846/pdfs/3050b.pdf>.
  - (33) Shi, Y.; Fritz, J. S. Separation of metal ions by capillary electrophoresis with a complexing electrolyte. *J. Chromatogr.* **1993**, 640, 473-479.
  - (34) Kuo, T.-C.; Kim, H.-K.; Cannon, D. M., Jr; Shannon, M. A.; Sweedler, J. V.; Bohn, P. W. Nanocapillary arrays effect mixing and reaction in multilayer fluidic structures. *Angew. Chem.* **2004**, 116, 1898-1901.
  - (35) Lead and Copper Rule Minor Revision; EPA 815-F-899-010; Environmental Protection Agency, 1999.
  - (36) Certificate of Analysis; CRM 010-100 Electroplating Sludge No. 2; Resource Technology Corp., Laramie, WY, 2003.
  - (37) Skoog, D. A.; West, D. M. *Analytical Chemistry*, 3rd ed.; Holt, Rinehart and Winston Press, New York, 1979.
  - (38) Tulock, J. J.; Shannon, M. A.; Bohn, P. W.; Sweedler, J. V. Microfluidic separation and gateable fraction collection for mass-limited samples. *Anal. Chem.* **2004**, 76, 6419-6425.

- (39) Swearingen, C. B.; Wernette, D. P.; Cropek, D. M.; Lu, Y.; Sweedler, J. V.; Bohn, P. W. Immobilization of a catalytic DNA molecular beacon on Au for Pb(II) detection. *Anal. Chem.* **2005**, ASAP.

## FIGURE CAPTIONS

FIGURE 1. The sensor is composed of a dual-labeled cleavable substrate DNA whose 5'- and 3'-end is labeled with a fluorophore (FAM) and a quencher (Dabcyl), respectively, and an enzyme strand whose 3'-end is labeled with a Dabcyl. Initially, the fluorescence of FAM is quenched because of the close proximity of the Dabcyl. In the presence of  $\text{Pb}^{2+}$ , the substrate DNA is cleaved, resulting in the release of fragments and a concomitant increase in fluorescence.

FIGURE 2. Schematic of a three-dimensional nanocapillary array interconnect (NAI) gateable microfluidic device. Both crossed-microfluidic channels are identical with dimensions of 50  $\mu\text{m}$  width, 30  $\mu\text{m}$  depth, and 14-mm length.

FIGURE 3. Electrical bias configurations for fluidic control of lead and DNAzyme within NAI/microfluidic device (2a and b). (a) on state and (b) off state. Temporal sequence of fluorescence images at the intersection of the crossed microchannels (2c-h). Source channel (horizontal) was filled with 1  $\mu\text{M}$   $\text{Pb}^{2+}$  in BGE (25 mM lactic acid, 25 mM HEPES, 50 mM NaCl) and receiving channel (vertical) was filled with hybridized DNAzyme in BGE. Dashed lines indicate the position of the horizontal source channel. Applied voltages were (c) all reservoirs were floated and (d) on state causing injection of  $\text{Pb}^{2+}$  solution. Lead solution is transferred from the source channel, across the NAI toward grounded reservoir. The reaction with DNAzyme produced fluorescence from cleaved DNA in the receiving channel. (e) During on state bias, the DNA cleavage reaction reached equilibrium and a constant fluorescent signal is maintained (captured image is  $\sim 40$  s after on state bias is applied).  $\text{Pb}^{2+}$  plug continued to move to the ground electrode and cleaved DNA moved toward the positive bias. (f)  $\sim 1$  s after off state bias is applied. (g)  $\sim 40$  s after off state bias is applied. Cleaved DNA moved toward the positive bias and the receiving channel was flushed with bulk hybridized DNAzyme solution. (h) Repetitive  $\text{Pb}^{2+}$  plug injection after switching back to the on state bias.

FIGURE 4. Plot of fluorescence enhancement as a function of lead ion concentration from 0.1, 1, 5, 10, 50, 100 and 200  $\mu\text{M}$ . Error bars represent  $\pm 1 \sigma$  ( $n=4$ ). Inset shows the plot of  $\ln(I_{\text{max}} - I)$  vs.  $[\text{Pb}^{2+}]$  demonstrating excellent linearity ( $r^2 = 0.982$ ) over the 0.1 to 100  $\mu\text{M}$  range.

FIGURE 5. Typical fluorescence signals during repetitive  $\text{Pb}^{2+}$  injection (100 nM in BGE). Detection was performed at the intersection of crossed channels. Electrical bias configurations are described for Figure 2a and b. On state was maintained for 20 s and switched to off state for 10 s, repetitively.

FIGURE 6. Plot of fluorescence enhancement as a function of lead ion concentration spiked in the electroplating sludge sample for standard addition calibration. Error bars represent  $\pm 1 \sigma$  ( $n=4$ ).

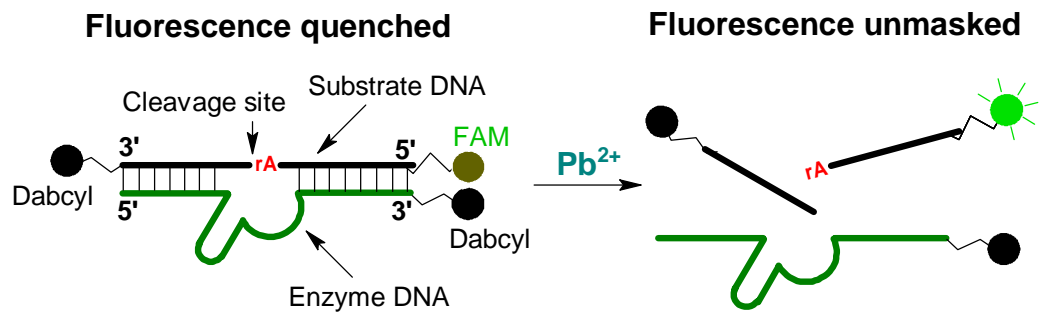
---

TABLE 1. Certified metal content in electroplating sludge reference material

element	concn, <sup>a</sup> mg/kg	element	concn, mg/kg	element	concn, mg/kg
Al	692.5 ± 82.5	Ba	173.3 ± 23.5	Ca	562.7 ± 33.0
Cr	79.5 ± 14.1	Cu	63,169.3 ± 2410.0	Fe	2,698.7 ± 814.5
Pb	119,344.0 ± 27453.0	Mg	(80.0)	Mn	17.5 ± 2.1
Hg	(1.4)	Ni	193.6 ± 15.0	Ag	56.4 ± 6.3
Na	(1,576.2)	Zn	182.6 ± 41.0		

<sup>a</sup> Certified and noncertified values (36), values in parentheses are not certified; certified values are determined on a dry weight basis; uncertainties are one standard deviation of the measurement; the uncertainty is obtained from 95% Confidence Intervals.

---



**Figure 1.**

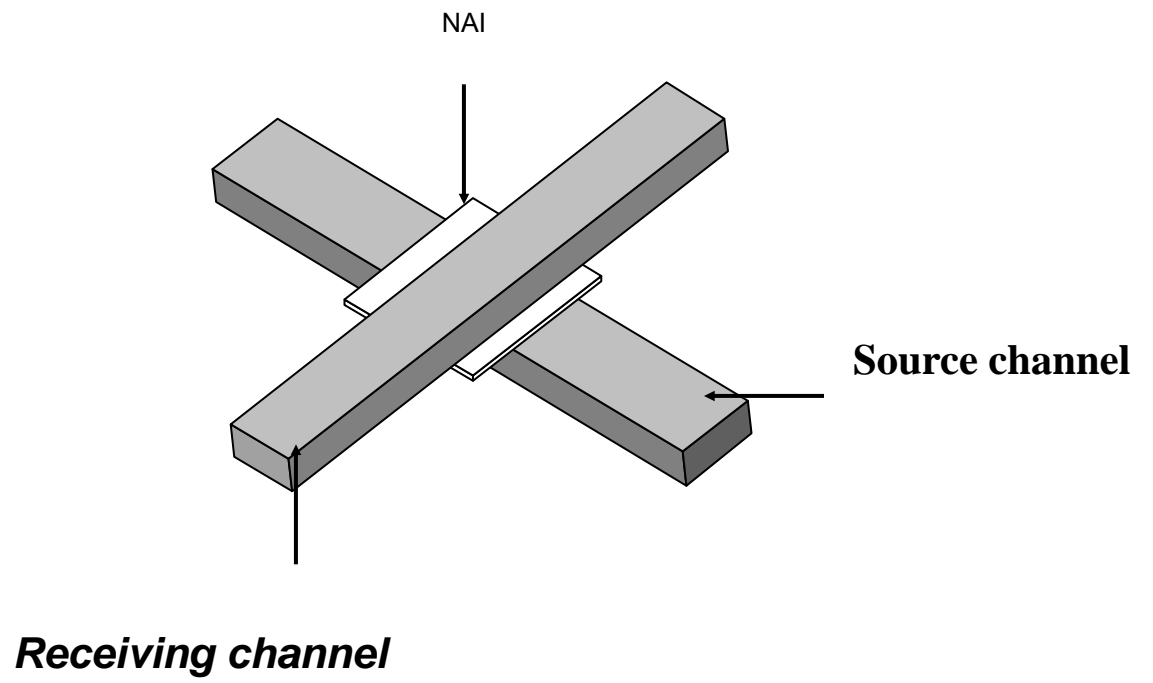


**Figure 2.**

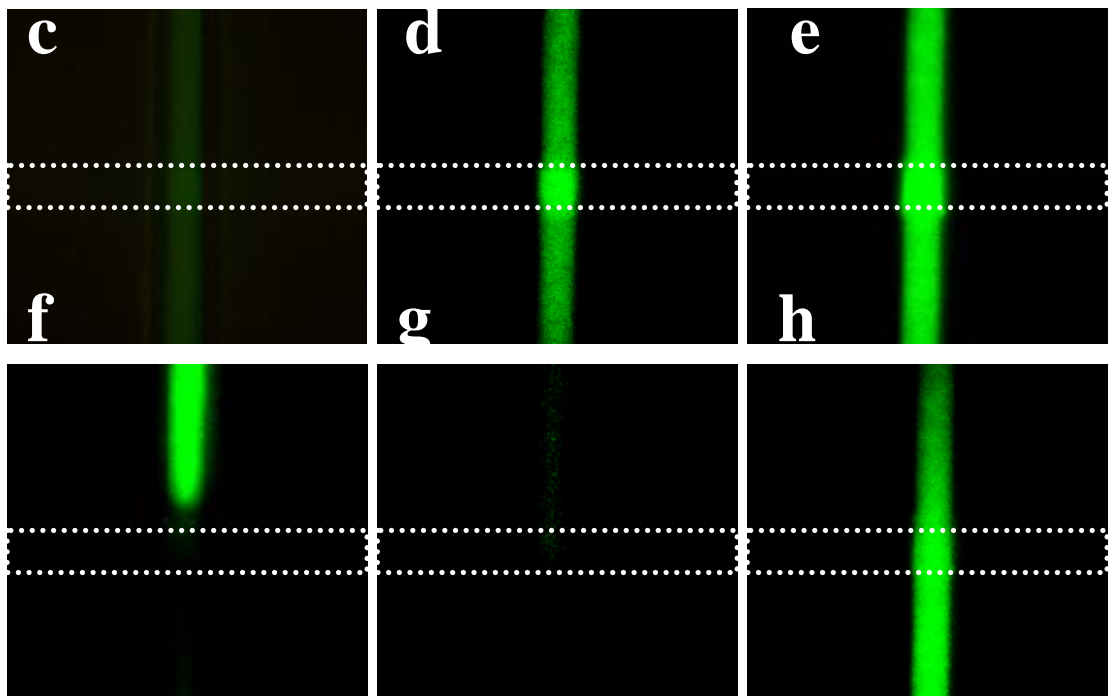
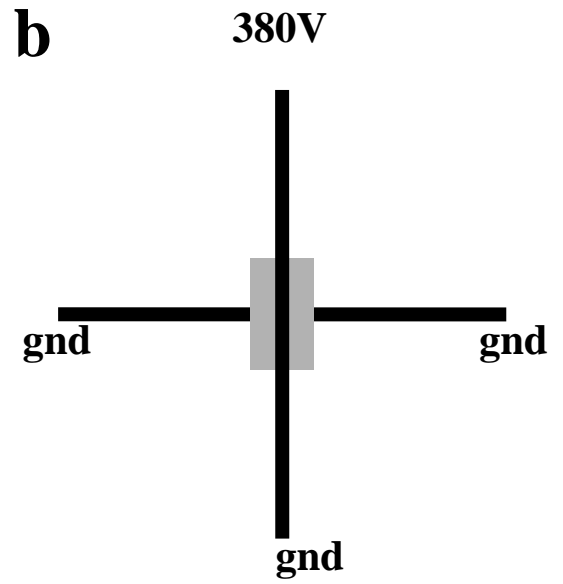
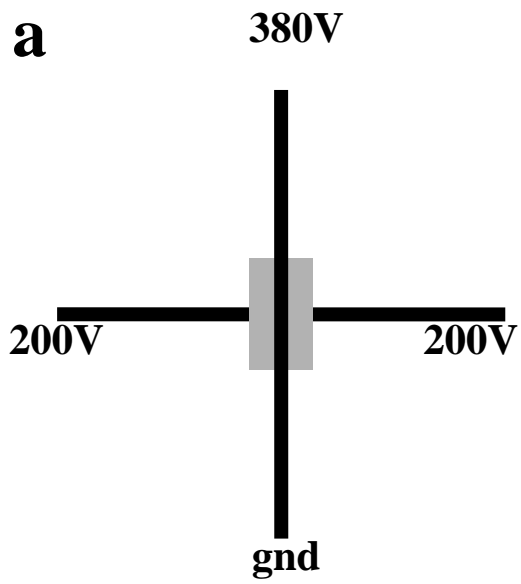


**Figure 3.**

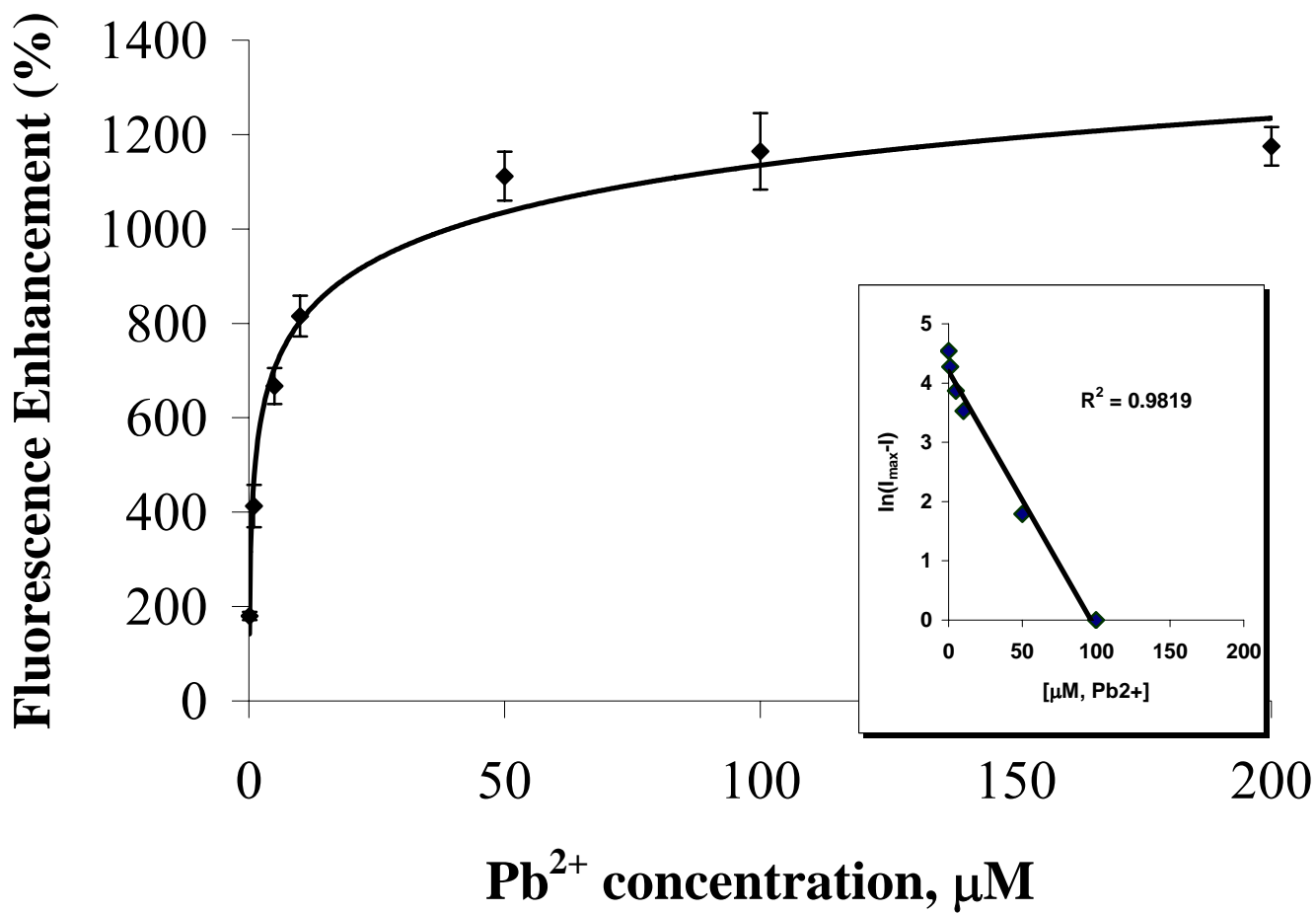


**Figure 4.**

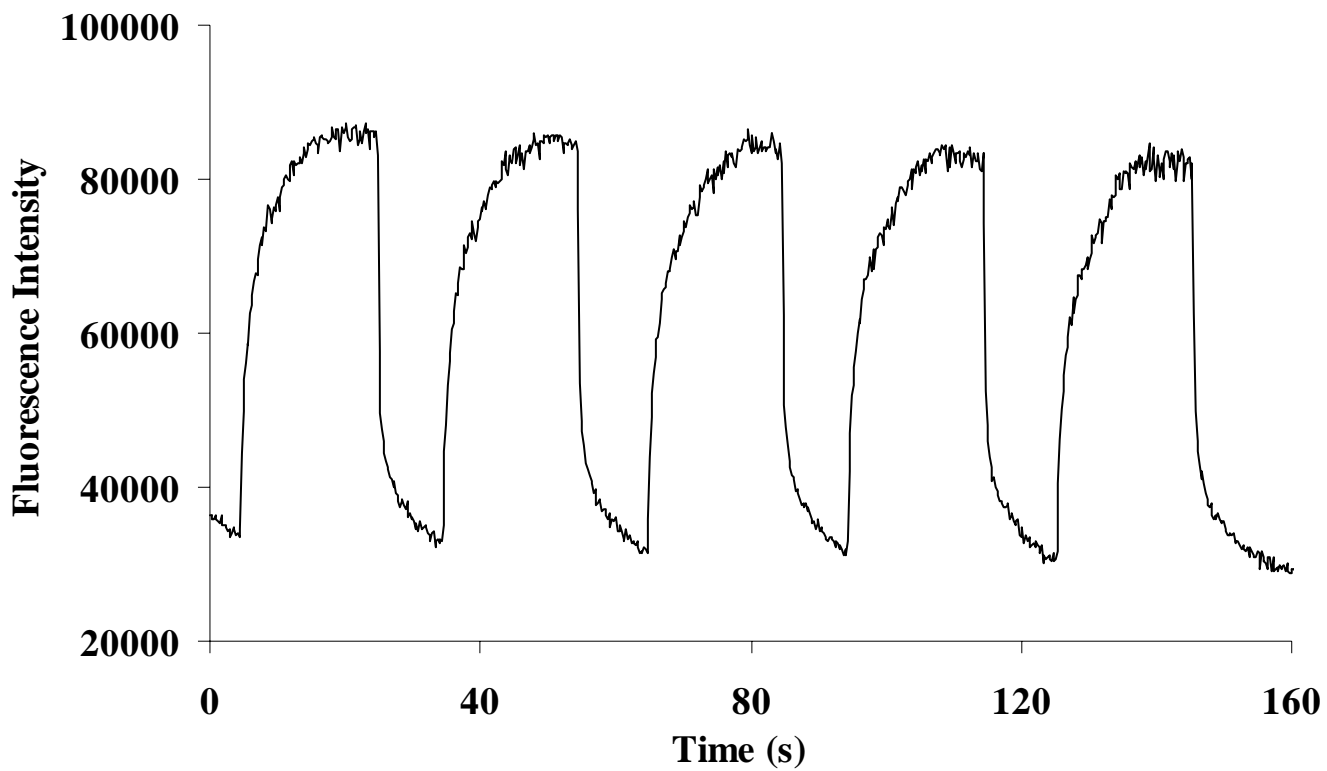


**Figure 5.**

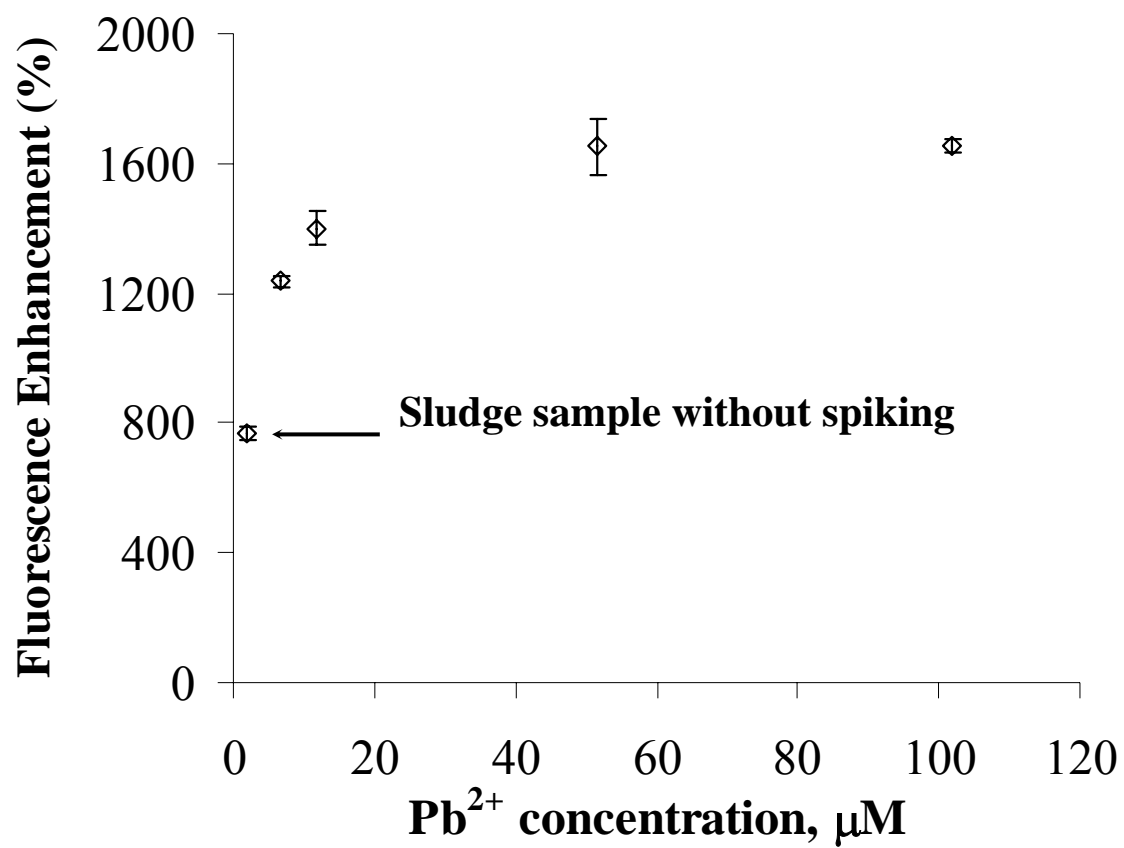


**Figure 6.**